NASA CR-165237
R80AEG458

National Aeronautics and
Space Administration

PROGRAM TO DEVELOP SPRAYED, PLASTICALLY DEFORMABLE COMPRESSOR SHROUD SEAL MATERIALS

FINAL REPORT
JUNE 29, 1976 - SEPTEMBER 29, 1980

BY
J.D. SCHELL and R.C SCHWAB
MATERIALS AND PROCESS TECHNOLOGY LABORATORIES
AIRCRAFT ENGINE GROUP
GENERAL ELECTRIC COMPANY
CINCINNATI, OHIO 45215

Prepared for
NATIONAL AERONAUTICS AND SPACE ADMINISTRATION
LEWIS RESEARCH CENTER
21000 BROOKPARK ROAD
CLEVELAND, OHIO 44135

NAS3-20054

1. Report No.	2. Government Accession No.	3. Recipient's Catalog No.
NASA-CR-165237		

4. Title and Subtitle	5. Report Date
PROGRAM TO DEVELOP SPRAYED, PLASTICALLY DEFORMABLE COMPRESSOR SHROUD MATERIAL - FINAL REPORT	January 1981
	6. Performing Organization Code

7. Author(s)	8. Performing Organization Report No.
R.C. Schwab and J.D. Schell	R80AEG458
	10. Work Unit No.

9. Performing Organization Name and Address	11. Contract or Grant No.
Aircraft Engine Group General Electric Company Cincinnati, OH 45215	NAS3-20054
	13. Type of Report and Period Covered
12. Sponsoring Agency Name and Address	Contractor Report
National Aeronautics and Space Administration Washington, D.C. 20546	14. Sponsoring Agency Code

15. Supplementary Notes

Project Manager, H.W. Scibbe; Technical Advisor, R.C. Bill
Mechanical Technologies Branch, Structures & Mechanical Technologies Division
NASA-Lewis Research Center, Cleveland, OH 44135

16. Abstract

A study of fundamental rub behavior for 10 dense, sprayed materials and eight current compressor-clearance materials has been conducted. A literature survey of a wide variety of metallurgical and thermophysical properties was conducted and correlated to rub behavior. Based on the results, the most promising dense rub material was Cu-9Al. Additional studies on the effects of porosity, incursion rate, blade solidity, and ambient temperature were carried out on aluminum bronze (Cu-9Al-1Fe) with and without a 515B Feltmetal underlayer.

A further development effort was conducted to assess the property requirements of a porous, aluminum bronze, seal material. This evaluation examined strength, thermal cycle capabilities, erosion and oxidation resistance, machinability, and abradability at several porosity levels.

17. Key Words (Suggested by Author(s))		18. Distribution Statement
Compressor		
Gas-Path Seal	Plasma Spray	UNCLASSIFIED - UNLIMITED
Abradability	Titanium blades	
Nickel-base alloys	Coatings	
Iron-base alloys	Erosion Resistance	

19. Security Classif. (of this report)	20. Security Classif. (of this page)	21. No. of Pages	22. Price*
UNCLASSIFIED	UNCLASSIFIED		

* For sale by the National Technical Information Service, Springfield, Virginia 22151

FOREWORD

This report describes the results of a study of the fundamental rub behavior of experimental sprayed materials and currently used compressor-clearance materials. The investigation was conducted from July 1976 through August 1980. In addition to the authors, the following General Electric Company personnel made significant technical contributions to this effort: W.P. Foster, J.P. Young, R.E. Bates, and J.C. Nickley in conducting the seal rub tests; W.R. Butts for directing in-house plasma spray operations; and Dr. W.R. Stowell and Dr. I.I. Bessen for technical guidance in analysis of the data. Dr. S.O. Brennom, while an employee of General Electric Company (currently with Union Carbide Corporation in Houston, Texas), contributed significantly to the overall effort.

TABLE OF CONTENTS

TABLE OF CONTENTS (Concluded)

LIST OF FIGURES

LIST OF FIGURES (Continued)

LIST OF FIGURES (Continued)

LIST OF FIGURES (Continued)

LIST OF FIGURES (Concluded)

LIST OF TABLES

LIST OF TABLES (Concluded)

1.0 SUMMARY

Ten metals were selected for the Task I, Phase I study of fundamental rub behavior on titanium compressor blades. A wide range of metallurgical characteristics (crystal structure, density, composition, and mechanical properties) and thermophysical properties (melting point, specific heat, thermal conductivity, and thermal expansion coefficient) were covered by the materials selected. These were Al, Fe, Cu, Zn, Cu-10Zn, Cu-5Al, Cu-9Al, Fe-6Al, Fe-13Cr, and Ni-13Cr. Such properties as impact strength, thermal conductivity, and melting point appear to play significant roles in rub behavior but do not completely account for the differences observed.

A number of current, compressor-clearance-control coatings were investigated in Task I, Phase II. These included Al, Metco 601, AlBronze/NiCg, 80/20 NiCg, AB-1, Feltmetal 515B, Al top coat over Feltmetal, and AlBronze top coat over Feltmetal. Results for the aluminum were in reasonable agreement with the data from Phase I. The only materials which caused blade wear were the AlBronze/NiCg and the 80/20 NiCg. On the basis of both Phases I and II, it was found that rub energy cannot be used as a screening test for compressor-clearance-control coatings.

As a result of Phases I and II, Cu-9Al was identified as the most promising clearance-control-coating material. In Phase III of Task I, Cu-9Al was studied at two porosity levels (with 20 and 40% Ekonol added) with a Feltmetal (FM) 515B underlayer and without the FM 515B underlayer. The 20% porosity material exhibited good rub characteristics both with and without the Feltmetal 515B underlayer for the Cu-9Al; therefore, it was selected for further evaluation.

In Task II an aluminum bronze (AlBr) alloy was used since it was expected to give similar rub behavior (composition: Cu-9.5Al-1Fe) and was more readily available than the Cu-9Al. Rub tests were conducted at 2.54, 25.4, and 254 μm/sec (0.0001, 0.001, and 0.01 in./sec) incursion rates at room temperature and 755 K (900° F) with 48 blades and with 12 blades. It was found that for the low incursion rate hot rubs were more severe than cold rubs, but at the higher incursion rate cold rubs were more severe than hot rubs. The presence of the Feltmetal 515B was beneficial in reducing blade wear.

Task III was an effort to more fully develop the AlBr/Ekonol material system into an acceptable seal material. Issues such as erosion resistance, thermal-cyclic ability, elevated-temperature stability, and smooth surface-finish capability were addressed. These properties [as well as room temperature, 755 K (900° F), and 867 K (1100° F) rub performance with Ti-6Al-4V and Inconel 718 blades] were determined over a range of compositions from AlBr + 20% Ekonol to AlBr + 5% Ekonol (about 30 to 70 volume percent metal in the deposited coating). In general, the titanium alloy blades always experienced more blade wear than Inconel 718 blades; blade wear was higher for as-sprayed

coatings than for exposed coatings, and the elevated-temperature rubs showed less blade wear but were less predictable in rub behavior features such as scabbing, scouring, blade pickup, and compaction of the porous coatings. A final powder-blend composition of AlBr + 12.5% Ekonol was recommended for rig rub testing under conditions closely simulating the engine operating environment. Blade wear was excessive both for Inconel 718 and for Ti-6Al-4V blades.

2.0 RECOMMENDATIONS

Future efforts to develop shroud seal materials should:

1. Concentrate on balanced-property, composite, seal materials consisting of a metal matrix with some porosity plus an inert, friable, filler material to add stability to the abradable coating.

2. Simultaneously address the blade-tip properties through use of tip treatments aimed at reducing frictional heat generation and preserving high blade-tip yield strengths during rub interactions.

3. Further address the wear mechanisms through detailed rub-energy and heat-flow measurements carried out under conditions closely simulated compressor-rub conditions.

4. Establish with greater certainty whether the melting points of copper-base alloys are sufficiently high to avoid sticky-debris problems under compressor-rub conditions.

3.0 INTRODUCTION

A major factor in the progress of aircraft-engine development has been continued improvement in performance. In turn, many performance improvements have been dependent upon advancements in materials and process technology. Improved compressor-clearance control has contributed to performance improvement through the application of abradable, gas-path-seal materials. These materials have included thermal-sprayed aluminum and nickel graphites, Feltmetals, and silicone rubbers.

Compressors for advanced turbine engines are designed to utilize higher pressure ratios, fewer stages (higher loading per stage), and higher tip speeds than prevail in current-production engines. Under these conditions, leakage over compressor blade tips results in substantial performance losses. Efforts to reduce those losses by decreasing tip clearances are frequently thwarted by excessive tip rubs caused by such events as transient compressor stalls, gyroscopic flight loads, and engine inlet distortion. These rubs lead to: (1) blade wear and consequent increased clearance, (2) blade-tip fatigue failures caused by excitation from rubbing, (3) generation of particulate debris that clogs air passages in cooled turbine hardware downstream, sticks to blades, and decreases performance, and (4) occasional thermal damage to rotor and stator components made of titanium alloy. Significant performance improvements could be made, both in current and future engines, with the development of rub coatings or rub materials that (1) are abradable under high-speed rubs and produce minimal damage to blade tips, (2) retain tight clearances, and (3) generate a nonsticking, nonreacting, rub debris.

Clearance-control seal materials have assisted designers in improving compressor efficiency; however, current materials are not adequate for advanced engines. Blade wear, erosion resistance, debris character, and/or surface-finish aspects are deficient. Plasma-sprayed aluminum, used on some engines, can wear blades or can be scoured depending on engine conditions. Flame-sprayed nickel graphite coatings, used in other engines, can wear blades or erode excessively depending on the composition and strength of the coating, and good surface finishes are difficult to obtain.

All of the materials that rub well, i.e., that produce little or no blade wear, display either of two characteristics: (1) they have low cohesive strength, or (2) they are easily, plastically deformed. The low-cohesive-strength materials wear by internal fractures under the blade rub; the plastically deformed materials visually and microscopically look smeared. On so called "hot rubs," the blade tips are worn and show similar plastic flow. Both fracture stress and flow stress are temperature dependent; therefore, the wear phenomena are intricately dependent on the generation of heat during a rub and the rate of heat loss from the rubbing interfaces.

The low-cohesive-strength materials have two inherent deficiencies: low erosion resistance and lack of good surface-finish capability. To date most dense materials have caused blade wear, blade-tip fatigue cracking, and/or

sticky debris. But they have inherently good surface-finish and erosion properties and offer great potential for improved performance in compressor shroud seals if the deficiencies can be eliminated. A basic understanding of the deformation processes occurring at the rub surfaces is needed in order to effectively identify solutions to blade-wear and fatigue-associated problems with dense rub materials. This is especially true with Ti-base blades.

The objectives of this program were: (1) to observe the rub behavior of titanium blades against dense, sprayed materials and determine the significant mechanical and physical properties, (2) to select dense materials, on the basis of the deduced properties, and subject them to a series of tests designed to meet compressor-clearance rub-material requirements, (3) to assess the effects of adding porosity to these materials, and (4) to evaluate the basic coating requirements imposed on a porous, abradable seal by the compressor environment.

The program was divided into three tasks. Task I consisted of three phases. In Phase I, 10 materials, displaying a range of metallurgical properties, were selected to evaluate the hot and cold rub-test behavior of the dense, sprayed coatings in order to determine the properties significant to rub behavior. Current-engine compressor-seal coatings were evaluated in Phase II and compared to the results of Phase I. Two experimental coating systems were selected based on the results of Phases I and II for use in Phase III where the effect of porosity on the coating rub behavior was examined.

For Task II, two coating systems were selected from Task I results. Further performance verification of the two systems was undertaken. Consideration was given to a wide range of rub-test parameters. The parameters being varied included ambient test temperature, number of blades used, and incursion rate.

Task III involved two interdependent efforts that broadened the Task II effort:

1. Consideration of such performance factors as thermal-shock resistance, the effects of long-term temperature exposures, erosion resistance, and smooth-surface-finish capabilities.

2. Determination of processing and material composition effects on rub performance.

Taking these effects into consideration, an AlBr + 12.5% Ekonol coating composition was selected for final evaluation in the Evendale Compressor Rub Simulator.

4.0 TEST PROGRAM

The test program was designed to identify a potential material system(s) as an improved compressor-clearance coating. To this end, a study was made of the rub behavior of a variety of dense, sprayed materials and current-engine compressor coatings. A flow chart for the test program is given in Figure 1.

4.1 TEST PROCEDURES, TASKS I AND II

The rub tester consisted of a steam-driven, rotating-blade fixture (Figure 2) capable of holding up to 48 blades and producing a maximum blade speed of 152 m/sec (500 ft/sec). The blade axis is parallel to the rotation axis. The shroud material is located on a static specimen (Figure 3) with the rub face in a plane perpendicular to the rotating axis or (intentionally) tilted at a small angle. The rub is made by translating the static member into the rotating blade tips. The ambient temperature of the rig can be set as high as 922 K (1200° F) with a drift in temperature of less than 11 K (20° F). A dynamometer stage mounted on the stator is capable of measuring shear forces as low as 2.2 N (0.5 lbf). The specimen substrate temperature and the rub force (dynamometer) were continuously monitored and recorded on a strip chart during the rub tests (Figure 4).

4.2 TASK I - FUNDAMENTAL RUB BEHAVIOR

4.2.1 Phase I - Significant Property Identification

4.2.1.1 Material Selection and Preparation

Basically, when a blade rubs into a seal the stronger material will resist wear, and the weaker material will take the wear. If one material has a low fracture strength, it will break away in pieces while the material with higher fracture strength remains intact. Similarly, if one material has a tendency to flow plastically (i.e., a low flow stress), it will wear by smearing while the other may not deform plastically at all. Complexities arise when one considers the effects of fracture stress and flow stress due to changes in the temperature of the rubbing members. There is never a certainty that both rubbing members are at the same temperature during a rub. Although all blade materials have high fracture strengths, they do not always have high flow stresses. Titanium alloys, in particular, lose strength rapidly with increasing temperature, and plastic flow sets in across Ti blade tips quite readily to produce burrs when the tip is overheated. Titanium blades that have been severely worn have shown a blue oxide across the tip, indicating that excessive temperatures have been experienced due to the energy dissipated during the rub.

TASK I

Phase I - Fully Dense Material Development

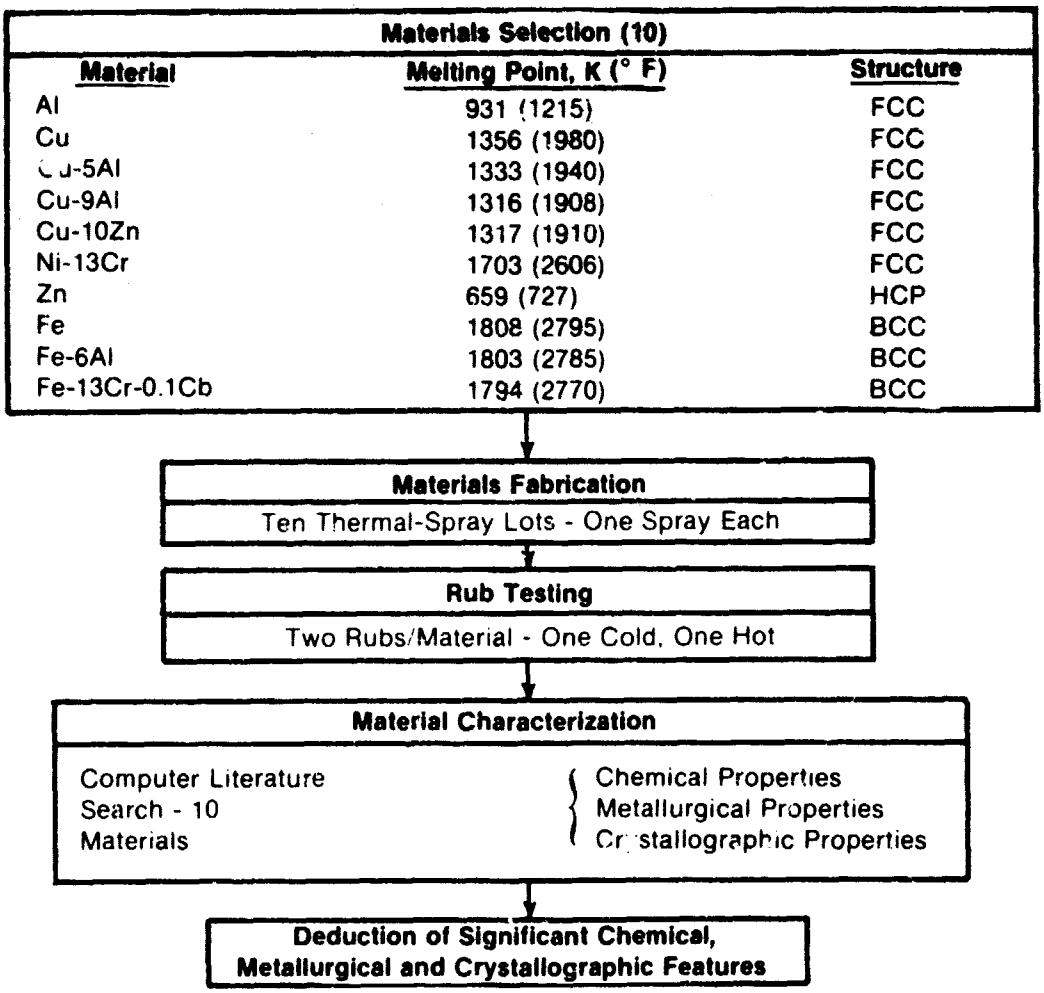

Figure 1. Test Program Flow Diagram.

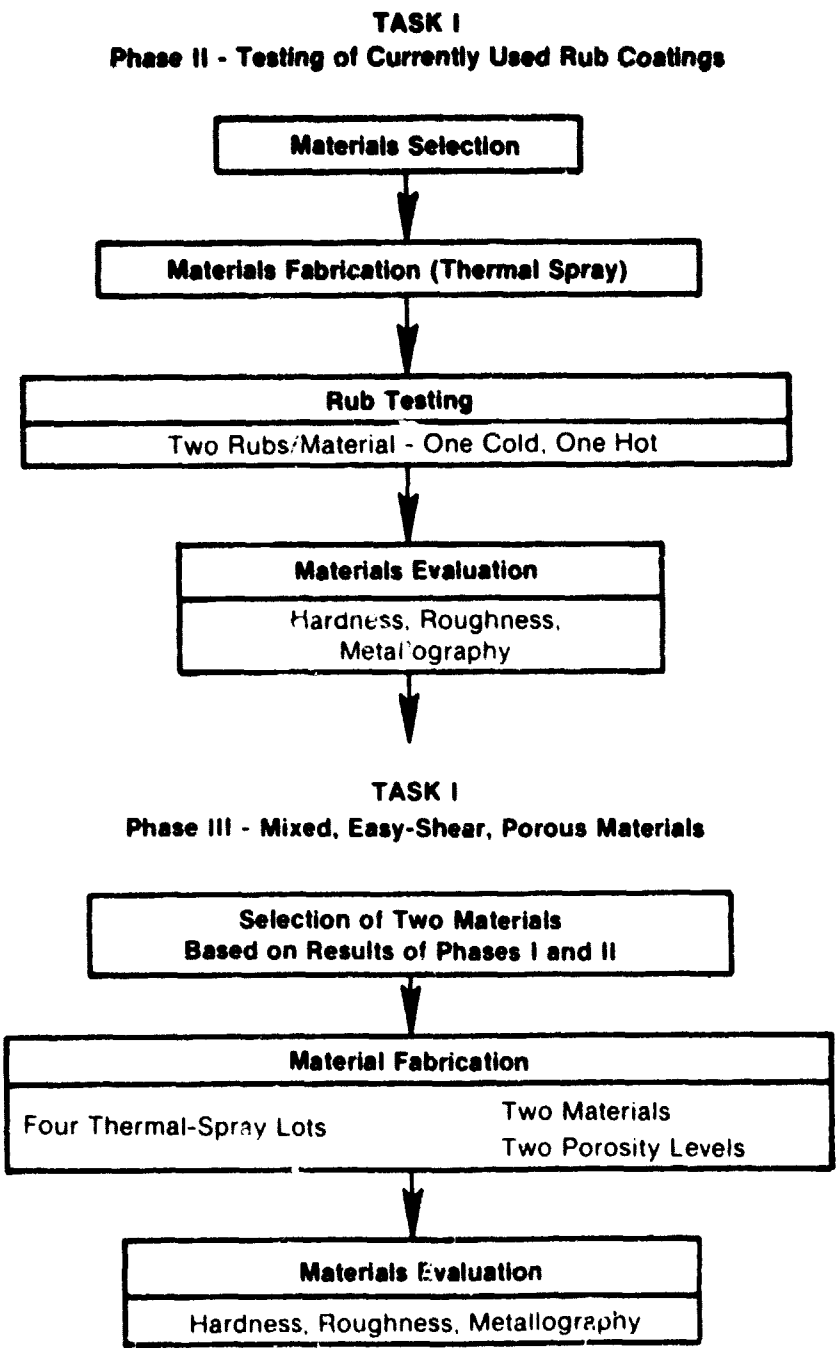

Figure 1. Test Program Flow Diagram (Continued).

TASK II
Rub-Test Parameter Evaluation

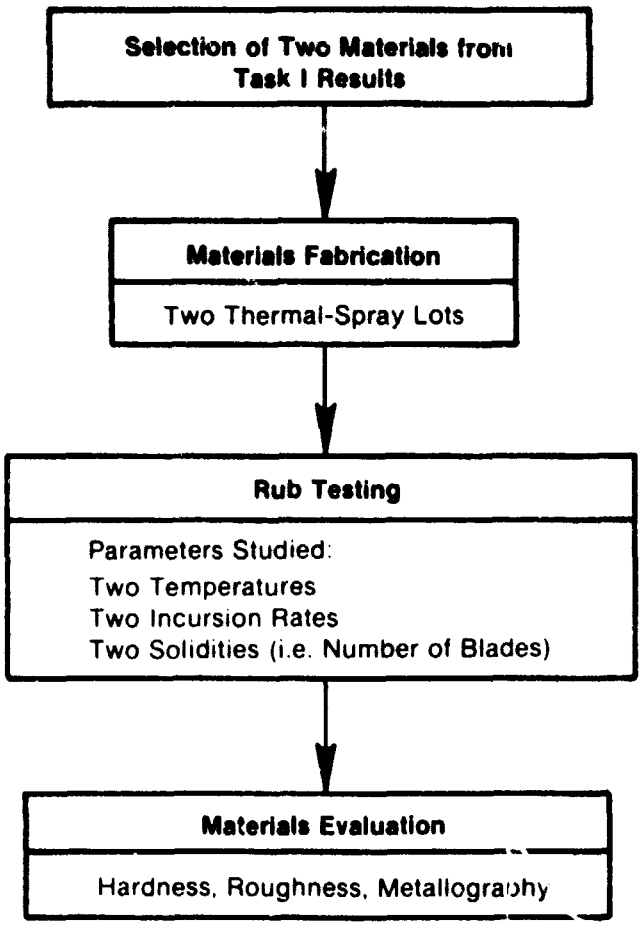

Figure 1. Test Program Flow Diagram (Continued).

Task III - Porous Aluminum Bronze Development

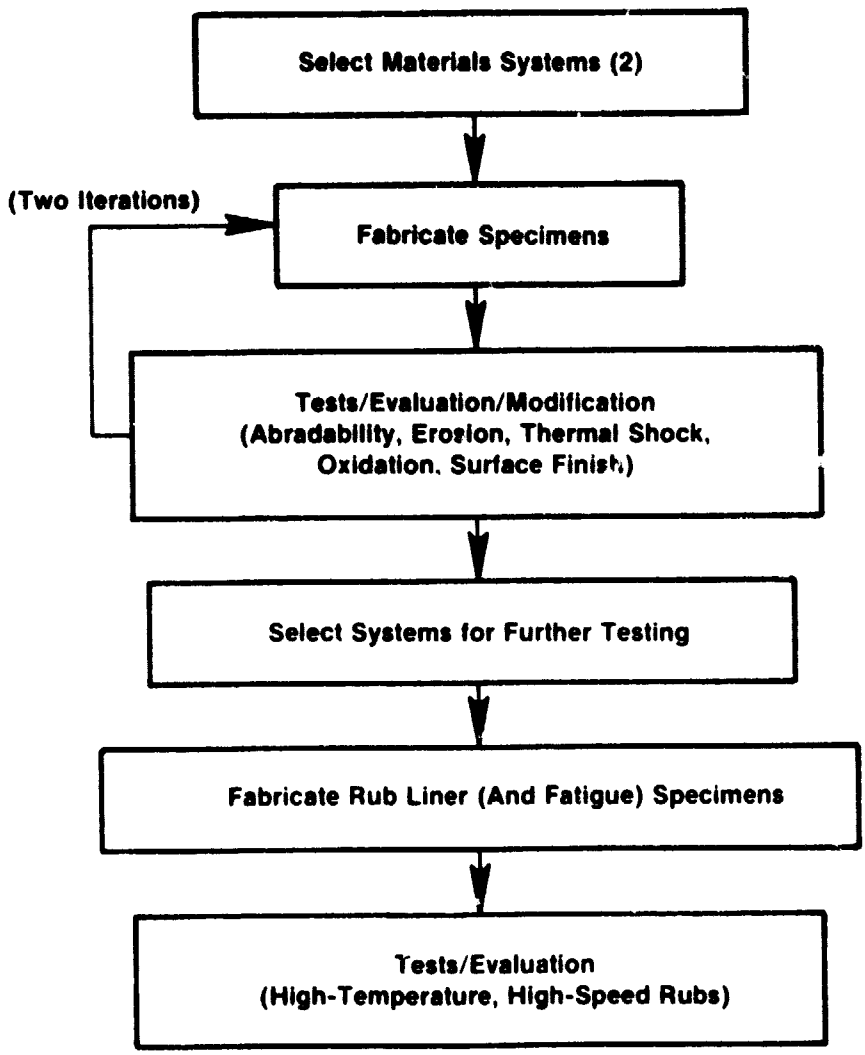

Figure 1. Test Program Flow Diagram (Concluded).

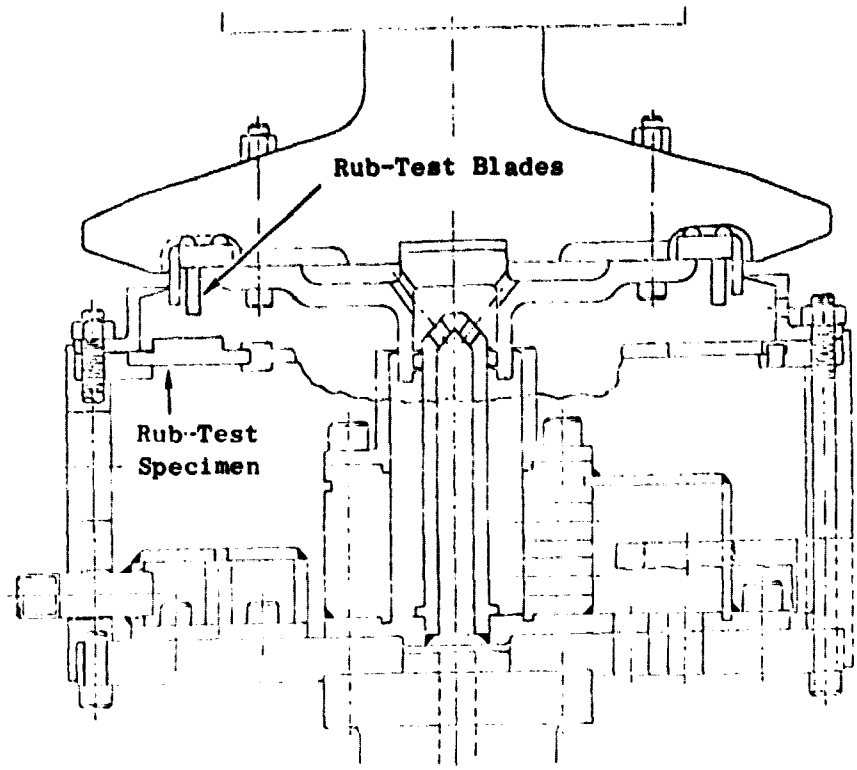

Figure 2. Schematic of the Rub-Test Rig Showing Blade and Stator Configuration.

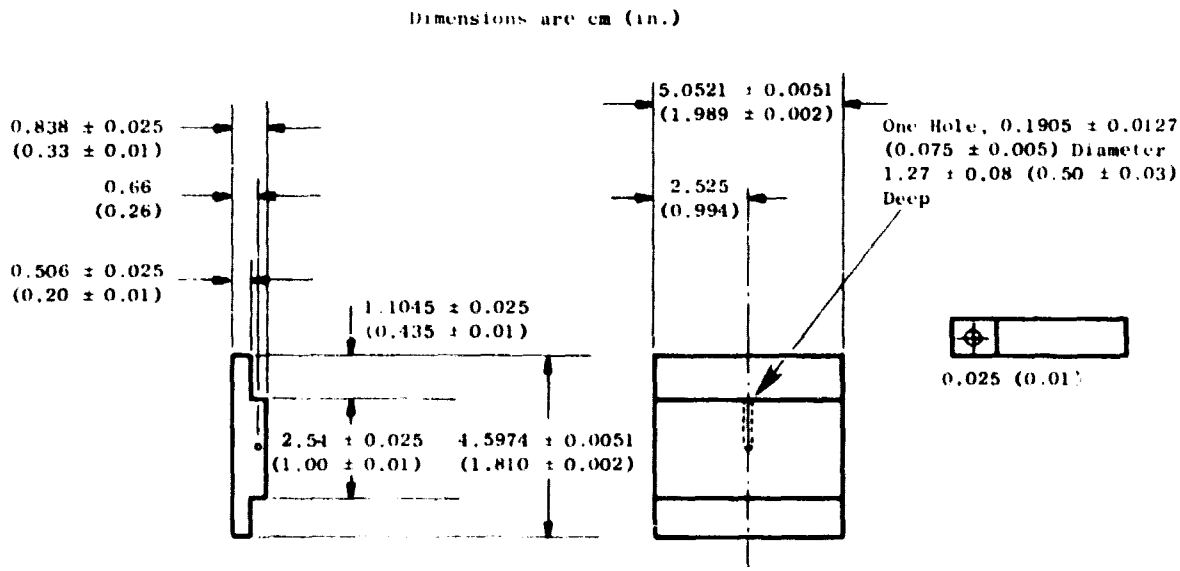

Figure 3. Rub-Test Specimens.

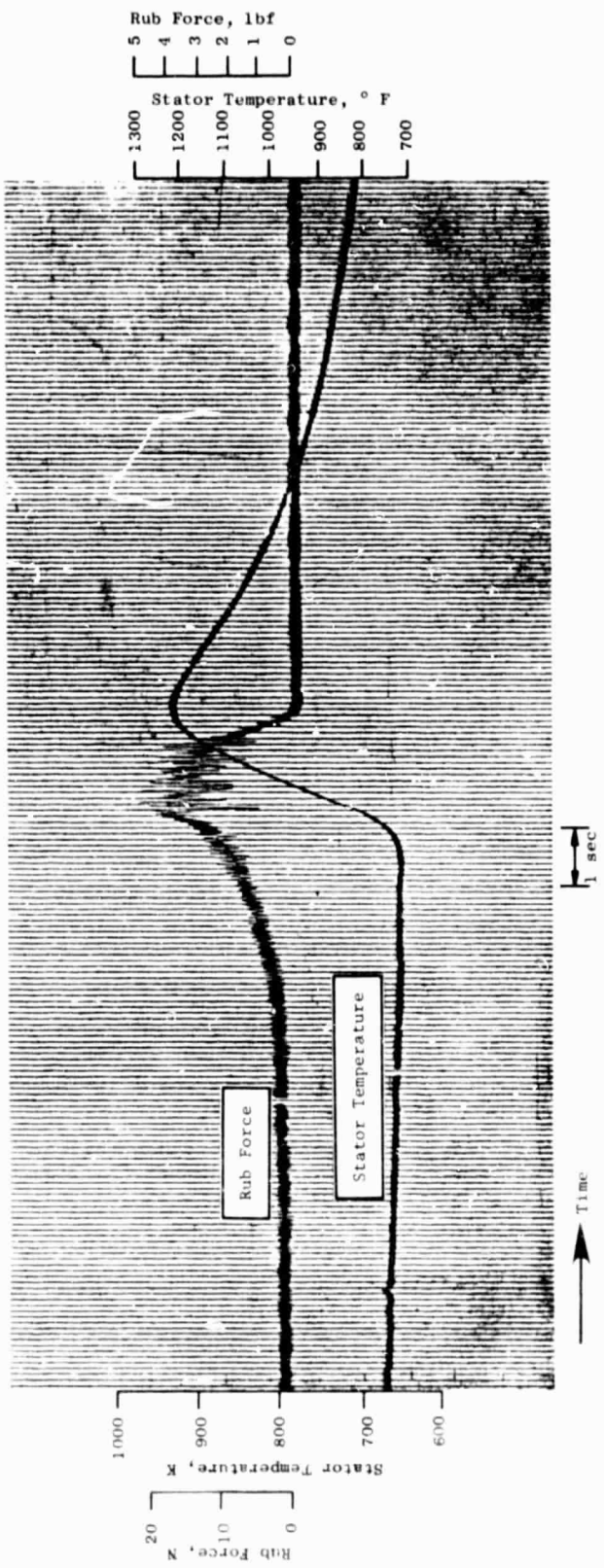

Figure 4. Strip Chart Trace of Test Specimen Temperature and Rub Force Vs. Time.

Analysis of blade rubbing requires dynamic consideration. Due to the heat generated at the blade tips during rubbing, there are probably competitive reactions such as work-hardening versus recrystallization. However, in the Lynn rub tester at blade tip speeds of 152 surface m/sec (500 ft/sec), a rub occurs every 2 msec, and recrystallization will not be kinetically favored unless the temperature is high enough for rapid lattice diffusion. Potential for recrystallization will be limited to a very thin, surface layer early in a rub but may extend a finite depth into the coating later in the rub. Specific parameters, such as depth of bite per blade and rub duration, will determine the extent that each competing interaction develops in a given rub.

Work-hardening will depend upon solute effects (lattice atomic size mismatch) and crystalline structure (number and efficiency of slip planes, cross-slip tendency, and stacking-fault energy). These parameters can be explored by varying alloy compositions while maintaining the same crystal structure and by studying materials with different crystal structures.

Considering the facts above, the following 10 materials were selected:

1. Al (FCC) - Aluminum is known to display easy shear when rubbed. It is a good reference material with a flow stress lower than Ti alloys.

2. Cu (FCC) - Copper provides higher working temperatures than aluminum although it will work-harden more due to lower stacking-fault energy. Copper also provides reference material for Cu-Al alloys.

3. Cu-5Al (FCC) - Aluminum addition adds oxidation resistance to copper, but it also reduces the stacking-fault energy (may increase work-hardening).

4. Cu-9Al (FCC) - This alloy, when sprayed as a mixture with nickel graphite, has shown good rub behavior with Ti-base blades. Stacking-fault energy is lower than Cu-5Al.

5. Cu-10Zn (FCC) - Zinc has a small mismatch effect on copper and should give additional information on alloying effects.

6. Ni-13Cr (FCC) - Ni-20Cr has been shown to wear Ti-base blades. The flow stress will be lowered by dropping the chromium content.

7. Zn (HCP) - Zinc is known to rub well and should be a good reference material for ideal rub behavior even though the low melting point makes it impractical for engine use.

8. Fe (BCC) - BCC crystals have more slip systems than FCC or HCP crystals, and iron (low in interstitial carbon and nitrogen) will have a relatively low flow stress even though the temperature capability is higher than that of the copper and aluminum alloys.

9. Fe-6Al (BCC) - Aluminum will add oxidation resistance to the iron while maintaining BCC structure.

10. Fe-13Cr-0.1Cb (BCC) - Chromium will add more oxidation resistance to the iron, and columbium will minimize carbide and nitride solute-hardening by forming columbium carbide and nitride precipitates.

Selected bulk properties, from the literature, of the 10 coating materials are compiled in Table I.

The surfaces of all rub-test panels were grit-blasted and thermally sprayed with a 0.1 to 0.2 mm (4 to 8 mil) bond coat of Metco 450 (nickel aluminide) to promote good adhesion of the 1.3 to 1.5 mm (0.050 to 0.060 in.) thick top coating. The as-sprayed coating densities were determined by water immersion (Table II). The low densities of the Fe-base alloys were due to porosity caused by incomplete particle melting during spraying. All coated panels were annealed prior to rub testing.

4.2.1.2 Dense-Coating Rub-Test Results

The rub parameters used for all the tests were:

Blade material:	Ti-6Al-4V
Number of blades:	48
Blade thickness:	0.635 mm (0.025 in.)
Incursion rate:	254 μm/sec (0.010 in./sec)
Incursion depth:	0.508 to 0.762 mm (0.020 to 0.030 in.)
Blade tip speed:	152 surface m/sec (500 ft/sec)
Ambient temperature:	310 and 755K (100 and 900° F)

The rub-test results are tabulated in Table III. Examination of the results revealed the following trends:

- All of the dense coatings with melting points greater than Al produced blade wear.

- Cu-base alloys caused more severe scabbing and blade wear than Fe- or Ni-base alloys during room-temperature tests. During elevated-temperature rubs, Cu-base alloys with Al additions showed a marked improvement in rub behavior. Cu-9Al coating was the most abradable (most coating wear) of all the materials with melting points greater than aluminum.

- For a given material, elevated-temperature rubs exhibited lower shear forces (rub energy) than those observed during room-temperature rubs, but the lower forces did not always result in proportionately reduced blade wear.

Table I. Bulk Properties of Phase I Coating Materials.

• Room temperature values unless otherwise stated

*Property	Al	Cu	Fe	Zn	Cu-10Zn	Cu-5Al	Cu-9Al	Fe-6Al	Fe-13Cr	Ni-13Cr	References
Atomic Composition, %	---	---	---	---	9.7Zn	11.0Al	18.9Al	11.7Al	13.9Cr	14.4Cr	1
Crystal Structure	FCC	FCC	BCC	HCP	FCC	FCC	FCC	BCC	BCC	FCC	2
Lattice Constant (A) a	4.049	3.615	2.866	2.665	3.635	3.661	3.664	2.883	2.871	3.563	
c	---	---	---	4.947	---	---	---	---	---	---	2
Melting Point, K (° F)	933 (1220)	1357 (1983)	1808 (2795)	692 (786)	1317 (1910)	1356 (1940)	1316 (1908)	1803 (2785)	1796 (2770)	1703 (2606)	3
Density, Mg/m^3	2.70	8.96	7.87	7.13	8.80	8.17	7.58	7.28(1)	7.77(1)	8.62(1)	4
Specific Heat, $kJ/kg*K^{-1}$ ($cal/g*^{-1}$)	0.900 (0.215)	0.385 (0.092)	0.460 (0.110)	0.385 (0.092)	0.377 (0.090)	0.414(2) (0.099)	0.435 (0.104)	0.417(3) (0.114)	0.460(2) (0.110)	0.435 (0.104)	4,5
Thermal Conductivity, $MW*m^{-3}/k$ ($cal*cm^{-3}/K*sec^{-1}$)	2.385 (0.570)	3.937 (0.941)	0.745 (0.178)	1.130 (0.270)	1.883 (0.450)	0.828 (0.198)	0.602 (0.144)	0.301 (0.072)	0.226(2) (0.054)	0.527(2) (0.138)	4,6
Thermal Expansion Coeff, $um/m*K^{-1}$	23.6	16.5	11.7	39.7	18.4	16.5	16.5	13.1	9.9(2)	13.5(2)	4,7
Young's Modulus, GPa (10^6 psi)	62 (9)	110 (16)	197 (28.5)	92 (13.4)	117 (17)	117 (17)	117 (17)	200 (29)	200 (29)	214 (31)	4,8,9
Shear Modulus, GPa (10^6 psi)	23 (3.4)	41 (6)	80 (11.6)	37 (5.4)	44 (6.4)	44 (6.4)	44 (6.4)	76 (11)	76 (11)	81 (11.7)	Calculated from 10
Tensile Strength (Annealed Condition), MPa (10^3 psi)	67 (6.8)	221 (32)	241 (35)	19 (2.8)	262 (38)	448 (65)	448 (65)	508 (73.7)	510 (74)	538 (78)	4,11,12,13
Yield Strength (Annealed Condition), MPa (10^3 psi)	12 (1.7)	69 (10)	103 (15)	2.4 (0.35)	83 (12)	172 (25)	172 (25)	412 (59.7)	303 (44)	276 (40)	4,11,12,13
Elongation, % (Annealed Condition)	35	45	40	---	50	55	40	25	25	30	4,11,12,13
Hardness, MN/m^2 Annealed	196	539	686	294	480	843	990	---	1410	1590	4,14
Hard	343	1225	1960	343	1400	1960	1960	3240	3920	2380	
Hot-Working Range, K (° F)	533-783 (500-950)	1033-1144 (1400-1600)	---	---	1033-1144 (1400-1600)	1089-1144 (1500-1600)	1033-1197 (1670-1695)	1478 (2200)	1478 (2200)	1478 (2200)	4,5,15,16
Recrystallization Temperature, K (° F)	561-589 (550-600)	572 (570)	475-575 (395-575)	283 (50)	644 (700)	622 (660)	867 (1100)	867 (1100)	---	---	4,12,17
Stacking-Fault Energy, mJ/m^2	200-238	40-70	---	---	36	4	2	---	---	---	11,18,19
Izod Impact Strength, J (ft-lbf)	---	41-54 (30-40)	---	---	41 (30)	---	14-20 (10-15)	---	---	---	

1. Calculated from lattice constants.
2. Estimated from Reference 4.
3. Estimated from rule of Dulong and Petit.

Table II. Densities of the Sprayed Coatings.

Material	Spray Technique	As-Sprayed Density
Al	Wire	90
Cu	Wire	86
Fe	Wire	80
Zn	Wire	90
Cu-10Zn	Wire	86
Cu-5Al	Plasma*	86
Cu-9Al	Plasma*	86
Fe-6Al	Plasma*	73
Fe-13Cr-0.1Cb	Plasma*	80
Ni-13Cr	Plasma*	82

*Powder Size: -140/+325 Mesh

- Substrate temperatures measured during rubs could be misleading, when making sample-to-sample comparisons, because of differences in rub-path lengths and depths caused by variances in scabbing and blade wear.

- The Phase I materials can be grouped into three basic categories based on rub behavior: (a) Al and Zn produced smooth rub paths and no blade wear; (b) Cu-base alloys (except for Cu-9Al hot rub) produced rough, scabbed, rub surfaces and blade wear; and (c) Fe- and Ni-base alloys produced blade wear but only light scabbing.

4.2.1.3 Coating Appearance and Microstructure

Al and Zn Coatings

1. The coatings were densified in areas beneath and adjacent to the rub path.

2. Heavy plastic deformation was obvious in both coatings. Subsurface flow lines were visible even without etching.

3. No blade metal was transferred to the coating surface.

Cu-base Coatings

1. The coatings were densified in areas beneath the rub path.

2. Significant amounts of blade metal transferred to the coating surface (scabbing).

3. Although the rub surfaces were oxidized, oxidation of the coating beneath the rub paths was minimal.

4. Cracking (probably thermal) was evident in the scabbed areas (Figure 5).

5. The blade tips were heavily burred on the edges; this is an indication of plastic deformation of the blades (Figure 6).

6. Reactions between the transferred blade metal and the coating were evident in the variety of phases present in the microstructure of the scabbed area (Figure 7). The reaction zones of Cu-5Al and Cu-9Al coatings were primarily at the edges and corner of the rub paths where scabbing usually initiated. Microprobe analysis normal to the surface and under the rub paths indicated that the phases ranged in composition from pure coating to pure blade metal. The Cu/Ti ratios in the intermediate regions were similar to that of the Cu-Ti eutectic. Exact phase identification was not attempted because the coating/blade-metal mixtures were quaternary alloys with unknown phase diagrams.

Table III. Phase I Rub-Test D

- Forty-Eight Ti-6Al-4V Blades, 0.635 mm (0.025 in.) t
- Incursion Rate: 0.254 mm/sec (0.010 in./sec)
- Incursion Depth: 0.508 mm (0.020 in.) to 0.762 mm (
- Blade Tip Speed: 152 Surface m/sec (500 ft/sec)

Coating	T_m, Melting Point, K	T_{Amb},(1) Ambient Temperature, K	T_{Max},(2) Maximum Temperature, K	ΔT,(3) K	$\frac{T_{Max}}{T_m}$	Maximum(4) Temperature-Rise Rate, K/sec	Minimum(5) Shear Force, N	Maximum(6) Shear Force, N	Maximum(7) Force-Rise Rate, N/sec	Aver Bl We m
Zn	629	311	400	89	0.61	52	---	<2.2	---	<0.
Al	931	297	611	314	0.66	---	7.1	10.2	6.2	<0.
Al	931	731	731	0	0.78	0	---	6.7	0.7	<0.
Cu*	1356	317	633	317	0.47	117	16.5	22.2	15.6	0.
Cu*	1356	694	831	136	0.61	53	1.8	4.3	4.1	0.
Fe*	1808	328	383	56	0.21	10	4.9	9.3	14.2	0.
Fe	1808	766	944	178	0.52	62	---	0.6	0.2	0.
Cu-5Al	1333	317	1039	722	0.78	150	18.2	32.0	64.1	1.
Cu-5Al	1333	766	894	128	0.67	50	4.9	6.2	10.7	0.
Cu-9Al	1316	317	1000	683	0.76	144	17.3	33.8	34.7	0.
Cu-9Al	1316	706	1022	317	0.78	83	9.3	14.7	23.6	0.
Cu-10Zn*	1317	333	456	122	0.34	49	14.2	22.7	34.7	0.
Cu-10Zn*	1317	744	936	192	0.71	88	---	2.8	1.8	0.
Fe-6Al*	1803	328	550	222	0.30	90	---	21.4	21.4	0.
Fe-6Al*	1803	772	914	142	0.51	100	---	2.6	0.1	0.
Fe-13Cr*	1794	328	533	205	0.30	96	---	12.5	16.5	0.
Fe-13Cr*	1794	811	972	161	0.54	78	---	2.2	1.6	0.
Ni-13Cr*	1703	322	364	42	0.21	7	---	10.7	10.2	0.
Ni-13Cr*	1703	719	786	67	0.46	16	---	5.8	2.2	0.

*Blade contacted only part of specimen surface

1. Temperature measured at the start of a test by a control thermocouple (T/C) embedded in the substrate 1.52 mm (0.06 in.)
2. Maximum temperature measured by control T/C during a test.
3. $T_{Max} - T_{Amb}$.
4. Maximum slope of the temperature/time trace of the control T/C during a test.
5. Lowest shear force recorded after the peak force was obtained.
6. Highest shear force recorded during test, usually occurring as a peak at the beginning of the test.
7. Maximum slope of the force/time trace during a test.
8. Average length change of three randomly selected blades.
9. Area under the force/time curve of a test multiplied by the velocity of the blades.
10. Rub energy divided by unit volume of coating removed.
11. Varied from 0.127 to -0.508 mm (0.005 to -0.020 in.).
12. Coating delaminated.

Phase I Rub-Test Data.

0.635 mm (0.025 in.) thick
(0.010 in./sec)
.020 in.) to 0.762 mm (0.030 in.)
m/sec (500 ft/sec)

(6) ,	Maximum(7) Force-Rise Rate, N/sec	Average(8) Blade Wear, mm	Average Depth of Rub, mm	Coating Hardness R_{15Y}	Rub-Surface Roughness rms, μm	Rub(9) Energy, kJ	E/V,(10) J/m^3	Rub-Surface Appearance
	---	<0.025	-0.762	84	1.02-1.14	---	---	Smooth
	6.2	<0.025	-0.914	89	1.27-1.52	3.701	3.38	Smooth
	0.7	<0.025	-0.787	---	---	0.968	0.99	Smooth
	15.6	0.965	0.152	88	>7.62	11.762	---	Heavily Scabbed
	4.1	0.660	0.178	85	3.30	1.396	---	Heavily Scabbed
	14.2	0.508	0.076	94	1.27	2.068	---	Lightly Scabbed
	0.2	0.635	-0.203	94	>7.62	0.141	0.58	Lightly Scabbed
	64.1	1.194	0.432	91	>7.62	10.442	---	Heavily Scabbed
	10.7	0.559	-0.406	91	>7.62	2.203	4.51	Moderately Scabbed
	34.7	0.660	Note 11	94	>7.62	10.548	1.72	Moderately Grooved and Scabbed
	23.6	0.356	-0.711	81	1.91	7.240	0.85	Lightly Grooved and Scabbed
	34.7	0.559	0.203	93	1.65	2.329	---	Heavily Scabbed
	1.8	0.660	0	82	3.05	1.171	---	Heavily Scabbed
	21.4	0.457	-0.178	90	>7.62	3.676	17.15	Lightly Scabbed
	0.1	0.279	-0.178	82	2.03	0.639	2.98	Lightly Scabbed
	16.5	0.483	-0.127	---	---	2.800	18.40	Lightly Scabbed
	1.6	0.483	-0.203	92	2.03-2.29	0.449	1.84	Lightly Scabbed
	10.2	0.381	Note 12	---	---	2.904	---	Lightly Scabbed
	2.2	0.330	0.178	---	3.05	1.960	---	Lightly Scabbed

rate 1.52 mm (0.06 in.) below the rub coating.

t.

FOLDOUT FRAME 2

Table III. Phase I Rub-Test D

- Forty-Eight Ti-6Al-4V Blades, 0.635 mm (0.025
- Incursion Rate: 0.254 mm/sec (0.010 in./sec)
- Incursion Depth: 0.508 mm (0.020 in.) to 0.7
- Blade Tip Speed: 152 Surface m/sec (500 ft/se

Coating	T_m, Melting Point, °F	T_{Amb},(1) Ambient Temperature, °F	T_{Max},(2) Maximum Temperature, °F	ΔT,(3) °F	$\frac{T_{Max}}{T_m}$	Maximum(4) Temperature-Rise Rate, °F/sec	Minimum(5) Shear Force, lbf	Maximum(6) Shear Force, lbf	Maximum(7) Force-Rise Rate, lbf/sec
Zn	727	100	260	160	93	93	---	<0.5	---
Al	1215	75	640	565	---	---	1.6	2.3	1.4
Al	1215	855	855	0	0	0	---	1.5	0.16
Cu*	1980	110	680	570	210	210	3.7	5.0	3.5
Cu*	1980	790	1035	245	96	96	0.4	0.96	0.92
Fe*	2795	130	230	100	18.5	18.5	1.1	2.1	3.2
Fe	2795	920	1240	320	112	112	---	0.13	0.04
Cu-5Al	1940	110	1410	1300	270	270	4.1	7.2	14.4
Cu-5Al	1940	920	1150	230	90.5	90.5	1.1	1.4	2.4
Cu-9Al	1908	110	1340	1230	260	260	3.9	7.6	7.8
Cu-9Al	1908	810	1380	570	150	150	2.1	3.3	5.3
Cu-10Zn*	1910	140	360	220	88.5	88.5	3.2	5.1	7.8
Cu-10Zn*	1910	880	1225	345	158	158	---	0.64	0.4
Fe-6Al*	2785	130	530	400	162	162	---	4.8	4.8
Fe-6Al*	2785	930	1185	255	180	180	---	0.58	0.015
Fe-13Cr*	2770	130	500	370	172	172	---	2.8	3.7
Fe-13Cr*	2770	1000	1290	290	141	141	---	0.5	0.36
Ni-13Cr*	2606	120	195	75	13	13	---	2.4	2.3
Ni-13Cr*	2606	835	955	120	28.5	28.5	---	1.3	0.49

*Blade contacted only part of specimen surface

1. Temperature measured at the start of a test by a control thermocouple (T/C) embedded in the substrate 1.52 mm (0.
2. Maximum temperature measured by control T/C during a test.
3. $T_{Max} - T_{Amb}$.
4. Maximum slope of the temperature/time trace of the control T/C during a test.
5. Lowest shear force recorded after the peak force was obtained.
6. Highest shear force recorded during test, usually occurring as a peak at the beginning of the test.
7. Maximum slope of the force/time trace during a test.
8. Average length change of three randomly selected blades.
9. Area under the force/time curve of a test multiplied by the velocity of the blades.
10. Rub energy divided by unit volume of coating removed.
11. Varied from 0.127 to -0.508 mm (0.005 to -0.020 in.).
12. Coating delaminated.

se I Rub-Test Data. (Concluded)

, 0.635 mm (0.025 in.) thick
c (0.010 in./sec)
(0.020 in.) to 0.762 mm (0.030 in.)
e m/sec (500 ft/sec)

mm(6) ar ce, f	Maximum(7) Force-Rise Rate, lbf/sec	Average(8) Blade Wear, in.	Average Depth of Rub, in.	Coating Hardness R_{15Y}	Rub-Surface Roughness rms, μin.	Rub(9) Energy, ft-lbf (Btu)	E/V,(10) ft-lbf/in.^{3}	Rub-Surface Appearance
.5	---	<0.001	-0.030	84	40-45	---	---	Smooth
.3	1.4	<0.001	-0.036	89	50-60	2730 (3.49)	152,000	Smooth
.5	0.16	<0.001	-0.031	---	---	714 (0.914)	44,600	Smooth
.0	3.5	0.038	0.006	88	>300	8675 (11.1)	---	Heavily Scabbed
.96	0.92	0.026	0.007	85	130	1030 (1.32)	---	Heavily Scabbed
.1	3.2	0.020	0.003	94	50	1525 (1.95)	---	Lightly Scabbed
.13	0.04	0.025	-0.008	94	>300	104 (0.133)	26,000	Lightly Scabbed
.2	14.4	0.047	0.017	91	>300	7702 (9.85)	---	Heavily Scabbed
.4	2.4	0.022	-0.016	91	>300	1625 (2.08)	203,000	Moderately Scabbed
.6	7.8	0.026	Note 11	94	>300	7780 (9.96)	77,600	Moderately Grooved and Scabbed
.3	5.3	0.014	-0.028	81	75	5340 (6.83)	38,100	Lightly Grooved and Scabbed
.1	7.8	0.022	0.008	93	65	1719 (2.2)	---	Heavily Scabbed
.64	0.4	0.026	0	82	120	864 (1.10)	---	Heavily Scabbed
.8	4.8	0.018	-0.007	90	>300	2711 (3.47)	772,000	Lightly Scabbed
.58	0.015	0.011	-0.007	82	80	471 (0.603)	134,000	Lightly Scabbed
.8	3.7	0.019	-0.005	---	---	2065 (2.64)	828,000	Lightly Scabbed
.5	0.36	0.019	-0.008	92	80-90	331 (0.425)	82,800	Lightly Scabbed
.4	2.3	0.015	Note 12	---	---	2142 (2.74)	---	Lightly Scabbed
.3	0.49	0.013	0.007	---	120	1446 (1.85)	---	Lightly Scabbed

strate 1.52 mm (0.06 in.) below the rub coating.

est.

FOLDOUT FRAME 2

Figure 5. Thermal Cracking in Scabbed Area of Cu Coating After Cold Rub. 10X

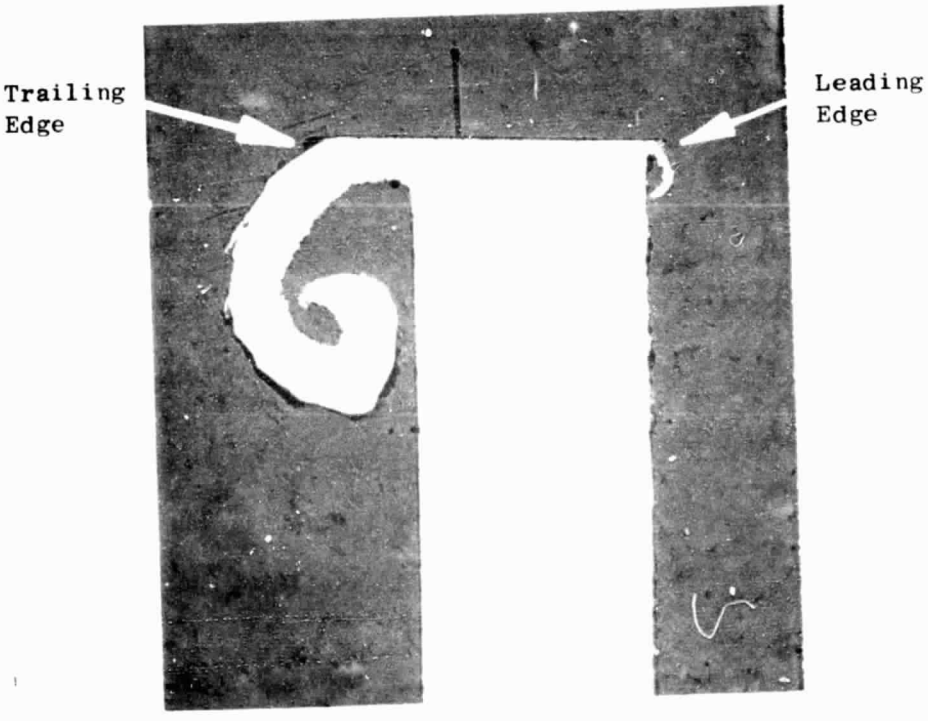

Figure 6. Burring of Ti-6Al-4V Blade Used for Cold Rub of Cu. 50X

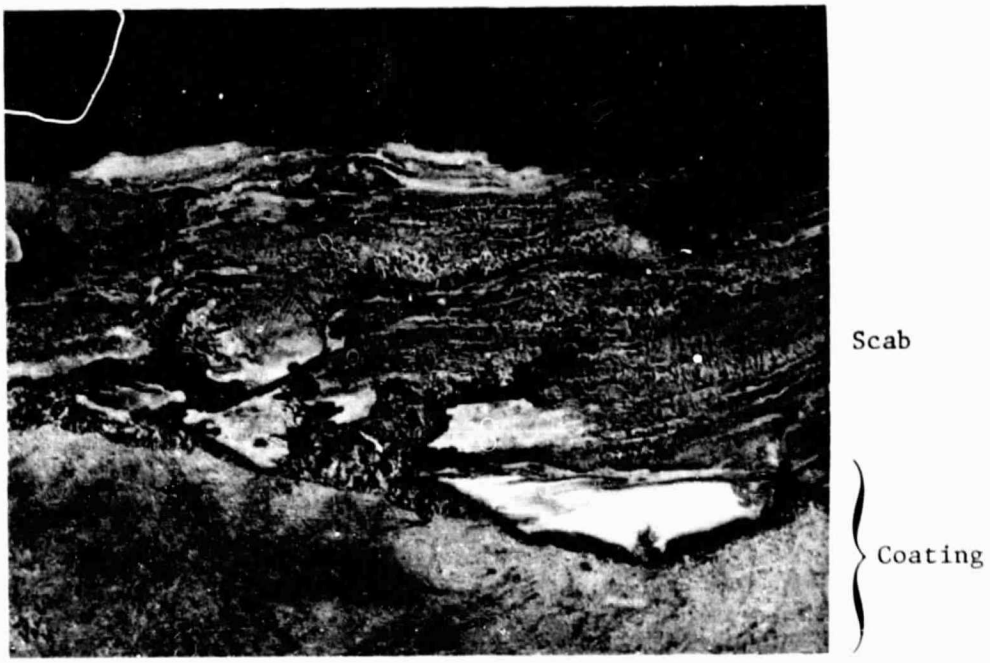

Figure 7. Microstructure of Cu Coating (Hot Rub) in a Scabbed Area Showing the Variety of Phases Present. 100X

7. The as-sprayed and annealed coatings had lamellar structures typical of thermally sprayed materials. After rubbing, the Cu-5Al coating showed evidence of recrystallization and twinning, but the lamellar structure was still present (Figure 8). The lamellar structure was absent in the Cu-9Al coating after rubbing (Figure 9). The grain size of the coating was smaller and more uniform than the Cu-5Al coating; this indicates that extensive cold-working and recrystallization had occurred during the rub.

Fe and Ni-base Coatings

1. The coatings were densified beneath the rub paths.

2. Only light scabbing was evident.

3. Cracking (probably thermal) of the coatings occurred perpendicular to the rub direction (Figure 10).

4. The blade tips were burred - indicating plastic deformation during the rub (Figure 11).

5. Reaction zones in the coatings were similar to, but less extensive than, those of the Cu-base coatings. As with the Cu-base alloy, microprobe examination revealed that the Fe/Ti ratios in the intermediate regions were close to that of the Fe-Ti eutectic.

4.2.1.4 Blade Microstructures

EDAX (Energy Dispersive X-ray) analysis in the scanning electron microscope (SEM) of blade tips from the Cu, Cu-10Zn, Cu-9Al, and Fe rubs indicated that, for the Cu-9Al and Fe rubs, significant coating material was transferred to the blade tip; the blades rubbed against Cu and Cu-10Zn were clean.

All blade tips, except those from the Zn and Al (hot) rubs, contain martensite. This indicates that the temperatures of the tips exceeded the β-transus temperature of Ti-6Al-4V = 1278 K (1840° F) during the rubs. When this occurs, the yield strength of the titanium alloy is drastically reduced, and blades wear more. A typical etched blade tip is shown in Figure 12. The extent of the martensitic zones was readily determined by optical microscopy, and measurements of the linear depth of martensitic transformation in the blade tips (in the direction perpendicular to the rub surface) are compiled in Table IV. As shown in the table, the blade tips from Cu-9Al rubs exhibit martensite zones that are significantly smaller than the zones associated with rubs of any of the other Cu-, Fe-, or Ni-base coatings. Assuming that the martensitic-zone size will be proportional to the highest temperature attained at the blade-tip/rub-surface interface during a rub, the Cu-9Al coating appears to be producing lower rub temperatures.

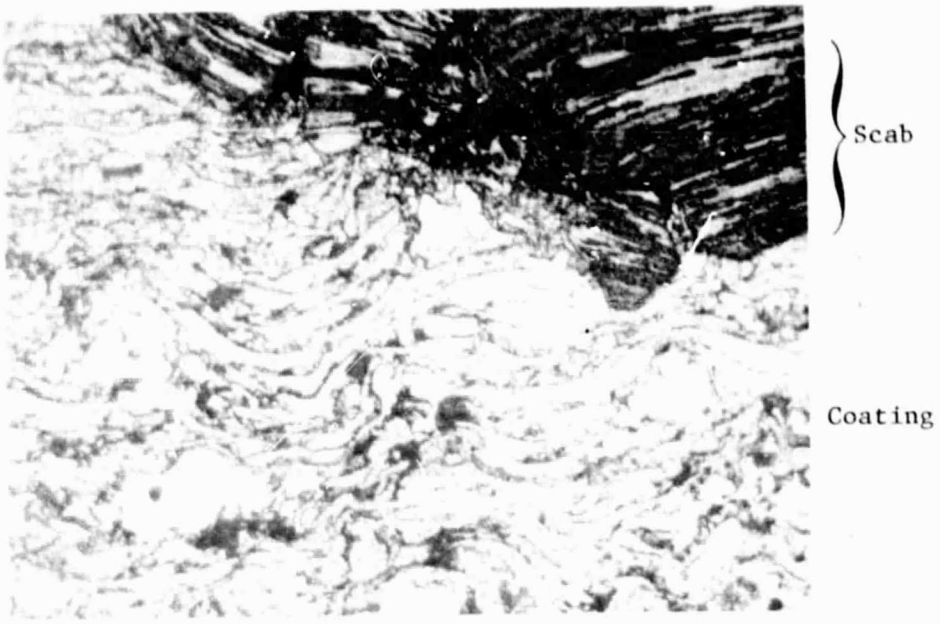

Figure 8. Microstructure of Cu-5Al Coating (Hot Rub) in Scabbed Area Showing the Lamellar Nature of the Coating and the Scab. 250X

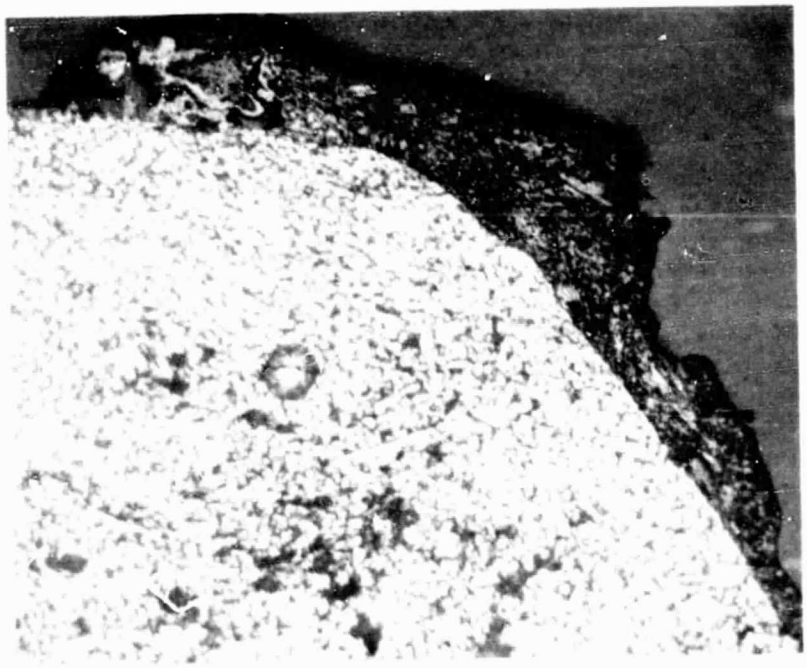

Figure 9. Microstructure of Cu-9Al (Hot Rub) Near Edge of Rub Path Showing a Light Scab and the Nonlamellar Nature of the Coating. 250X

a. Fe-13Cr

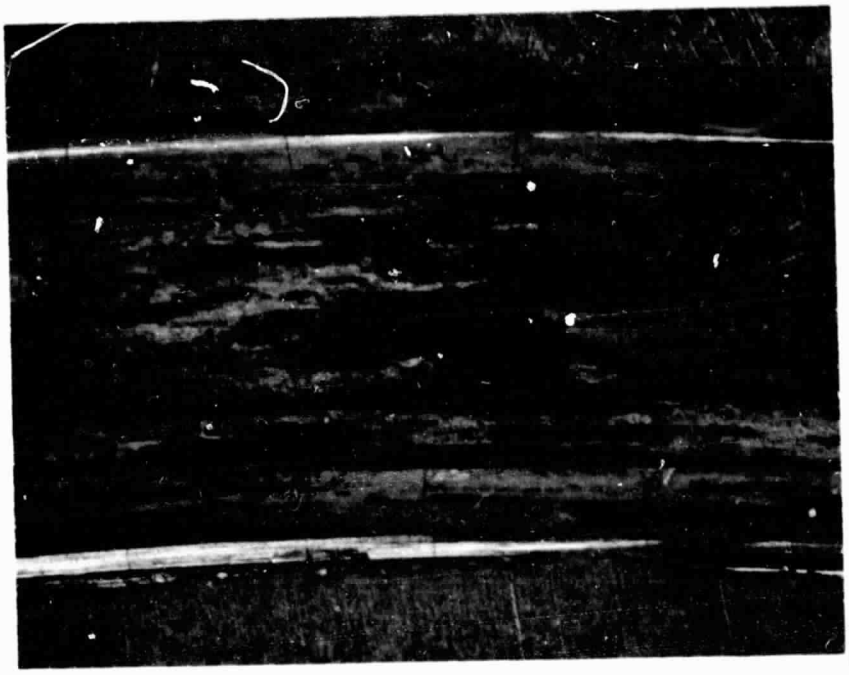

b. Ni-13Cr

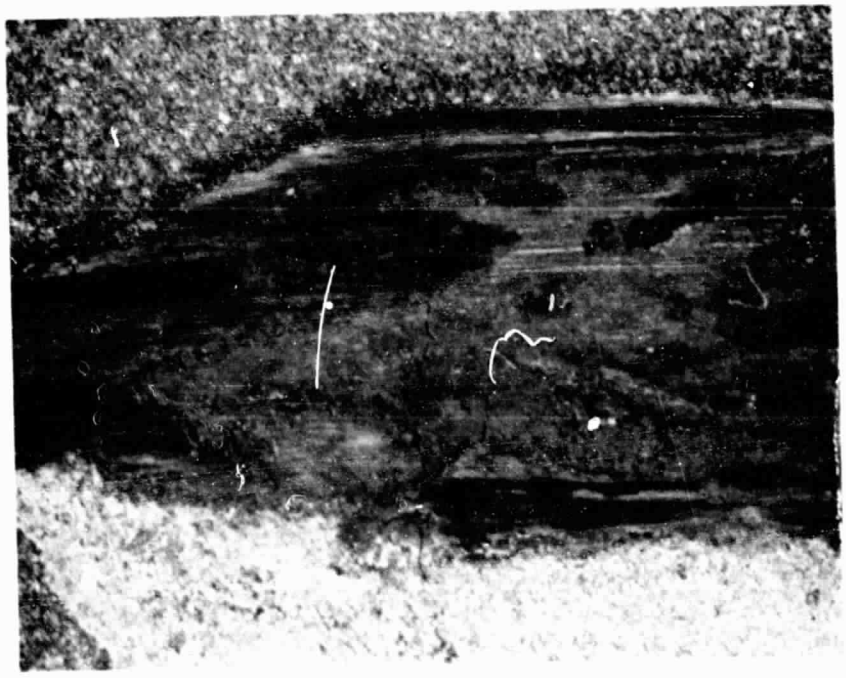

Figure 10. Thermal Cracking, Perpendicular to Rub Direction, of Fe-13Cr and Ni-13Cr Cold Rubs.

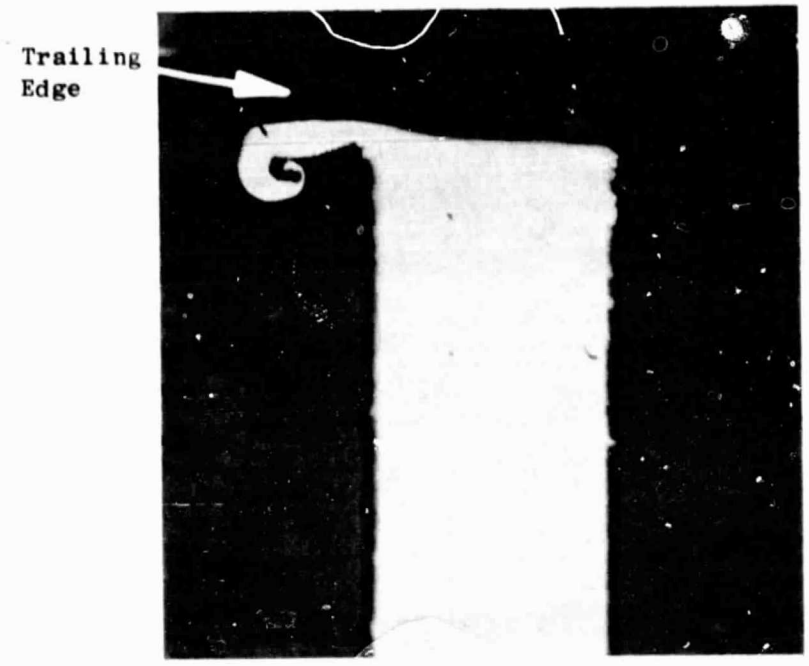

Figure 11. Burring in a Ti-6Al-4V Blade used in Fe Cold Rub (Typical of Fe- and Ni-Based Coatings. 10X

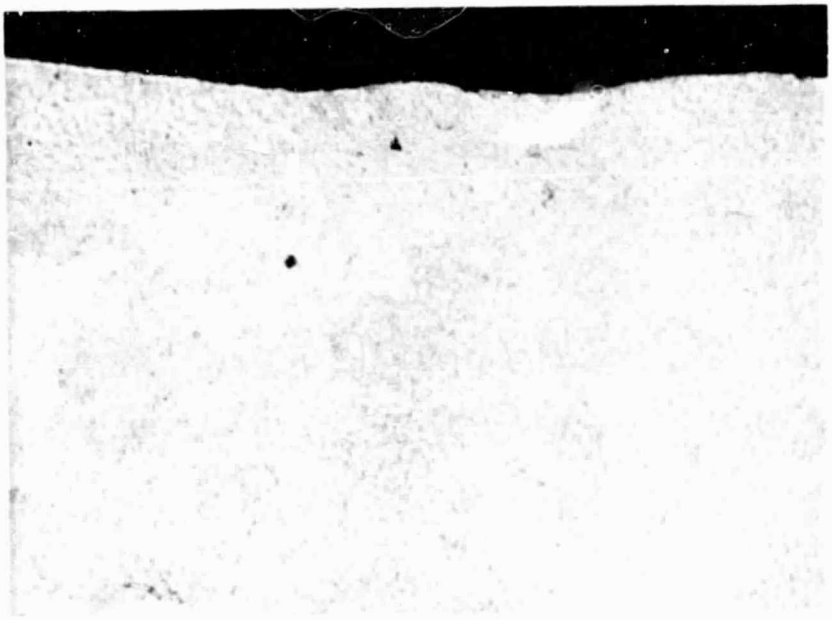

Figure 12. Structure of Ti-6Al-4V Blade Tip, from Room-Temperature Rub of Fe Coating, Showing Complete Transformation to Martensite. 250X

Table IV. Martensitic Transformation Depths.

Rub Coating	Ambient Test Temperature	Depth of Martensitic Zone at Blade Tip, mm	
		Min.	Max.
Zn	Room Temperature	0	0
Al	Room Temperature	0	<0.1
Al	Hot	0	0
Cu	Room Temperature	0.5	0.6
Cu	Hot	1.0	1.2
Fe	Room Temperature	0.7	0.8
Fe	Hot	1.3	1.4
Cu-5Al	Room Temperature	0.6	1.1
Cu-5Al	Hot	0.4	0.9
Cu-9Al	Room Temperature	0	0.3
Cu-9Al	Hot	0	0.4
Cu-10Zn	Room Temperature	0.3	0.6
Cu-10Zn	Hot	0.5	0.9
Fe-6Al	Room Temperature	0.8	0.9
Fe-6Al	Hot	1.1	1.2
Fe-13Cr	Room Temperature	0.8	1.1
Fe-13Cr	Hot	1.5	1.7
Ni-13Cr	Room Temperature	0.2	0.3
Ni-13Cr	Hot	1.4	1.6

Table IV shows that for all coatings except Al and Cu-5Al there is a clear increase in martensitic-zone size (blade-tip temperature) as the ambient test temperature is increased. Phase I rub-test data (Table III) showed that, for a given material, as the ambient test temperature was increased the rub energy decreased. A comparison of data from Tables III and IV leads to the conclusion that, in most cases, the reduction in rub energy with increased temperature (ambient test or blade tip) may merely be a reflection of the general inverse flow-stress/temperature relationship of most materials. In the case of the weaker coatings (Al and Zn), the flow stress of the coatings would be expected to drop more rapidly with temperature than the flow stresses of the Ti-6Al-4V blades. In the case of the stronger coatings (Cu-, Fe-, and Ni-base), the extreme temperature sensitivity of the flow stress of Ti-6Al-4V at temperatures above 811 K (1000° F) may be the dominant factor. This general type of behavior would explain why low-energy rubs cannot always be expected to produce low blade wear. Unfortunately, improved rub coatings cannot be identified on the basis of elevated-temperature mechanical properties alone since it has become evident that, in many cases, metallurgical reactions can occur during rubs.

4.2.1.5 Property Considerations

Property differences between Cu and Cu-Al alloys have been examined in an effort to identify key features which might account for the improvement in rub behavior produced by Al additions to Cu. Selected properties of the Phase I materials are compiled in Table I. As shown in the table, the primary property differences between Cu and Cu-Al alloys occur for melting point, thermal conductivity, tensile and yield strengths, hardness, recrystallization temperature, stacking-fault energy, and impact strength. It should be noted that the bulk-material properties will apply to spray-coating materials on a microscopic basis, but on a macroscopic basis coating properties such as tensile strength, hardness, and thermal conductivity will be lower than bulk properties due to the lamellar structure and porosity associated with spray coatings.

Possible effects of the property differences on the rub behavior of coatings are discussed below:

Thermal Conductivity, Melting Point - The lower thermal conductivities of the Cu-Al alloys as compared to pure copper would be expected to produce hotter rubs due to the decreased ability of the coatings to conduct frictionally generated heat away from the rub paths. The rub and microstructural data showed that temperatures reached by Cu-Al coatings and substrates directly beneath the rub paths were higher than those reached by Cu coatings, but temperatures reached by blade tips during rubs (martensitic-zone size) indicated that the actual rub surfaces of the coatings may have been hotter than the rub surfaces of the Cu-Al coatings. These data are consistent because the Cu coatings would be able to conduct more heat away from the rub path in lateral directions, thus, resulting in lower temperatures directly beneath the rub path.

There has been some evidence that high-speed, sliding contact between two materials may result in the formation of a thin molten layer at the rub interface; this could act as a lubricant to reduce the friction coefficient and subsequent wear damage (Reference 20). If this phenomenon had occurred during the rub tests, the temperatures reached by blade tips would have been proportional to the melting points of the coating materials. Blade-tip temperatures (as indicated by martensitic-zone size) reached during rubs of Cu, Cu-5Al, and Cu-9Al coatings were of the same order as the melting points of the coatings (Table V). Examination of the blade tips and coatings revealed that some melting had taken place (complicated by eutectic reactions). However, Cu-10Zn, which has the same melting point as Cu-9Al and a lower thermal conductivity than Cu, did not show any significant improvement over Cu when rubbed; this indicates that the improved rub behavior of Cu-Al alloys cannot be attributed solely to melting-point and thermal-conductivity differences.

Tensile Strength, Yield Strength, Hardness - The higher tensile and yield strengths and hardnesses of the Cu-Al alloys show that these materials are stronger and more difficult to plastically deform than Cu. Because of the higher strengths, Cu-Al alloys would be expected to require more force (energy) for deformation, and rub-force (shear) data from Phase I tests show that

higher forces were generated during rubs of Cu-Al alloys. However, Cu rubs caused more blade wear than Cu-9Al rubs, indicating that mechnical strength differences cannot account for the improved rub behavior of Cu-Al alloys.

Table V. Melting-Point/Martensitic-Depth Relationships.

Coating	Coating Melting Point, K (° F)	Martensite Depth In Blade Tips, mm
Cu	1357 (1983)	1.0 to 1.2
Cu-5Al	1333 (1940)	0.4 to 0.9
Cu-9Al	1315 (1908)	0.0 to 0.4

Recrystallization Temperature Stacking-Fault Energy - The recrystallization temperatures and stacking-fault energies of Cu and Cu-Al alloys are significantly different. However, the combined effects of these properties (along with recrystallization, work-hardening, and recovery rates) result in good hot-working characteristics and hot-working temperature ranges, 1033 to 1200 K (1400 to 1700° F), that are similar for Cu and Cu-Al alloys. This indicates that general hot-working characteristics are not obvious causes of the observed differences in rub behavior.

Impact Strength - Impact strength is the only mechanical property examined that indicates Cu-Al coatings should behave differently than either Cu or Cu-10Zn coatings. As shown in Table I, the impact strengths of Cu and Cu-10Zn are approximately 2 to 3 times as large as the impact strength of Cu-9Al (at room temperature). Since impact testing imposes high strain rates (10^3/sec) on materials and rub-test blades "impact" a coating at high speeds, it is possible that the response of a dense coating to shock loading may be an important factor in rub behavior.

In Summary - Examination of the rub test, metallographic, and physical-property data from Phase I materials revealed no obvious key features for abradable, high-melting-point materials although Al additions to Cu improved the rub behavior of dense, spray coatings.

R.C. Bill has proposed a "Figure of Merit" to rank rub performance of materials based on the adiabatic heating of seal materials by rub-induced deformation until hot-working temperature range is reached:

Figure of Merit = (Tensile Strength) • (Elongation) • ρCp • $(T_{hw} - T_{amb})$

where:

ρ = density
Cp = specific heat
T_{hw} = hot-working temperature
T_{amb} = ambient temperature

The "Figure of Merit" was calculated for each of the coatings, using the properties listed in Table I, and plotted against a rub performance factor (coating wear minus blade wear) for each test in Figure 13. It appears that the rub performances of the materials do show some correlation with the "Figure of Merit," but different wear mechanisms are indicated depending on the degree of abradability/abrasiveness of the coating.

Several areas which warrant further attention have been identified:

1. The apparent ability of Al additions to Cu to reduce Cu-Ti eutectic reactions during rubs.

2. The potential for easy plastic deformation of near-eutectoid Cu-Al alloys.

3. The potential for surface melting/lubrication during rubs.

4. The role of impact behavior on the response of a material to high-velocity rubs.

5. "Figure of Merit"/rub-performance correlations which include the blade material properties and heat partitioning between coating and blade.

4.2.2 Phase II - Current Compressor-Clearance Coatings

4.2.2.1 Material Selection and Preparation

There are two major types of compressor-clearance coatings currently in use: (a) the easily plastically deformed coatings and (b) the low-cohesive-strength coatings. Table VI lists the coatings used for Phase II rub testing. Plasma-sprayed Al was chosen as an example of a plastically deformable coating currently in use. The low-cohesive-strength coatings were chosen to cover a wide range of abradability among the current compressor coatings.

The Feltmetal underlayer was added to some of the Phase I coatings in order to study the effect of a compliant layer underneath the rub coatings. The Feltmetal pad has low thermal conductivity due to high porosity, and the effect of this on the rub of the coatings was also to be assessed.

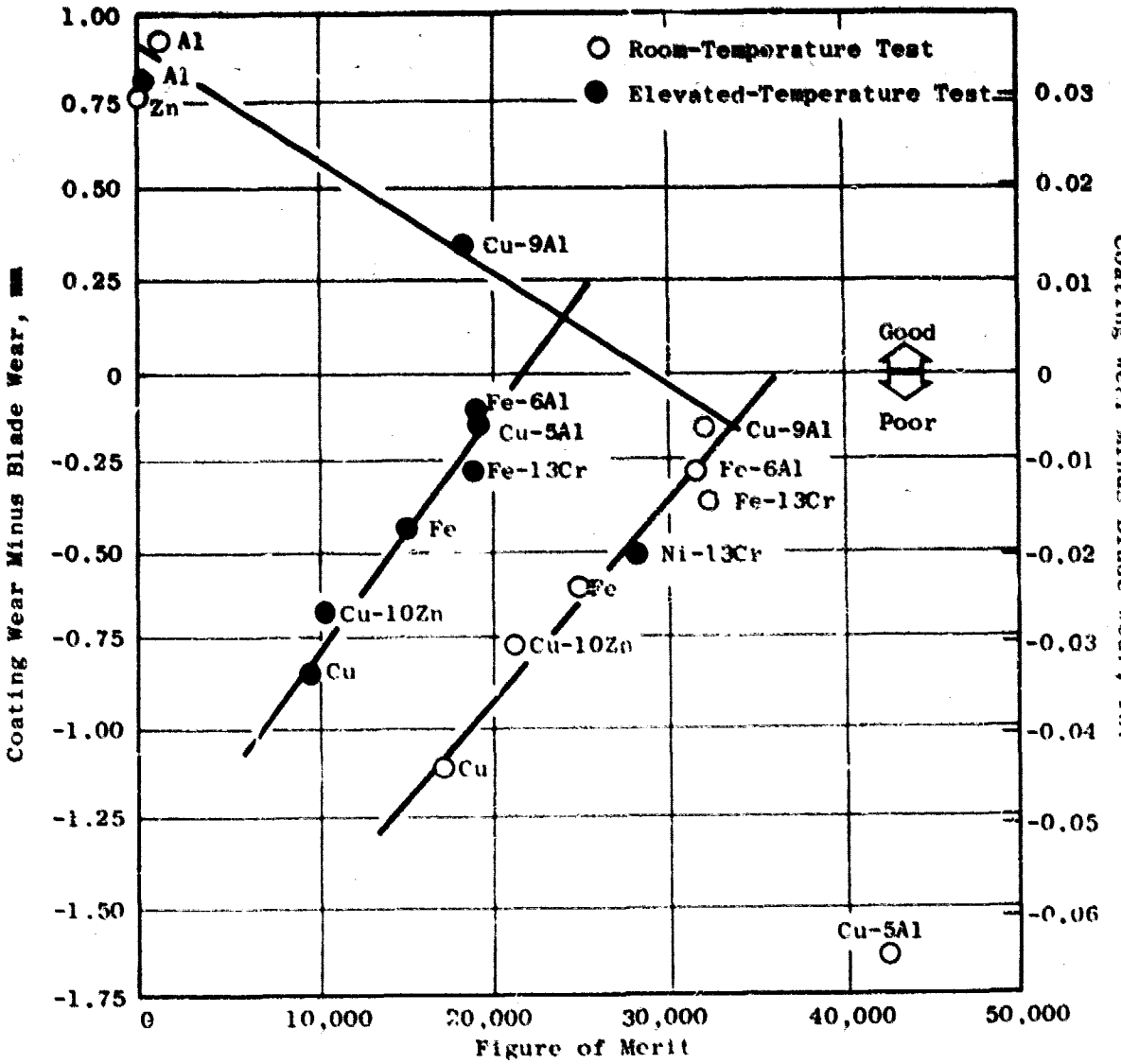

Figure 13. Rub Performance Versus "Figure of Merit."

4.2.2.2 Rub-Test Results

The results of the rub tests of Phase II coatings are presented in Table VII. Only two materials, AlBr/NiCg and 80/20 NiCg, caused blade wear. Microstructural examination of these coatings revealed that the rub surfaces of the samples which caused blade wear were compacted to various degrees during the rubs (Figures 14 and 15). The 80/20 NiCg cold-rub specimen which did not wear blades did not have a compacted surface. Some surface compaction also occurred in Feltmetal 515B specimens (Figure 16); however, the compaction was less than that observed for AlBr/NiCg and 80/20 NiCg specimens, and the FM 515B specimens did not wear blades.

Table VI. Phase II Rub-Test Coatings.

Plastically Deformable Coatings	
• Al (Dense, Plasma Sprayed)	
Low-Cohesive-Strength, Abradable Coatings	
• Metco 601	Porous, Thermal Sprayed
• Aluminum Bronze/Nickel Graphite (AlBr/NiCg)	Porous, Thermal Sprayed
• 80/20 Nickel Graphite (NiCg)	Porous, Thermal Sprayed
• AB-1	Porous, Sintered
• Feltmetal 515B	Porous, Sintered
Modified Phase I Coatings	
• Plasma-Sprayed Al Over Feltmetal	
• Plasma-Sprayed AlBr Over Feltmetal	

The lowest rub forces were observed for the Metco 601, AB-1, and Al/Feltmetal rubs. The highest rub forces were produced during AlBr/NiCg and 80/20 NiCg rubs where blade wear occurred, but the force associated with the cold Al rubs, which did not wear blades, was also high. The rub energies calculated from the rub-force/time curves appear to support the Phase I observation that rub-force/energy and blade wear do not correlate with respect to different materials. Even when rub energy has been adjusted on a unit-volume basis (last column of Table VII), there are no obvious trends to the blade wear and rub-energy data except that the denser Phase II materials (Al, AlBr/NiCg, and 80/20 NiCg) cause higher rub force and energy generation in most cases.

The AlBr/NiCg and 80/20 NiCg specimens were the only materials that produced significant substrate temperature rises during both hot and cold rubs. Heat discoloration on the surfaces of these samples was quite obvious. Discoloration also indicated that the rub surfaces of the FM 515B and AlBr/

Table VII. Phase II Rub-Test D

- Forty-Eight Ti-6Al-4V Blades, 0.635 mm (0.025 i
- Incursion Rate: 0.254 mm/sec (0.010 in./sec)
- Incursion Depth: 0.508 mm (0.020 in.) to 0.762
- Blade Tip Speed: 152 Surface m/sec (500 ft/sec

Coating	T_{Amb}, K	T_{Max}, K	ΔT, K	Maximum Temperature-Rise Rate, K/sec	Maximum Shear Force, N	Maximum Force-Rise Rate, N/sec	Average Depth of Rub, mm	Average Blade Wear, mm	Coati Hardn R_{15Y}
Al	319	561	242	110.0	14.7	13.92	0.686	<0.025	73
Al	728	783	56	24.7	4.4	1.01	0.711	<0.025	73
Metco 601	311	381	69	24.4	1.8	1.51	0.940	<0.025	56
Metco 601	756	756	0	---	<1.1	---	0.914	<0.025	55
AlBr/NiCg	311	742	431	166.7	17.8	25.35	0.737	0.102	74
AlBr/NiCg	756	964	208	97.2	8.0	10.36	0.584	0.152	72
80/20 NiCg	322	617	294	119.4	12.0	7.83	0.660	<0.025	57
80/20 NiCg	769	978	208	161.1	18.7	19.13	0.432	0.102	50
AB-1	322	322	0	---	<1.1	---	0.889	<0.025	<0
AB-1	756	756	0	---	<1.1	---	0.737	<0.025	<0
Feltmetal 515B	311	339	28	10.7	6.7	7.56	0.711	<0.025	<0
Feltmetal 515B	783	783	0	---	4.0	4.54	0.508	<0.025	<0
Al/Feltmetal(1)	311	339	28	8.3	1.8	3.02	0.787	<0.025	---
Al/Feltmetal(1)	742	742	0	---	<1.1	---	0.660	<0.025	<0
AlBr/Feltmetal(1)	756	756	0	---	4.0	7.34	0.660	0(3)	---

1. Specimens were prepared by NASA.
2. Feltmetal was too soft for hardness reading.
3. Pickup of 0.025 mm.

VII. Phase II Rub-Test Data.

-4V Blades, 0.635 mm (0.025 in.) Thick

.254 mm/sec (0.010 in./sec)

0.508 mm (0.020 in.) to 0.762 mm (0.030 in.)

152 Surface m/sec (500 ft/sec)

Average Depth of Rub, mm	Average Blade Wear, mm	Coating Hardness R_{15Y}	Rub-Surface Rougness rms, μm	Rub Energy, kJ	Rub Energy/ Unit Volume of Coating Removed, J/m^3	Rub-Surface Appearance
0.686	<0.025	73	1.27-1.52	4.128	5.02	Smooth, dense
0.711	<0.025	73	1.52	0.938	1.10	Smooth, dense
0.940	<0.025	56	>7.62	0.828	0.73	Deeply grooved
0.914	<0.025	55	1.27-1.52	---	---	Lightly grooved
0.737	0.102	74	3.05-5.08	7.469	8.44	Lightly scabbed
0.584	0.152	72	>7.62	2.817	4.02	Lightly scabbed
0.660	<0.025	57	2.79-7.62	4.219	5.31	Smooth, porous
0.432	0.102	50	7.62	3.543	6.82	Lightly scabbed
0.889	<0.025	<0	7.62	---	---	Smooth, porous
0.737	<0.025	<0	4.57	---	---	Smooth, porous
0.711	<0.025	<0[2]	1.78-2.03	1.588	1.86	Smooth, porous
0.508	<0.025	<0[2]	2.54-3.81	0.940	1.54	Lightly grooved
0.787	<0.025	---	---	0.719	0.76	Lightly grooved
0.660	<0.025	<0[2]	1.27-1.40	---	---	Lightly grooved
0.660	0[3]	---	---	0.823	1.04	Smooth, spalled in some areas

FOLDOUT FRAME 2

Table VII. Phase II Rub-Test

- Forty-Eight Ti-6Al-4V Blades, 0.635 mm (0.025 in.
- Incursion Rate: 0.254 mm/sec (0.010 in./sec)
- Incursion Depth: 0.508 mm (0.020 in.) to 0.762 m
- Blade Tip Speed: 152 Surface m/sec (500 ft/sec)

Coating	T_{Amb}, °F	T_{Max}, °F	ΔT, °F	Maximum Temperature-Rise Rate, °F/sec	Maximum Shear Force, lbf	Maximum Force-Rise Rate, lbf/sec	Average Depth of Rub, in.	Average Blade Wear, in.
Al	115	550	435	198.0	3.3	3.13	0.027	<0.001
Al	850	950	100	44.4	1.0	0.226	0.028	<0.001
Metco 601	100	225	125	43.9	0.41	0.340	0.037	<0.001
Metco 601	900	900	0	---	<0.25	---	0.036	<0.001
AlBr/NiCg	100	875	775	300.0	4.0	5.7	0.029	0.004
AlBr/NiCg	900	1275	375	175.0	1.8	2.33	0.023	0.006
80/20 NiCg	120	650	530	215.0	2.7	1.76	0.026	<0.001
80/20 NiCg	925	1300	375	290.0	4.2	4.3	0.017	0.004
AB-1	120	120	0	---	<0.25	---	0.035	<0.001
AB-1	900	900	0	---	<0.25	---	0.029	<0.001
Feltmetal 515B	100	150	50	19.2	1.5	1.70	0.028	<0.001
Feltmetal 515B	950	950	0	---	0.9	1.02	0.020	<0.001
Al/Feltmetal(1)	100	150	50	15	0.41	0.68	0.031	<0.001
Al/Feltmetal(1)	875	875	0	---	<0.25	---	0.026	<0.001
AlBr/Feltmetal(1)	900	900	0	---	0.9	1.65	0.026	0(2)

1. Specimens were prepared by NASA.
2. Feltmetal was too soft for hardness reading.
3. Pickup of 0.001 in.

FOLDOUT FRAME 2

VII. Phase II Rub-Test Data. (Concluded)

lades, 0.635 mm (0.025 in.) Thick

m/sec (0.010 in./sec)

mm (0.020 in.) to 0.762 mm (0.030 in.)

rface m/sec (500 ft/sec)

um -Rise e, ec	Average Depth of Rub, in.	Average Blade Wear, in.	Coating Hardness R_{15Y}	Rub-Surface Roughness rms, μin.	Rub Energy, ft-lbf	Rub Energy/ Unit Volume of Coating Removed, ft-lbf/in.^{3}	Rub-Surface Appearance
13	0.027	<0.001	73	50-60	3045	226,000	Smooth, dense
226	0.028	<0.001	73	60	692	49,400	Smooth, dense
340	0.037	<0.001	56	>300	611	33,000	Deeply grooved
-	0.036	<0.001	55	50-60	---	---	Lightly grooved
7	0.029	0.004	74	120-200	5509	380,000	Lightly scabbed
33	0.023	0.006	72	>300	2078	181,000	Lightly scabbed
76	0.026	<0.001	57	110-300	3112	239,000	Smooth, porous
3	0.017	0.004	50	300	2613	307,000	Lightly scabbed
-	0.035	<0.001	<0	300	---	---	Smooth, porous
-	0.029	<0.001	<0	180	---	---	Smooth, porous
70	0.028	<0.001	<0(2)	70-80	1171	83,600	Smooth, porous
02	0.020	<0.001	<0(2)	100-150	693	69,300	Lightly grooved
68	0.031	<0.001	---	---	530	34,200	Lightly grooved
-	0.026	<0.001	<0(2)	50-55	---	---	Lightly grooved
65	0.026	0(2)	---	---	607	46,700	Smooth, spalled in some areas

FRAME 2

a. Cold Rub, 311 K (100° F)

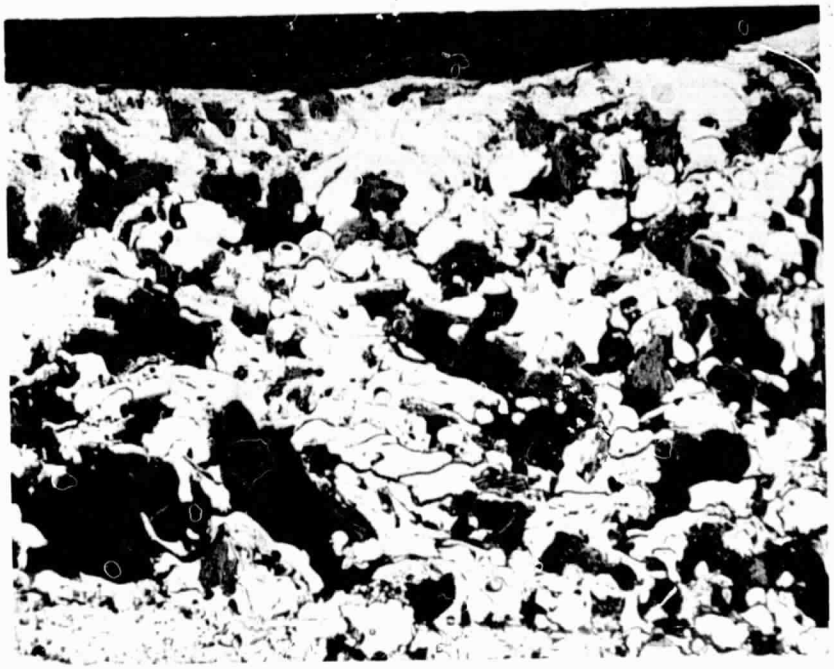

b. Hot Rub, 756 K (900° F)

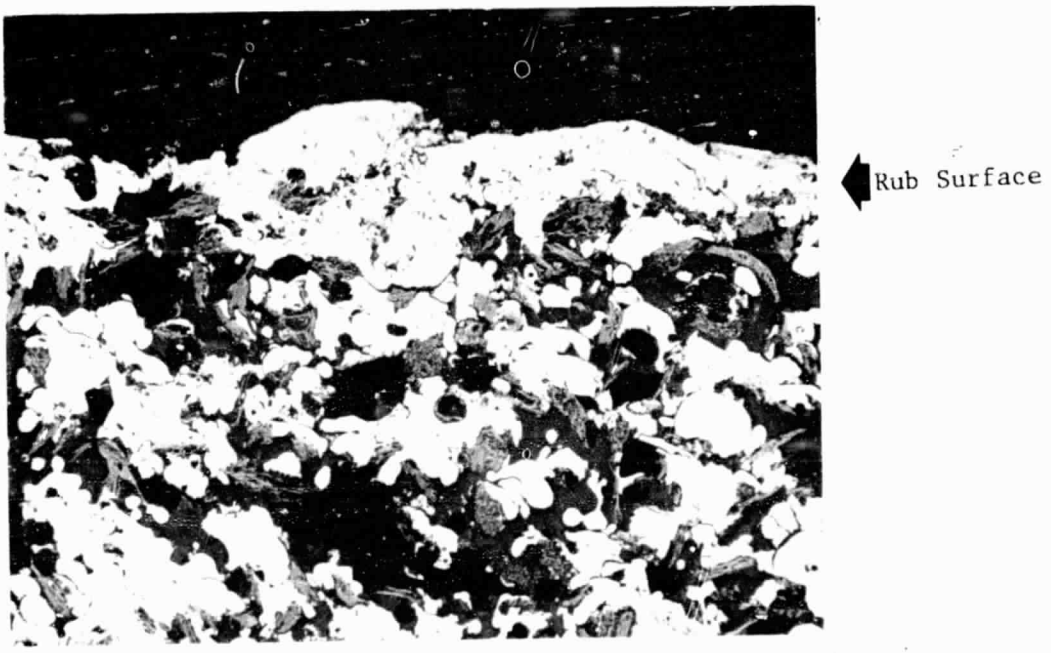

Figure 14. Cross Sections of Rub Paths Showing Compaction of AlBr/NiCg. 100X

a. Cold Rub, 322 K (120° F)

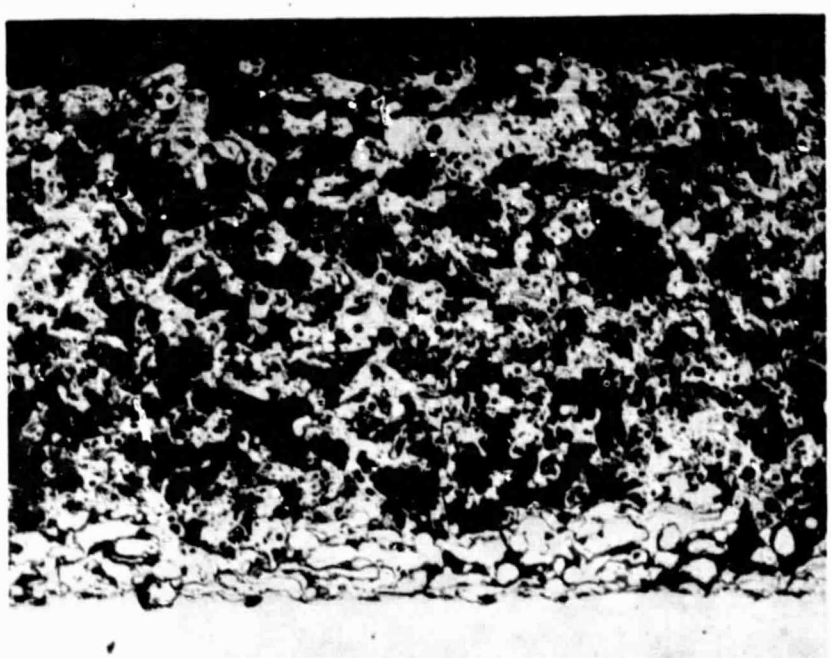

b. Hot Rub, 770 K (925° F)

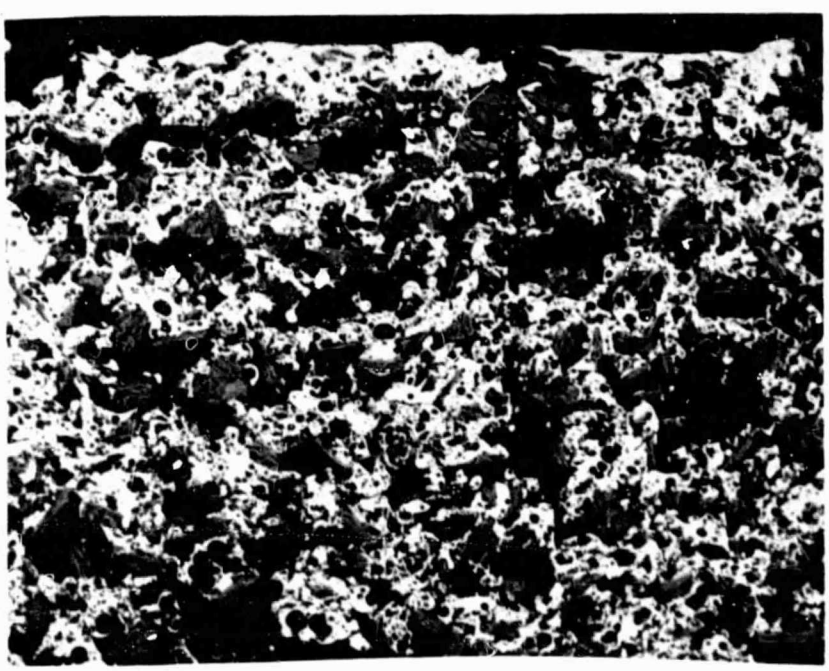

Figure 15. Cross Sections of Rub Paths of 80/20 NiCg Showing Compacted and Noncompacted Surfaces. 100X

a. Cold Rub, 311 K (100° F)

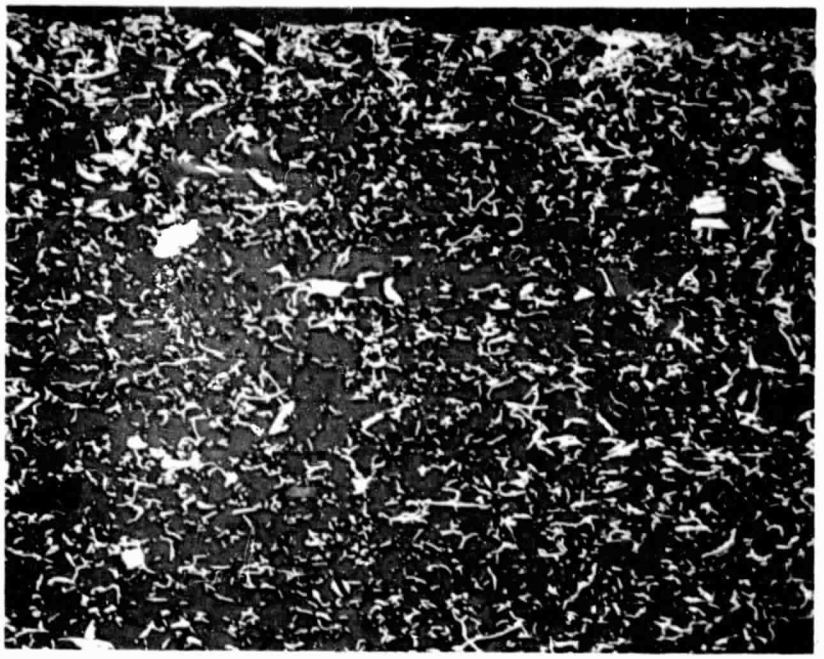

b. Hot Rub, 783 K (950° F)

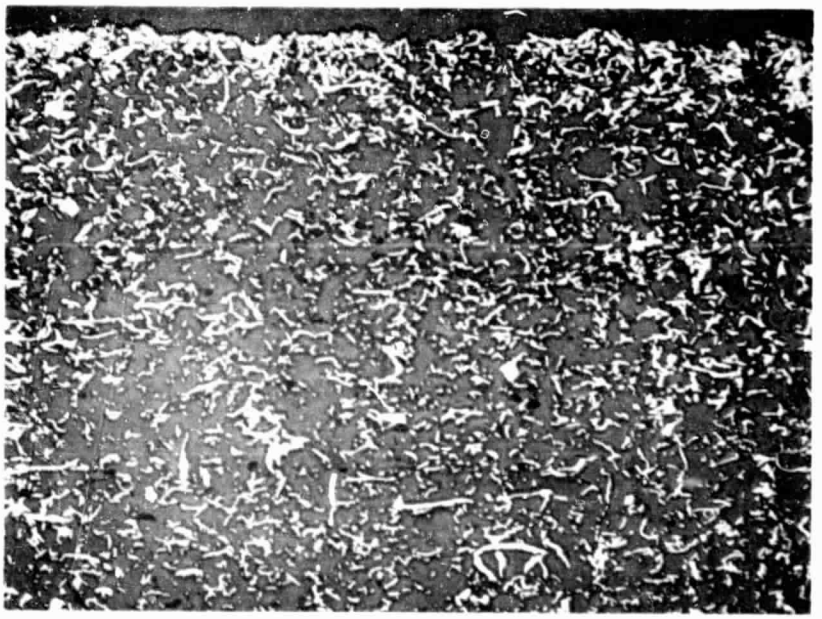

Figure 16. Cross Sections of Rub Paths Showing Minor Compaction of Feltmetal 515B. 50X

Feltmetal specimens were hotter than the 755 K (900° F) ambient test temperature, but the low thermal conductivity of the Feltmetal caused the substrate temperatures to remain virtually unchanged.

Microexamination of blade tips revealed only one unexpected feature: approximately 25.4 μm (1 mil) of pick-up on blades from the AlBr/Feltmetal rub (Figure 17). The material on the tip is dense and uniform; this indicates that severe deformation or possibly melting took place during the rub. Since Cu-9Al wore blades (Phase I testing) and the AlBr (Cu-9Al-1Fe)/Feltmetal did not, it is apparent that the addition of the Feltmetal layer between the spray coating and the substrate is reducing the severity of rubs.

The most distinctive coating microstructure was that of the Al/Feltmetal and AlBr/Feltmetal materials supplied by NASA. The spray materials on the Feltmetals remained essentially intact during rubs and resulted in smooth, dense, rub surfaces with only minor compaction of the supporting Feltmetal (Figure 18). It is notable that the Al/FM rubs resulted in lower shear forces than did either Al or FM alone; this indicates a possible synergistic effect for the Al/FM combination. For the AlBr/FM, approximately one-half of the AlBr spalled from the Feltmetal during the rub, but the remaining material had a smooth finish. The reason for the AlBr spallation has not been established.

A comparison of data from Phase I and Phase II tests on aluminum (Table VIII) shows that for the same test conditions the measured temperatures, shear forces, and rub-energies are in reasonable agreement.

As shown in Table IX, blade tips from rub tests which resulted in blade wear exhibited martensite (in agreement with Phase I results); blade tips from rubs which did not cause blade wear do not contain martensite with the exception of blades from the 80/20 NiCg (cold) and AlBr/FM (hot) rubs. The presence of martensite in all blade tips which were worn during Phase I and Phase II rubs indicates that blades are wearing only when tip temperatures exceed 1278 K (1840° F). At these elevated temperatures, the flow stress of Ti-6Al-4V is known to be less than 34.5 MPa (5 ksi), indicating it may be necessary for a dense rub coating material to have a very low bulk flow stress at 922 K (1800° F) or higher if wear of Ti-base blades is to be avoided during rubs.

In summary, the only Phase I and Phase II materials which have produced the target goals (no blade wear and smooth, dense, rub surfaces) are Al and Al/Feltmetal. Cu-9Al produced a smooth rub surface during hot rubbing but wore blades; however, AlBr(Cu-9-Al-1Fe)/Feltmetal produced a rub that did not wear blades. And AlBr spalled during the rub, indicating that some modification of the AlBr/Feltmetal system might also produce a material capable of providing smooth, dense, rub surfaces.

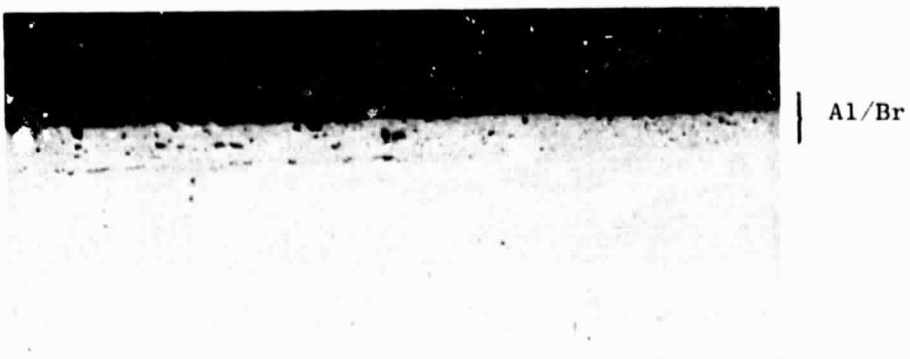

Figure 17. Blade Tip from AlBr/Feltmetal Hot Rub Showing Uniform Pickup Layer of AlBr. 250X

a. Al/Feltmetal Cold Rub, 311 K (100° F)

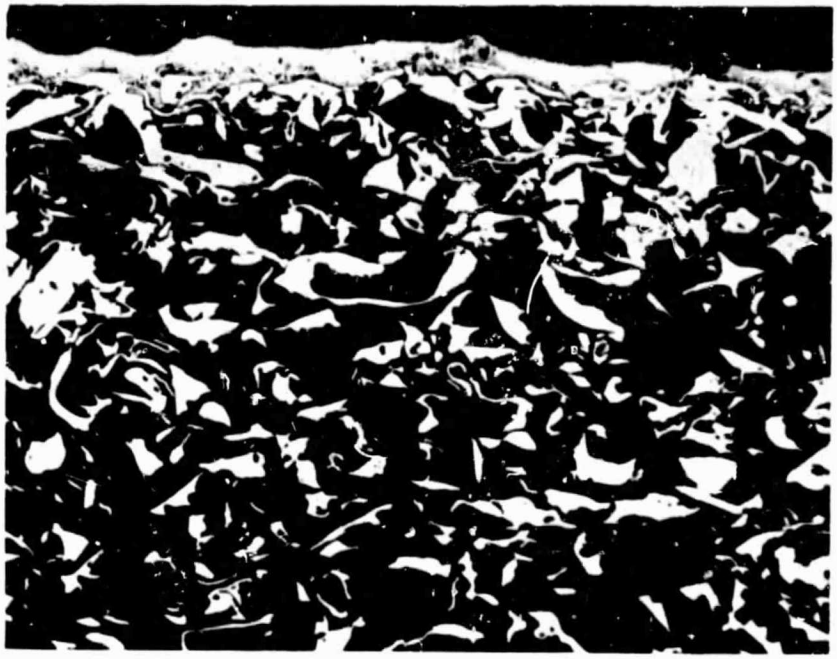

b. AlBr/Feltmetal Hot Rub, 756 K (900° F)

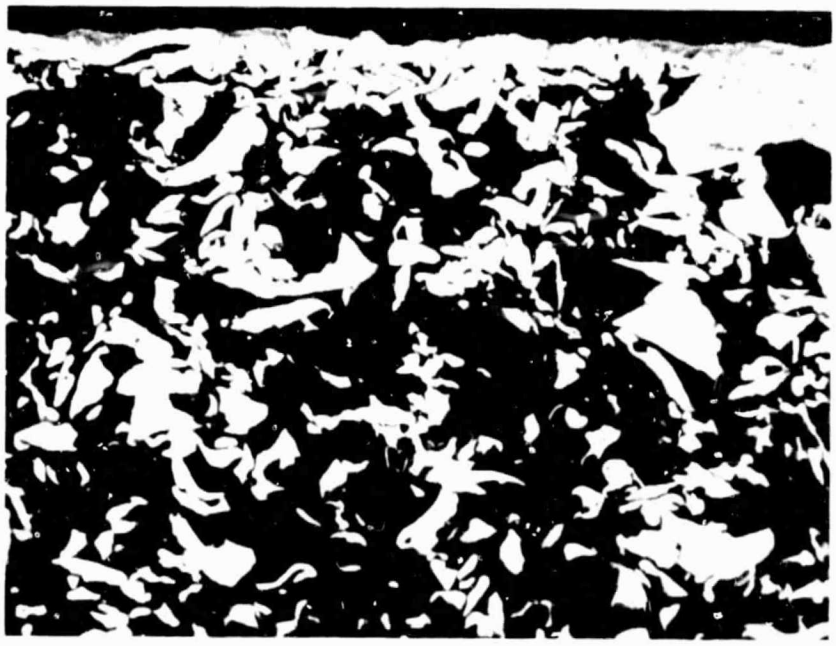

Figure 18. Cross Sections of Rub Paths from Metal-Spray/Feltmetal Materials. 100X

Table VII. Aluminum Rub-Test Data.

Coating	T_{Amb}, K	T_{Max}, K	ΔT^*, K	Maximum Shear Force, N	Average Depth of Rub, mm	Average Blade Wear, mm	Rub-Surface Roughness rms, μm	Rub Energy, kJ	Rub Energy/Unit Volume of Coating Removed, J/m^3
Al (Phase I, Annealed)	297	611	314	10.2	0.914	<0.025	1.27-1.52	3.701	3.377
Al (Phase I, Annealed)	731	731	0	6.7	0.813	<0.025	---	0.968	0.991
Al (Phase II, As-Sprayed)	319	561	242	14	0.686	<0.025	1.27-1.52	.128	5 021
Al (Phase II, As-Sprayed)	728	782	56	4.4	0.711	<0.025	1.52	0.938	1.098

Coating	T_{Amb}, °F	T_{Max}, °F	ΔT^*, °F	Maximum Shear Force, lbf	Average Depth of Rub, in.	Average Blade Wear, in	Rub-Surface Roughness μin.	Rub Energy, ft-lbf	Rub Energy/Unit Volume of Coating Removed, $ft-lbf/in.^3$
Al (Phase I, Annealed)	75	640	565	2.3	0.036	<0.001	50-60	2730	152,000
Al (Phase I, Annealed)	855	855	0	1.5	0.032	<0.001	---	714	44,600
Al (Phase II, As-Sprayed)	115	550	435	3.3	0.027	<0.001	50-60	3045	226,000
Al (Phase II, As-Sprayed)	850	950	100	1.0	0.028	<0.001	60	692	49,400

*$T_{Max} - T_{Avg}$

Table IX. Martensitic Transformation Depths.

Rub Test	Blade Wear, μm (in.)	Depth of Martensitic Zone at Blade Tip, mm	
		Min	Max
Al (cold)	<25.4 (0.001)	0	0
Al (hot)	<25.4 (0.001)	0	0
Al/Feltmetal (cold)	<25.4 (0.001)	0	0
Al/Feltmetal (hot)	<25.4 (0.001)	0	0
AlBr/NiCg (cold)	102 (0.004)	0.4	0.5
AlBr/NiCg (hot)	152 (0.006)	1.0	1.1
AlBr/Feltmetal (hot)	-25.4 (0.001)*	0.1	0.5
80/20 NiCg (cold)	<25.4 (0.001)	0.4	0.5
80/20 NiCg (hot)	102 (0.004)	0.9	1.1
Feltmetal 515B (cold)	<25.4 (0.001)	0	0
Feltmetal 515B (hot)	<25.4 (0.001)	0	0
AB-1 (cold)	<25.4 (0.001)	0	0
AB-1 (hot)	<25.4 (0.001)	0	0
Metco 601	<25.4 (0.001)	0	0
Metco 601	<25.4 (0.001)	0	0

*Pickup

4.2.3 Phase III - Porosity Effects

4.2.3.1 Material Selection and Preparation

Coating wear (depth of rub) minus blade wear was used to rank the rub performance of the Phase I coatings (Table X) and to select a coating for the study of porosity on rub behavior. Cu-9Al ranked the highest of the Cu-, Fe-, and Ni-based coatings. In the case of the Cu-9Al hot rub, a depth of rub and a rub surface similar to pure Al (Figure 19) were exhibited.

Phase II results indicated that a Feltmetal layer under sprayed AlBr coatings tended to reduce blade wear. Therefore, the following coating systems were selected to study the effects of porosity on rub behavior:

(1a) Cu-9Al + 20 volume percent Ekonol
(1b) Cu-9Al + 40 volume percent Ekonol
(2a) Cu-9Al + 20 volume percent Ekonol/Feltmetal 515B
(2b) Cu-9Al + 40 volume percent Ekonol/Feltmetal 515B

Ekonol, a polyester powder marketed by Metco Inc. as Metco 600, was selected as the nonmetallic component to be sprayed with the Cu-9Al powder to reduce the density of the spray deposit (introduce porosity) because it is similarly used in other rub coatings such as Metco 601.

Table X. Rub Performance Ranking, Phase I Coatings.

Ranking	Coating	Coating Wear-Blade Wear, mm (in.)
1	Al (C)	0.914 (0.036)
2	Al (H)	0.787 (0.031)
3	Zn (C)	0.762 (0.030)
4	Cu-9Al (H)	0.356 (0.014)
5	Fe-6Al (H)	-0.102 (-0.004)
6	Cu-9Al (C)	-0.152 (-0.006)
6	Cu-5Al (H)	-0.152 (-0.006)
8	Fe-6Al (C)	-0.279 (-0.011)
8	Fe-13Cr (H)	-0.279 (-0.011)
10	Fe-13Cr (C)	-0.356 (-0.014)
11	Fe (H)	-0.432 (-0.017)
12	Ni-13Cr (H)	-0.508 (-0.020)
13	Fe (C)	-0.584 (-0.023)
14	Cu-10Zn (H)	-0.660 (-0.026)
15	Cu-10Zn (C)	-0.762 (-0.030)
16	Cu (H)	-0.838 (-0.033)
17	Cu (C)	-1.118 (-0.044)
18	Cu-5Al (C)	-1.626 (-0.064)

Prior to spraying, rub-test panels without Feltmetal were grit-blasted and sprayed with 0.127 mm (0.005 in.) of Metco 450 bond coat; panels with brazed-on Feltmetal were very lightly grit-blasted with an S.S. White Model D air abrasive (dental type) and cleaned ultrasonically in methyl ethyl ketone (MEK) to remove any entrapped grit. Approximately 0.89 mm (0.035 in.) of coating was applied to panels without Feltmetal. The surfaces of the spray coatings were somewhat uneven due to the traverse fixturing and rates used; therefore, the surfaces of all coatings were evened by gentle abrasion with 140 grit SiC paper. Final coating thicknesses were 0.76 to 0.89 mm (0.030 to 0.035 in.) for panels without Feltmetal and 0.38 to 0.51 mm (0.015 to 0.020 in.) for panels with Feltmetal.

The spray parameters used for both the 20% and 40% Ekonol mixtures were:

Gun - Metco 3MB
Console - Avco
Powder Feeder - Plasmadyne
Nozzle - GH
kW - 21 (550 amp/38 volts)
Powder Port - No. 1
Spray Distance - 7.62 cm (3 in.)
Spray Angle - 90°
Spray Rate - 2.5 kg/hr (5.5 lbm/hr)
Primary Gas - Ar at 2.83 m^3/hr, 0.69 MPa (100 ft^3/hr, 100 psi)
Secondary Gas - H_2 at 0.14 m^3/hr, 0.55 MPa (5 ft^3/hr, 80 psi)

a. Al

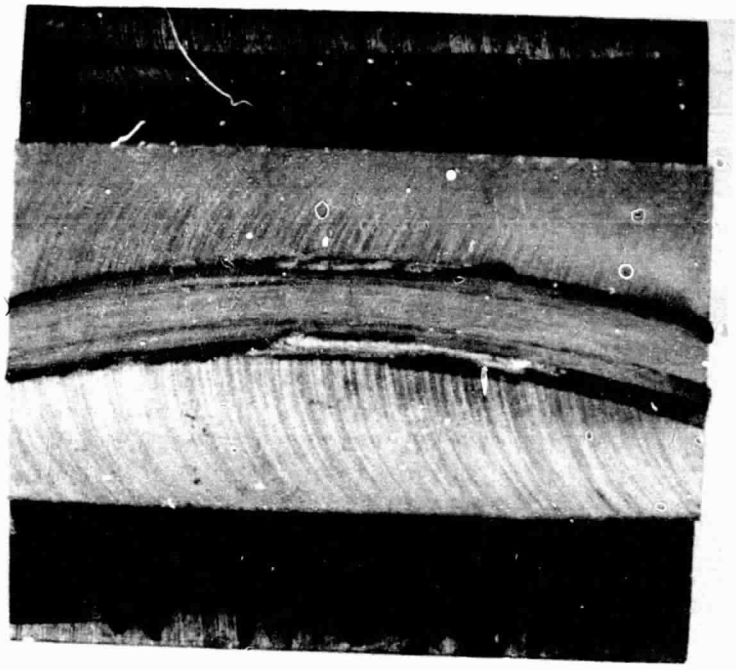

b. Cu-9Al

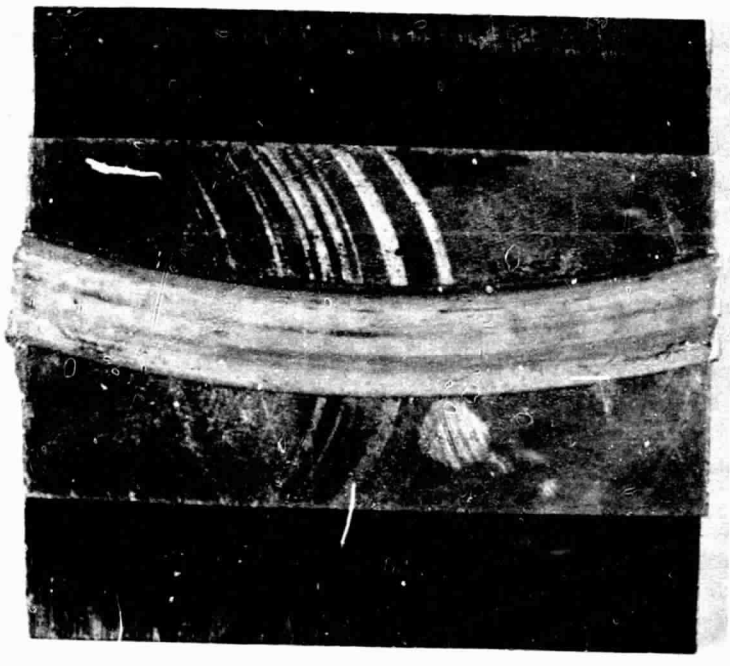

Figure 19. Comparison of Cu-9Al Rub Surface and the Al Rub Surface After Hot Rubs. 2X

4.2.3.2 Rub-Test Results

Phase III rub-test conditions were identical to those used in Phases I and II. The results are tabulated in Table XI (page 49). The following trends were derived from Phase III rub-test results:

1. Significant substrate temperature rises occur only when measurable blade wear or pick-up occurs (this generalization is complicated by the low thermal conductivity of Feltmetal).

2. Significant substrate temperature rise rates occur only for Cu-9Al + 20% Ekonol specimens.

3. The highest rub forces are associated with either blade wear or pick-up.

4. The presence of a Feltmetal underlayer does not cause a significant reduction in rub forces in relation to the spray-coating materials.

5. Cu-9Al + 20% Ekonol spray coatings with and without the Feltmetal underlayer yielded partially or completely smooth, smeared, rub surfaces, ≈ 3.81 μm (150 μin) rms, after 755 K (900° F) rubs (Figure 20).

Metallographic examination of c oss sections of the rub specimens yielded the following information:

1. Cu-9Al + 20% Ekonol and Cu-9A + 40% Ekonol coatings with or without the Feltmetal underlayer have not been compacted under the rub paths (Figure 21).

2. Coatings with the Feltmetal underlayer were not pushed into the felt during rubs.

3. In smooth, rubbed areas there is only a thin layer of smeared material. At very high magnification, there appear to be some small Cu-Ti eutectic zones in the smeared areas.

4. Substantial amounts of Ekonol have been lost from hot-rub specimens and from areas adjacent to the rub paths of cold-rub specimens with Feltmetal underlayers.

Metallographic examination of etched blade tips revealed thin zones of martensite, <25.4 μm (1 mil), in blade tips from rubs which caused blade wear or pick-up. These zones are much smaller than those observed in blade tips from rubs of CuAl or AlBr materials (no Ekonol) in Phase I and Phase II tests, indicating that tip temperatures were not greatly in excess of the β-transus temperature of ≈1278 K (1840° F) for Ti-6Al-4V. It may be postulated that, where scabs are not formed on rub surfaces, the surface temperature during rubs will be limited by the melting point of the rub

a. Without Feltmetal Underlayer

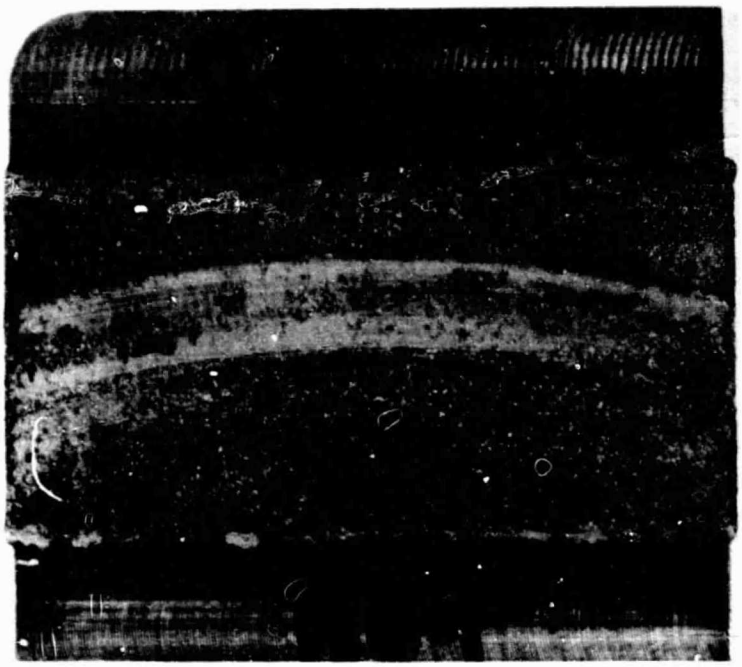

b. With Feltmetal Underlayer

Figure 20. The Hot-Rub Surfaces of the Cu-9Al + 20% Ekonol. 2X

a. Beneath Rub Path

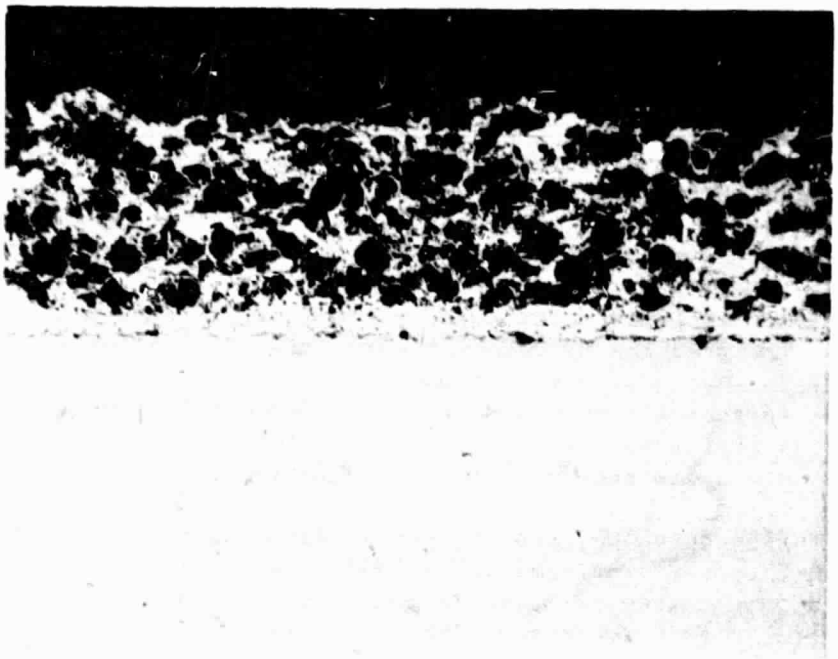

b. Away from Rub Path

Figure 21. Cross Sections of Cu-9Al + 20% Ekonol Coating. 50X

coating; in the case where scabs are formed, the temperature at the rub surface would be expected to be somewhere between the melting point of the coating and the melting point of Ti-6Al-4V, 1922 K (3000° F), depending on the extent of scabbing.

The pickup measured by micrometer on blade tips from Cu-9Al + 20% Ekonol/Feltmetal rubs was clearly evident microscopically. In addition, minor pickup not measurable by micrometer was observed on blade tips from Cu-9Al + 20% Ekonol rubs; the coating material picked up on the blade tips appeared to have reacted with the blade tips to form a Cu-Ti eutectic. Examination of the blade tips in the SEM and microprobe reveal the presence of Ti (Figure 22) in the pickup material. The presence of detectable amounts of titanium in the coating pickup indicates that a significant amount of diffusion occurred during the rub and gives further support to previous evidence that the temperature of the rub surfaces approached or exceeded the melting point of Cu-9Al, ≈1314 K (1910° F), since only a few seconds were available for the diffusion process.

Because of the encouraging, smooth, rub surfaces observed for hot rubs of Cu-9Al + 20% Ekonol systems, preliminary erosion tests were run to determine if materials with this degree of porosity would provide adequate erosion resistance. Standard, room-temperature, erosion tests showed the erosivity numbers [seconds to erode 25.4 μm (1 mil) of coating] to be 15.4 for Cu-9Al + 20% Ekonol and 6.9 for Cu-9Al + 40% Ekonol. Based on erosion resistance of currently used coatings, the Cu-9Al + 20% Ekonol would appear to have adequate erosion resistance in the as-sprayed condition, but the erosion resistance of the Cu-9Al + 40% Ekonol would be marginal.

The conclusions that can be drawn from evaluation of the Phase III rub data are:

1. The addition of porosity to Cu-9Al coatings significantly reduced blade wear in relation to the wear observed for dense Cu-9Al in Phase I tests.

2. Cu-9Al + 20% Ekonol spray coatings, particularly with a Feltmetal interlayer, have demonstrated the capability for yielding smooth rub surfaces under one set of rub-test conditions and have demonstrated erosion resistance considered acceptable in relation to spray coatings currently used in engine applications.

3. Cu-9Al + 40% Ekonol coatings are highly abradable. However, they have rougher rub surfaces than Cu-9Al + 20% Ekonol coatings, and they have marginal resistance to erosion.

4. Good rubs of the sprayed Feltmetal specimens cannot be explained by reduced shear forces. The compliance or low thermal conductivity of the Feltmetal may be more important factors than reduced rub forces.

a. Backscatter Image b. Cu Microprobe Scan c. Ti Microprobe Scan

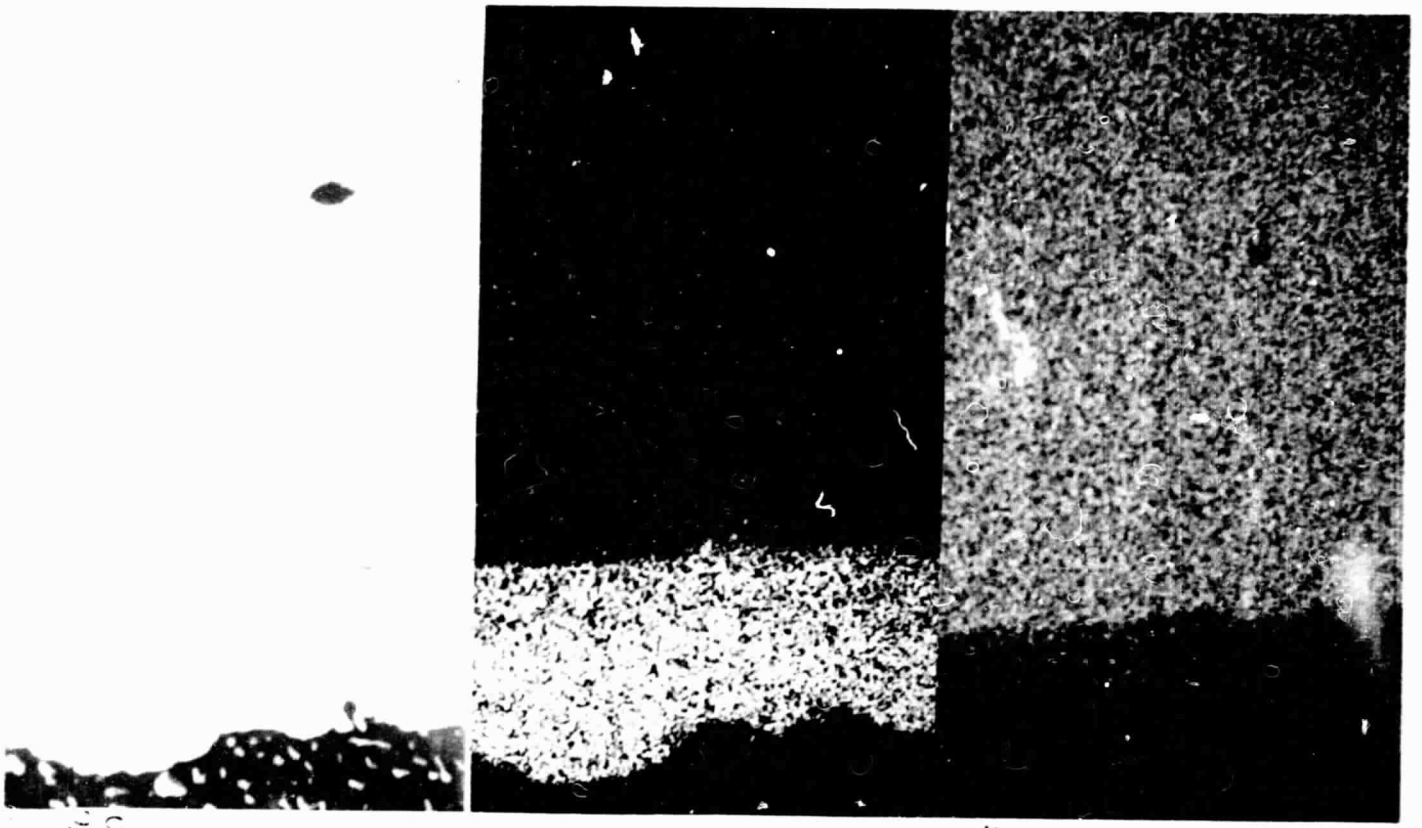

Figure 22. Ti-6Al-4V Blade Tip from Hot Rub with Cu-9Al + 20% Ekonol/Feltmetal, Showing Cu-9Al Pickup. 500X

4.3 TASK II - RUB-TEST PARAMETERS

4.3.1 Material Selection and Preparation

Cu-9Al + 20% Ekonol with and without the Feltmetal underlayer demonstrated the capability of yielding smooth rub surfaces with a significant reduction in blade wear over the dense coatings; this was coupled with erosion resistance considered acceptable for engine applications. These two coating systems were therefore selected to determine the effect of rub parameters in Task II.

AlBr (Metco 51F) powder was used in preference to Cu-9Al because of availability. The nominal composition of Metco 51F is Cu-9.5Al-1Fe. The rub behavior of Metco 51F was expected to be similar to Cu-9Al.

The spray parameters for the coatings were identical to those previously used in Phase III, Task I.

Prior to spraying, rub-test panels without Feltmetal were grit-blasted and sprayed with 0.127 mm (0.005 in.) of Metco 450 bond coat; panels with Feltmetal were very lightly grit blasted with an S.S. White Model D air abrasive (dental type) and cleaned ultrasonically. Approximately 0.762 mm (0.030 in.) of the AlBr + 20% Ekonol coating was applied to all panels, and they were sprayed in one operation to ensure uniform coating properties.

4.3.2 Test Results

The test parameters selected for study were: (a) the incursion rate, (b) the solidity (i.e., number of blades used), and (c) the test temperature. Two different incursion rates [2.54 and 25.4 μm/sec (0.0001 and 0.001 in./sec)], two solidity variations (48 and 12 blades), and two test temperatures [RT and 755 K (900° F)] were examined. The remaining test parameters were identical to those of Task I.

The test results are listed in Table XII. The following trends were observed from the Task II rub-test results:

1. The maximum rub temperatures exceed those observed for 0.254 mm/sec (10.0 mil/sec) rubs of Cu-9Al + 20% Ekonol during Phase III, Task I testing.

2. The maximum shear forces also exceed those observed for 0.254 mm/sec (10.0 mil/sec) rubs of Cu-9Al + 20% Ekonol during Phase III, Task I testing.

3. Some rub-force curves show cyclic force versus time behavior during part or all of the tests.

4. At 2.54 μm/sec (0.0001 in./sec) incursion rates, hot rubs are more severe than cold rubs; at 25.4 μm/sec (0.001 in./sec) incursion rates, hot rubs are less severe than cold rubs.

Table XI. Phase III Rub-Test R

- Forty-Eight Ti-6Al-4V Blades, 0.635 mm (0.025 in.) Thick
- Incursion Rate: 0.254 mm/sec (0.01 in./sec)
- Incursion Depth: 0.508 mm (0.020 in.) to 0.762 mm (0.03
- Blade Tip Speed: 152 surface m/sec (500 ft/sec).

Coating System	T_{Amb}, K	T_{Max}, K	ΔT, K	Max. Temperature-Rise Rate, K/sec	Max. Shear Force, N	Max. Force-Rise Rate, N/sec	Average Depth of Rub, mm	Av Bl We
Cu-9Al + 20% Ekonol	322	672	350	250	12.5	16.5	0.533	0
Cu-9Al + 20% Ekonol	767	850	83	78	2.8	2.6	0.381	0
Cu-9Al + 40% Ekonol	317	333	17	8	<1.1	---	0.711	<0
Cu-9Al + 40% Ekonol	769	769	0	3	<1.1	---	0.406	<0
Cu-9Al + 20% Ekonol/Feltmetal	28	367	56	16	11.6	14.2	1.067	0
Cu-9Al + 20% Ekonol/Feltmetal	761	772	11	7	4.9	9.8	0.406	0
Cu-9Al + 40% Ekonol/Feltmetal	28	28	0	0	<1.1	---	1.016	<0
Cu-9Al + 40% Ekonol/Feltmetal	761	772	11	5	1.9	18.7	0.635	<0

Coating System	T_{Amb}, °F	T_{Max}, °F	ΔT, °F	Max. Temperature-Rise Rate, °F/sec	Max. Shear Force, lbf	Max. Force-Rise Rate, lbf/sec	Average Depth of Rub, in.	W
Cu-9Al + 20% Ekonol	120	750	630	450	2.8	3.7	0.021	
Cu-9Al + 20% Ekonol	920	1070	150	140	0.64	0.58	0.015	
Cu-9Al + 40% Ekonol	110	140	30	15	<0.25	---	0.028	
Cu-9Al + 40% Ekonol	925	925	0	5	<0.25	---	0.016	
Cu-9Al + 20% Ekonol/Feltmetal	100	200	100	29	2.6	3.2	0.042	
Cu-9Al + 20% Ekonol/Feltmetal	910	930	20	12	1.1	2.2	0.016	
Cu-9Al + 40% Ekonol/Feltmetal	100	100	0	0	<0.25	---	0.040	
Cu-9Al + 40% Ekonol/Feltmetal	910	930	20	9.1	0.42	4.2	0.025	

1. Pickup of 0.102 mm (0.004 in.) on blade tip.
2. Pickup of <0.025 mm (0.001 in.) on blade tip.
3. Feltmetal too soft for hardness reading.

. Phase III Rub-Test Results.

, 0.635 mm (0.025 in.) Thick
: (0.01 in./sec)
0.020 in.) to 0.762 mm (0.030 in.)
m/sec (500 ft/sec).

Max. Force-Rise Rate, N/sec	Average Depth of Rub, mm	Average Blade Wear, mm	Coating Hardness R_{15Y}	Rub-Surface Roughness rms, μm	Rub-Surface Appearance
16.5	0.533	0.102	58	3.81-4.32	Lightly grooved, scabbed
2.6	0.381	0.051	43	2.54-7.62	Smooth, pullout in some areas
---	0.711	<0.025	---	---	Smooth, porous, pullout in some areas
---	0.406	<0.025	---	---	Porous, pullout in some areas
14.2	1.067	0[1]	<0[3]	2.54-5.08	Lightly grooved, scabbed, Feltmetal pullout in some areas
9.8	0.406	0[2]	---	---	Smooth, ≈ 3.81 μm (150 μin.) rms
---	1.016	<0.025	<0[3]	>7.82	Rubbed into Feltmetal
18.7	0.635	<0.025	<0[3]	7.62	Rubbed into Feltmetal

Max. Force-Rise Rate, lbf/sec	Average Depth of Rub, in.	Average Blade Wear, in.	Rub Surface Roughness rms, μin.
3.7	0.021	0.004	150-170
0.58	0.015	0.002	100-300
---	0.028	<0.001	---
---	0.016	<0.001	---
3.2	0.042	0[1]	100-200
2.2	0.016	0[2]	---
---	0.040	<0.001	>300
4.2	0.025	<0.001	300

FOLDOUT FRAME 2

Table XII. Task II Rub-T

- Ti-6Al-4V Blades, 0.635 mm (
- Rub Depth: 0.508 mm (0.020
- Blade Tip Speed: 152 surfac

Coating System	No. of Blades	Incursion Rate, μm/sec	T_{Amb}, K	T_{Max}, K	ΔT, K	Max. Shear, Force, N	A D R
AlBr + 20% Ekonol	48	2.48	322	728	406	15.1(1)	
AlBr + 20% Ekonol	48	2.48	733	994	261	15.1(1)	
AlBr + 20% Ekonol	48	24.8	322	700	378	13.3	
AlBr + 20% Ekonol	48	24.8	761	1061	300	9.3	
AlBr + 20% Ekonol	48	248	744	967	222	---	
AlBr + 20% Ekonol	12	24.8	317	506	189	12.5(1)	
AlBr + 20% Ekonol	12	24.8	694	978	228	6.7(1)	
AlBr + 20% Ekonol/Feltmetal	48	2.48	317	367	50	9.3(1)	
AlBr + 20% Ekonol/Feltmetal	48	2.48	744	861	61	1.8	
AlBr + 20% Ekonol/Feltmetal	48	24.8	322	378	56	7.6	
AlBr + 20% Ekonol/Feltmetal	48	24.8	739	783	44	3.6	

Coating System	No. of Blades	Incursion Rate, in./sec	T_{Amb}, °F	T_{Max}, °F	ΔT, °F	Max. Shear, Force, lbf	A D R
AlBr + 20% Ekonol	48	0.0001	120	850	730	3.4(1)	
AlBr + 20% Ekonol	48	0.0001	860	1330	470	3.4(1)	
AlBr + 20% Ekonol	48	0.001	120	800	680	3.0	
AlBr + 20% Ekonol	48	0.001	910	1450	540	2.1	
AlBr + 20% Ekonol	48	0.01	880	1280	400	---	
AlBr + 20% Ekonol	12	0.001	110	450	340	2.8(1)	
AlBr + 20% Ekonol	12	0.001	890	1300	410	1.5(1)	
AlBr + 20% Ekonol/Feltmetal	48	0.0001	110	200	90	2.1(1)	
AlBr + 20% Ekonol/Feltmetal	48	0.0001	880	1090	110	0.4	
AlBr + 20% Ekonol/Feltmetal	48	0.001	120	220	100	1.7	
AlBr + 20% Ekonol/Feltmetal	48	0.001	870	950	80	0.8	

1. From cyclic force versus time curve.
2. Feltmetal too soft for hardness reading.

FOLDOUT FRAME

le XII. Task II Rub-Test Results.

-4V Blades, 0.635 mm (0.025 in.) Thick
th: 0.508 mm (0.020 in.) to 0.762 mm (0.030 in.)
ip Speed: 152 surface m/sec (500 ft/sec).

ΔT, K	Max. Shear, Force, N	Average Depth of Rub, mm	Average Blade Wear, mm	Coating Hardness R_{15Y}	Rub-Surface Roughness rms, μm	Rub-Surface Appearance
406	15.1(1)	0.737	0.076	57	3.81	Light scabbing
261	15.1(1)	0.279	0.356	48	2.29-2.41	Heavy scabbing, light pullout
378	13.3	0.635	0.127	54	3.81	Light scabbing
300	9.3	0.330	0.025	70	2.54-5.08	Light scabbing
222	---	0.457	0.152	72	2.29-2.54	Smooth, no scabbing
189	12.5(1)	0.381	0.483	58	2.54-6.35	Very light scabbing
228	6.7(1)	0.152	0.178	63	2.03-2.41	Light scabbing
50	9.3(1)	0.991	0.051	<0(2)	>7.62	Spalled
61	1.8	0.457	0.051	<0(2)	0.89-1.27	Heavy scabbing with surface cracking
56	7.6	0.711	0.229	<0(2)	3.81	Moderate scabbing, some pullout
44	3.6	0.356	<0.025	<0(2)	3.81-4.06	Light scabbing, moderate pullout

T, F	Max. Shear, Force, lbf	Average Depth of Rub, in.	Average Blade Wear, in.	Rub-Surface Roughness rms, μin.
730	3.4(1)	0.029	0.003	150
670	3.4(1)	0.011	0.014	90-95
680	3.0	0.025	0.005	150
640	2.1	0.013	0.001	100-200
600	---	0.018	0.006	90-100
440	2.8(1)	0.015	0.019	100-250
410	1.5(1)	0.006	0.007	80-95
490	2.1(1)	0.039	0.002	>300
410	0.4	0.018	0.002	35-50
500	1.7	0.028	0.009	150
480	0.8	0.014	<0.001	150-160

FOLDOUT FRAME 2

5. More blade wear was produced in 12-blade tests than in 48-blade tests, but maximum temperatures and shear forces are lower for the 12-blade tests.

6. Blade wear for 48-blade tests of AlBr + 20% Ekonol is comparable to blade wear observed for Phase III, Task I tests of Cu-9Al + 20% Ekonol except for the hot, 2.54 μm/sec (0.0001 in./sec) rub, but more scabbing is evident with the AlBr + 20% Ekonol.

7. Blade wear is reduced when a Feltmetal underlayer is present.

The martensitic transformations of the Task II rub blades, determined metallographically (Table XIII), were deeper than those observed in Phase III, Task I. This is in accord with the higher shear forces, amount of blade wear, and maximum rub temperatures observed.

All Task II blades had a uniform pickup of coating material at the tip (Figure 23) ranging from 1.27 to 5.08 μm (0.00005 to 0.0002 in.). Blades with martensite depths of greater than 25.4 μm (0.1 mil) tended to show heavy burring on the trailing edge but very little coating pickup on the leading edge. No burring was observed on the blades that had less than 2.54 μm (0.1 mil) martensite (Figure 24), and there was coating pickup on the tip.

The increased temperatures, forces, depth of martensitic transformation and scabbing observed for AlBr + 20% Ekonol tests with respect to Cu-9Al + 20% Ekonol tests could be attributed to the effects of changing incursion rates during tests and/or a slightly decreased abradability of the AlB + 20% Ekonol. Rub results for AlBr + 20% Ekonol and Cu-9Al + 20% Ekonol from nearly duplicate tests at the 254 μm/sec (0.01 in./sec) showed nearly the same coating wear, but the blade wear was 0.152 mm (0.006 in.) for the former and only 0.051 mm (0.002 in.) for the latter. The following evidence points to probable decreased abradability of the AlBr + 20% Ekonol as compared to the prior Cu-9Al + 20% Ekonol material.

1. The erosivity number (seconds required to erode 25.4 μm (1 mil) of coating) of the AlBr + 20% Ekonol is ≈20 versus ≈15 for the Cu9Al + 20% Ekonol tested in Phase III, Task I.

2. The microstructure of the AlBr + 20% Ekonol, while not grossly different from that of the Cu-9Al + 20% Ekonol, shows the AlBr matrix to be slightly denser and more contiguous than the Cu-9Al matrix (Figure 25).

Prior experience with abradable coatings has shown that increased erosion resistance and higher densities will be accompanied by decreased abradability.

The reason for the higher erosion resistance and density of the AlBr + 20% Ekonol, which was sprayed with the same parameters as the Cu9Al + 20% Ekonol, is believed to be the finer size distribution of the AlBr (Metco 51F). As shown in Table XIV, the size distribution of the AlBr is shifted toward the -325 mesh size range; the Cu-9Al size distribution is centered about the -270

Table XIII. Martensitic Transformation Depths, Task II Coatings.

Rub Coating	Number of Blades	Incursion Rate, μm/sec (in./sec)	Ambient Test Temperature	Depth of Martensitic Zone at Blade Tip, mm	
				Min.	Max.
AlBr + 20% Ekonol	48	2.54 (0.0001)	Room Temperature	0	0
AlBr + 20% Ekonol	48	2.54 (0.0001)	Hot	0	0
AlBr + 20% Ekonol	48	25.4 (0.001)	Room Temperature	0	<0.1
AlBr + 20% Ekonol	48	25.4 (0.001)	Hot	0	<0.1
AlBr + 20% Ekonol	48	254 (0.010)	Hot	0	0.1
AlBr + 20% Ekonol	12	25.4 (0.001)	Room Temperature	<0.1	0.1
AlBr + 20% Ekonol	12	25.4 (0.001)	Hot	0.1	0.9
AlBr + 20% Ekonol/Feltmetal	48	2.54 (0.0001)	Room Temperature	0	<0.1
AlBr + 20% Ekonol/Feltmetal	48	2.54 (0.0001)	Hot	<0.1	0.2
AlBr + 20% Ekonol/Feltmetal	48	25.4 (0.001)	Room Temperature	0	0
AlBr + 20% Ekonol/Feltmetal	48	25.4 (0.001)	Hot	0	0.1

- Forty-Eight Blades
- Incursion Rate: 25.4 μm/sec (0.001 in./sec)

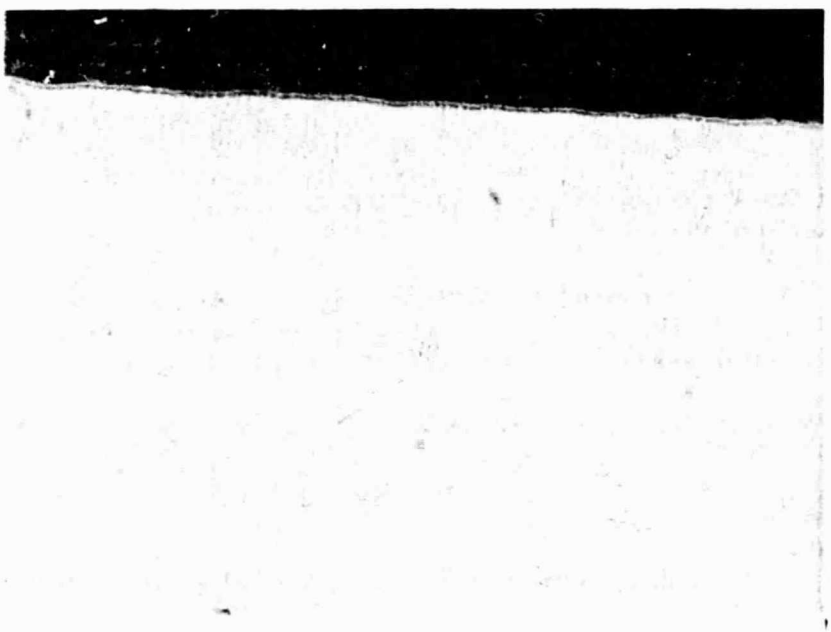

Figure 23. Pickup of Coating Material on Blade Tip During Cold Rub of AlBr + 20% Ekonol/ Feltmetal, Typical of All Task II Blades. 500X

a. No Martensite

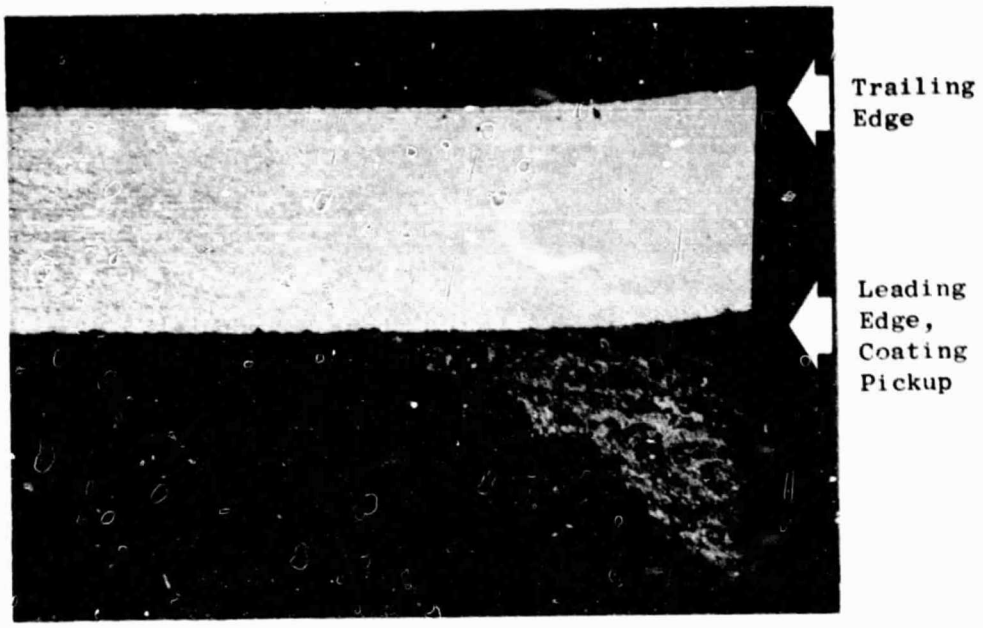

b. Martensite Zone

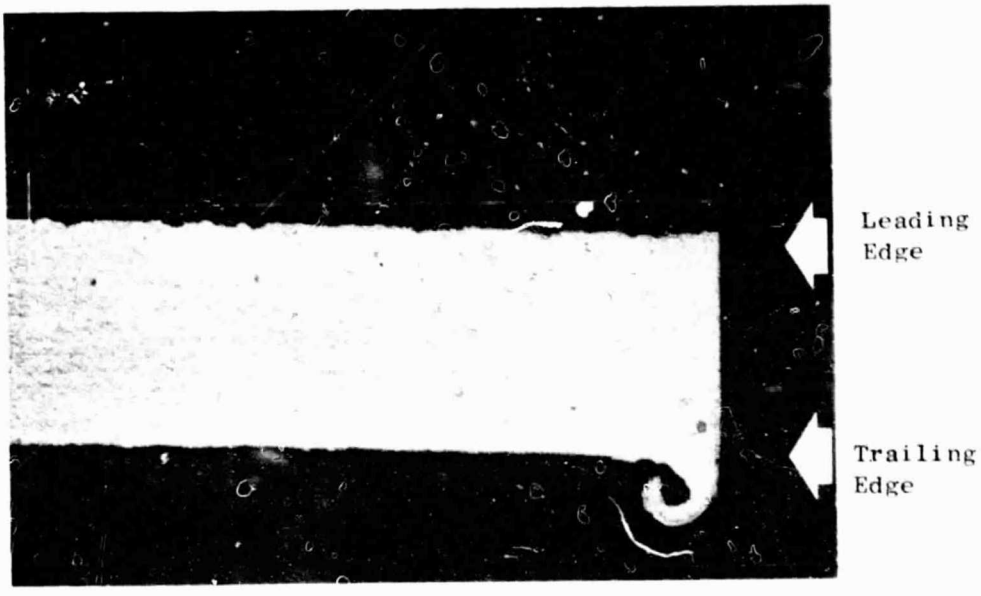

Figure 24. Ti-6Al-4V Blade Apperance for Rubs in Which (a) No Martensite Formed and (b) Martensite Did Form. 100X

a. Cu-9Al + 20% Ekonol

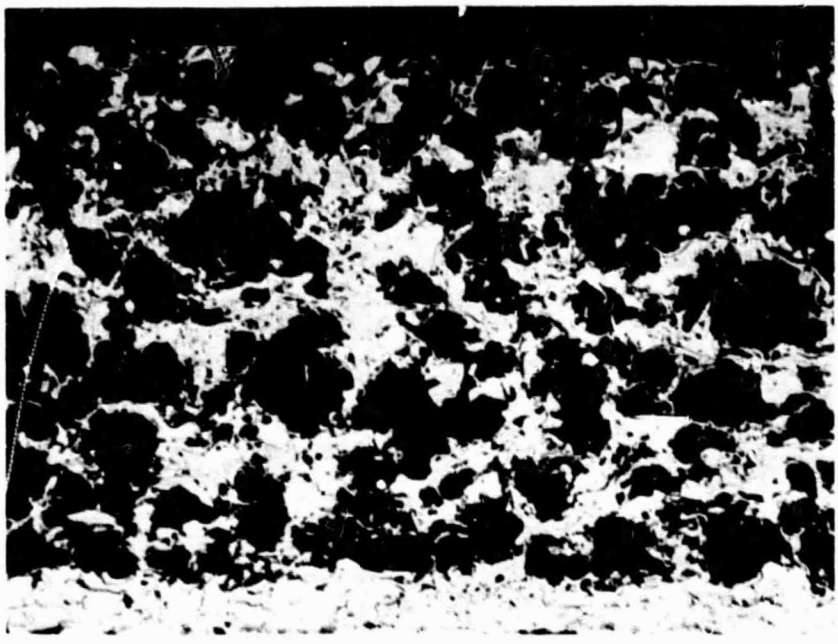

b. AlBr + 20% Ekonol

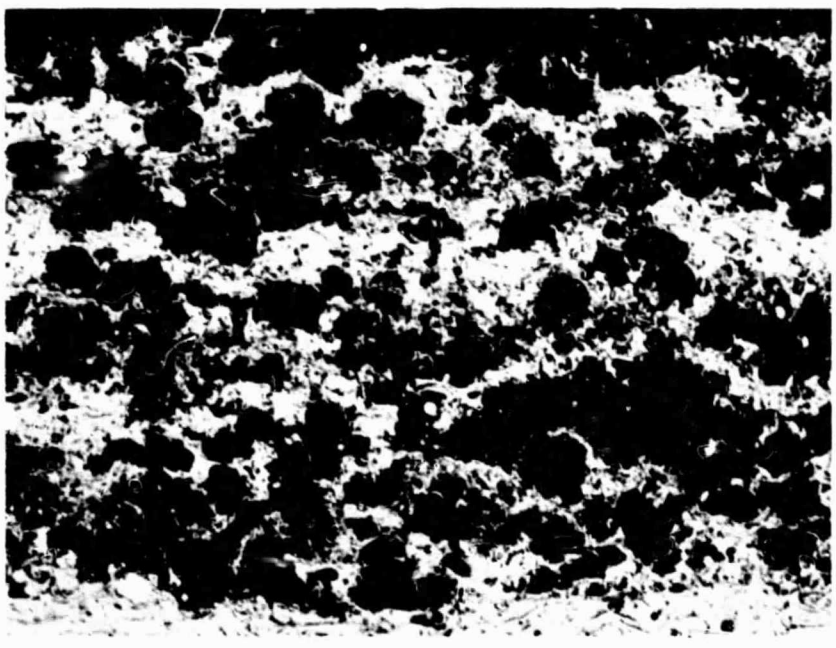

Figure 25. Microstructures of Cu-9Al + 20% Ekonol and AlBr + 20% Ekonol Showing the Slightly Increased Density of AlBr + 20% Ekonol. 100X

Forty-Eight Ti-6Al-4V Blades,
0.635 mm (0.025 in.) Thick

Incursion Depth: 0.508 to 0.762 mm
(0.020 to 0.030 in.)

Blade Tip Speed: 152 Surface m/sec (500 ft/sec)

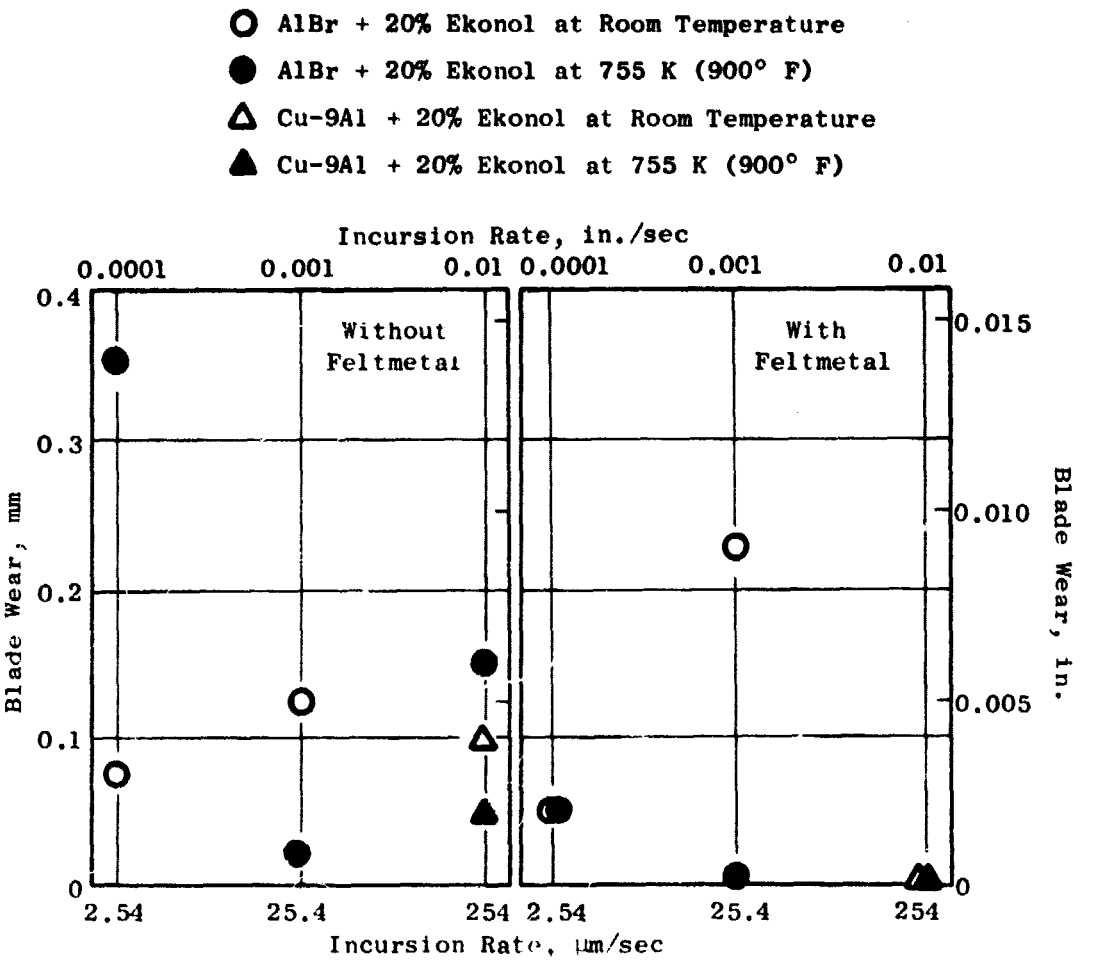

Figure 26. Blade Wear Versus Incursion Rate.

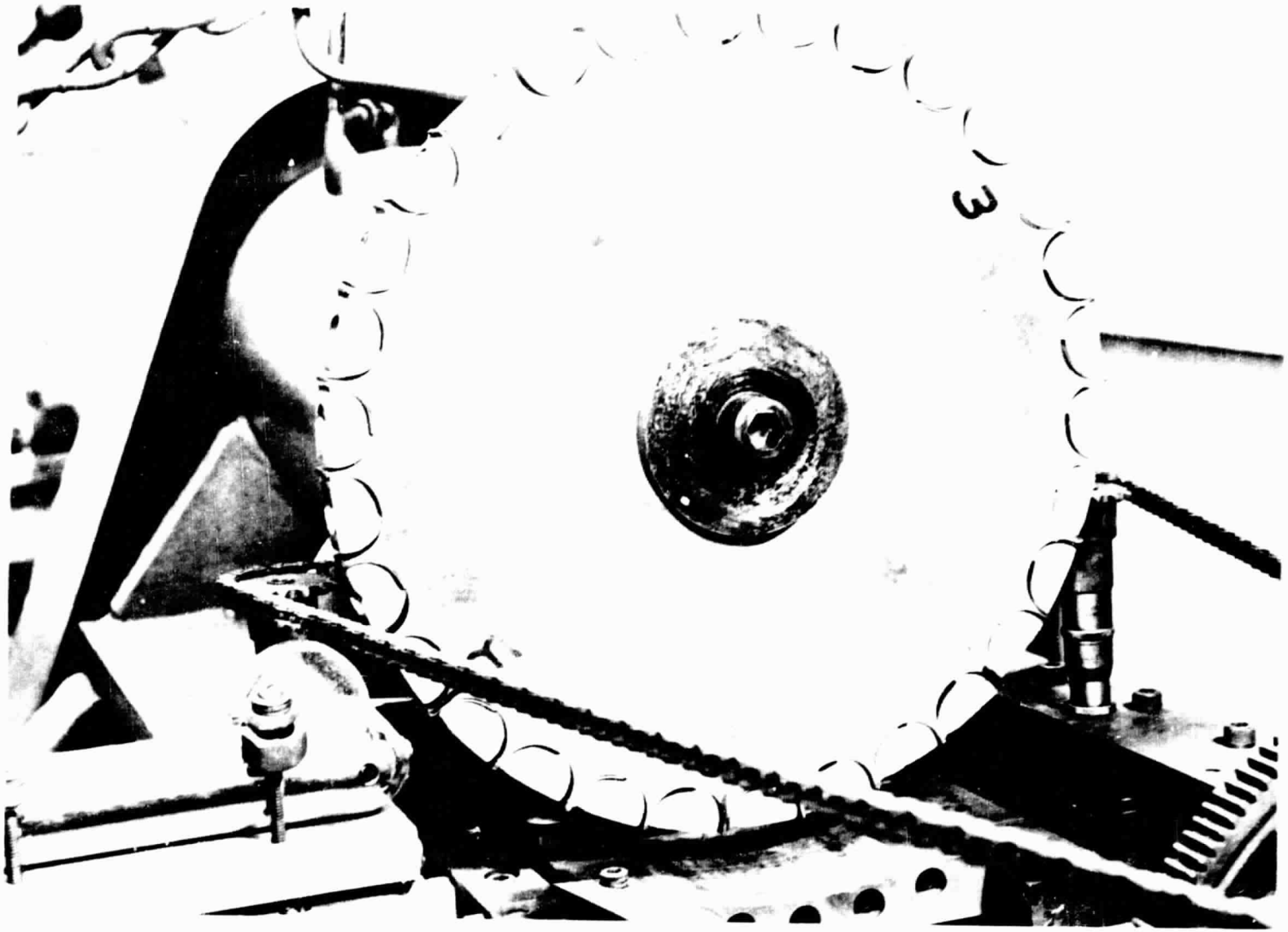

Figure 27. Abradability Tester.

versus 152 m/sec (750 versus 500 ft/sec) but was limited to room-temperature rub testing. The abradable material was sprayed on curved rub panels matched to the blade tip radius of a rotating wheel holding up to 30 blades. During the test, after the desired rotational speed of the wheel has been attained, the platform is slowly raised to allow incursion of the blades into the abradable material. This rate of incursion can be varied from 2.54 to 254 μm/sec (0.1 to 10 mils/second) and approximates most of the rotor/stator incursion rates experienced in a typical engine. For Task III, incursion rates of 2.54, 25.4, and 254 μm/sec (0.1, 1.0, and 10 mils/sec) were used with six blades in the wheel. The duration of the test is usually controlled to give a 381 to 508 μm (15 to 20 mil) total incursion of blades into the seal material [e.g., 15 to 20 seconds at 25.4 μm/sec (1.0 mil/sec)].

The second additional rub test used in Task III utilized the Evendale Compressor Rub Simulator (Figure 28). It is a modified B-29 turbosupercharger with the compressor impeller machined smooth, to act as a flywheel, and a remachined turbine disk with replaceable blades. The shroud, which is both segmented and replaceable, is hydraulically actuated at variable incursion rates in either of two selected modes (uniform and single point). The turbine is driven by a regulated shop-air supply. Air heating is provided by a controllable, in-line combustor fueled by propane gas. The entire vehicle is operated by one man from a remote control panel.

The capabilities of the Compressor Simulator are summarized as follows:

- Rub Velocities - 0 to 356 m/sec (1500 ft/sec)
- Test Temperature - 60 to 922 K (80 to 1200° F)
- Blade -
  - Stagger Angle - 45°
  - Thickness - 0.889 mm (0.035 in.)
  - Solidity - 1.2
  - Tip Radius - 16 cm (6.3 in.)
  - Chord - 2.54 cm (1.0 in.)
  - Uniform Rub (360°) - 0.508 mm (0.020 in.) Depth
- Single Point Rub - 0.76 mm (0.030 in.) Depth
- Variable Incursion Rates
  - Uniform - 0.508 to 1.524 mm/sec (20 to 60 mil/sec)
- - Single Point - 0.54 μm/sec to 2.54 mm/sec (0.1 to 100 mil/sec)

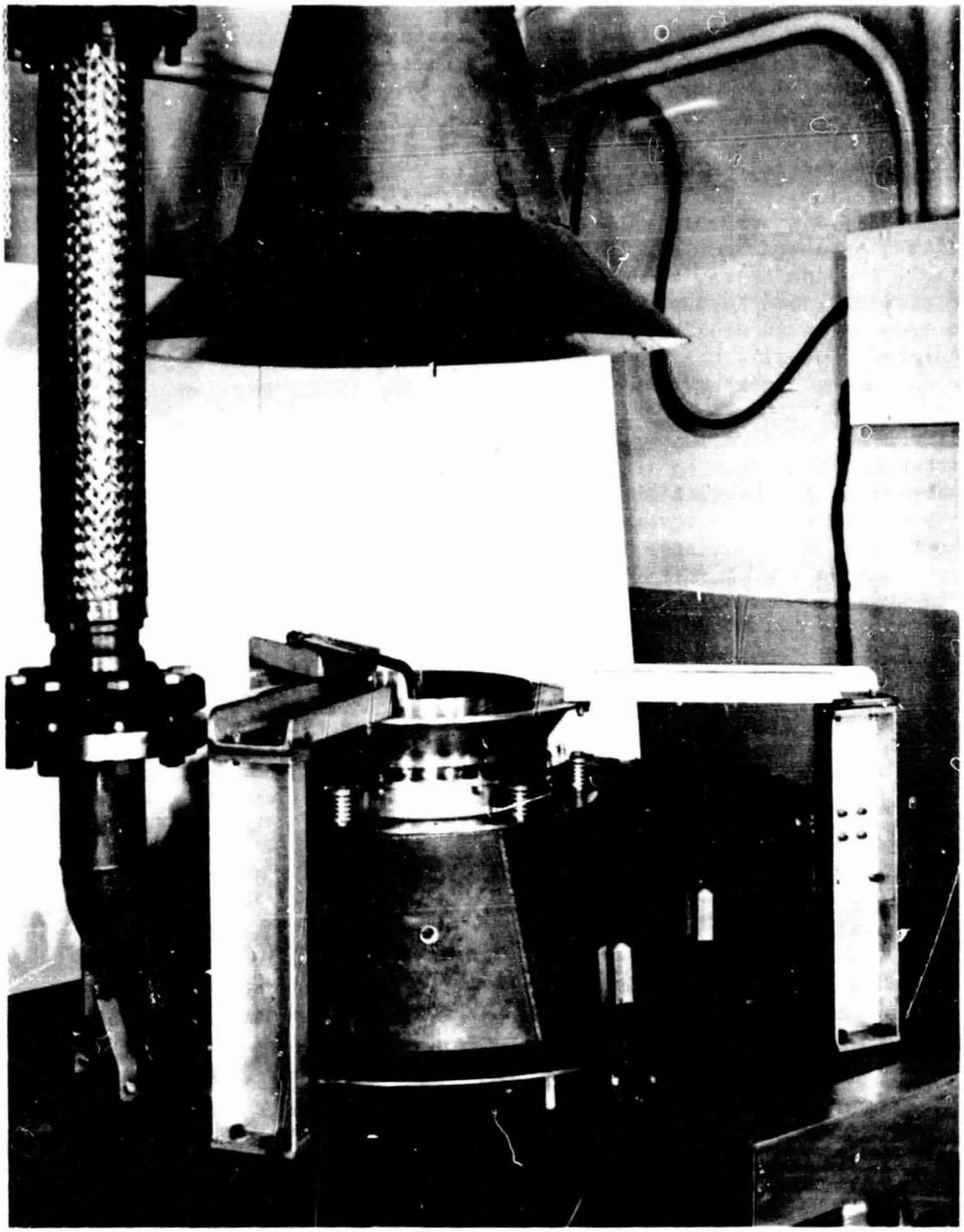

Figure 28. Evendale Compressor-Rub Simulator.

The rub test was selected for final evaluation of the recommended coating composition because it can closely match compressor temperatures, blade tip speeds, number of blades, incursion rates, and geometry over a wide range of conditions typical of General Electric engines.

A cold particle-erosion test was also employed in Task III. Fifty-micrometer Al_2O_3 particles were jetted through a standard nozzle at 276 kPa (40 psi) air pressure with a 20° impingement angle onto a 2.54 x 5.08 cm (1 x 2 in.) specimen set 10.16 cm (4 in.) from the nozzle. Like most particle-erosion tests, it provided a bench mark of material density, cohesive strength, and hardness by measuring pit depth in a standard length of time from which an erosivity number [seconds to erode 25.4 μm (1 mil)] can be calculated. Usually the more resistant materials, being dense, are less permeable to gas penetration and more resistant to gas erosion.

Coating cohesive strengths of Task III materials were evaluated in a standard tensile bond test by including a set of 2.54-cm (1-in.), round buttons of the appropriate substrate material in each spray run. Some of the coated tensile bond buttons were preexposed at 755 or 867 K (900 or 1100° F) for 50 hours prior to testing. The as-sprayed and preexposed buttons were bonded to 2.54-cm (1-in.) mandrels with FM123-5 adhesive. A hydraulically loaded Baldwin Tensile Machine was used to pull the coatings in uniaxial tension at a constant loading rate of 5.3 to 6.2 kN (1200 to 1400 lbf) per minute. The average value of three tests has been reported for each coating.

The ability of the coatings to withstand oxidation and thermal cycling was also considered in Task III. A standard, thermal-cycle test, used at GE, that has been of use in screening abradable coatings, involves depositing the coating material on the appropriate substrate material and giving it up to 50 thermal cycles. The substrate material chosen for the current work was M152 steel (new CF6 compressor-casing material). The thermal cycle consisted of placing the room-temperature sample into a 755 K (900° F) furnace, holding it a sufficient time to achieve thermal equilibrium (about one hour), removing it from the furnace, and force-cooling it by a large fan for the first 30 minutes after removal from the furnace. The samples were inspected under a 30X stereomicroscope every five cycles for evidence of thermal cracking, spallation, and blistering. Samples which exhibited one of these conditions or which successfully completed 50 thermal cycles were sectioned, metallographically prepared, and inspected at higher magnifications.

4.4.2 Initial Materials Selection and Preparation

The AlBr + 20% Ekonol and AlBr + 20% Ekonel/Feltmetal 515B were initially selected for further evaluation. The first approach to restoring the good abradability characteristics of Task I, Phase III was to purchase a special cut of aluminum bronze power (Lot 3223) that closely matched the seive analysis of the Cu-9Al used in Task I, Phase III. The mesh size distributions of these powder lots are given in Table XV. (Also included in Table XV is Lot 3322A which was used in subsequent portions of Task II.)

Table XV. Particle Size Distributions for Task I, Phase III and Task III Powders.

Sieve Fraction	Cu-9Al	AMI 332	
	Lot 189	Lot 3223	Lot 3322A
+170	7.7%	5.7%	7.3%
-170/+200	15.6%	8.8%	8.5%
-200/+270	32.0%	13.5%	19.2%
-270/+325	23.7%	51.9%	42.2%
-325	19.4%	18.9%	22.8%

The specimens were fabricated by an outside vendor in the same manner as Task II specimens. The spray parameters used were:

Gun - Metco 3MB
Console - Avco
Powder Feeder - Plasmadyne
Nozzle - GH
kW - 21 (460 amp. 45 V)
Powder port - No. 1
Spray Distance - 7.62 cm (3 in.)
Spray Angle - 90°
Spray Rate - 2.5 kg/hr (5.5 lbm/hr)
Primary Gas - Ar at 2/83 m^3/hr (100 ft^3/hr)
Secondary Gas - H_2 at 0.14 m^3/hr (5 ft^3/hr)

These parameters varied slightly from those used in Task I, Phase III and Task II in that a higher voltage and lower current were used to obtain the 21 kW power setting.

The specimens fabricated included Evendale room-temperature rub-test panels; Lynn elevated-temperature rub-test panels, particulate-erosion specimens, machinability samples, and thermal-shock samples.

4.4.3 Test Results

The Evendale (room temperature) rub-test results are summarized in Table XVI. Rubs were made on as-sprayed and coatings preexposed at 755 or 867 K (900 or 1100° F)/150 hours. The only tests showing blade wear were the 2.54 and 25.4 μm/sec (0.0001 and 0.001 in./sec) incursion rates with Ti-6Al-4V blades, on panels with no Feltmetal. The first-iteration panels rubbed by Ti-6Al-4V are shown in Figure 29. The most noticeable feature on these rub panels was material pullout in layers. This was particularly severe on those panels with the Feltmetal 515B underlayer. The panels rubbed by Inconel 718 were similar in appearance.

Table XVI. AlBr + 20% Ekonol/Feltmetal Room-Temperature Rub Test.

- All tests conducted with 48 blades at 152 m/sec (500 ft/sec) Tip Speed.

Coating	Blade Material	Temperature of 50-Hour Coating Preexposure, K (° F)	Rub Rate, μm/sec (in./sec)	Test Temp, K (° F)	Coating Wear, mm (in.)	Blade Wear, mm(in.)
AlBr + 20% Ekonol	Ti-6Al-4V	---	2.54 (0.0001)	755 (900)	0.483 (0.019)	0.00
AlBr + 20% Ekonol	Ti-6Al-4V	---	25.4 (0.001)	755 (900)	0.635 (0.025)	0.00
AlBr + 20% Ekonol	Ti-6Al-4V	---	254 (0.01)	755 (900)	0.660 (0.026)	0.00
AlBr + 20% Ekonol/Feltmetal	Ti-6Al-4V	---	2.54 (0.0001)	755 (900)	0.610 (0.024)	0.00
AlBr + 20% Ekonol/Feltmetal	Ti-6Al-4V	---	25.4 (0.001)	755 (900)	0.711 (0.028)	0.00
AlBr + 20% Ekonol/Feltmetal	Ti-6Al-4V	---	254 (0.01)	755 (900)	1.143 (0.045)	0.00
AlBr + 20% Ekonol/Feltmetal	Ti-6Al-4V	755 (900)	2.54 (0.0001)	755 (900)	1.372 (0.054)	0.00
AlBr + 20% Ekonol/Feltmetal	Ti-6Al-4V	755 (900)	25.4 (0.001)	755 (900)	0.787 (0.031)	0.00
AlBr + 20% Ekonol/Feltmetal	Ti-6Al-4V	755 (900)	254 (0.01)	755 (900)	0.813 (0.032)	0.00
AlBr + 20% Ekonol	Ti-6Al-4V	755 (900)	2.54 (0.0001)	755 (900)	0.762 (0.030)	0.00
AlBr + 20% Ekonol	Ti-6Al-4V	755 (900)	25.4 (0.001)	755 (900)	0.660 (0.026)	0.00
AlBr + 20% Ekonol	Ti-6Al-4V	755 (900)	254 (0.01)	755 (900)	0.940 (0.037)	0.00
AlBr + 20% Ekonol	Inco 718	---	25.4 (0.0001)	867 (1100)	0.737 (0.029)	0.00
AlBr + 20% Ekonol	Inco 718	867 (1100)	25.4 (0.001)	867 (1100)	0.914 (0.036)	0.00
AlBr + 20% Ekonol/Feltmetal	Inco 718	867 (1100)	25.4 (0.001)	867 (1100)	0.711 (0.028)	0.00
AlBr + 20% Ekonol/Feltmetal	Inco 718		25.4 (0.001)	867 (1100)	1.067 (0.042)	0.00

a. Rub Paths; Six Blades, 229 Surface m/sec (750 ft/sec)

	AlBr + 20% Ekonol		AlBr + 20% Ekonol/Feltmetal	
50-Hour Preexposure:	As Sprayed	755 K (900° F)	As Sprayed	755 K (900° F)
Rub No.:	309	313	312	315
Rate, μm/sec:	2.54	2.54	2.54	25.4
(in./sec)	(0.0001)	(0.0001)	(0.0001)	(0.001)
Blade Wear, mm:	0.1043	0	0	0
(in.)	(0.0045)			

Rub No.:	310	314	311	316
Rate, μm/sec:	25.4	25.4	25.4	25.4
(in./sec)	(0.001)	(0.001)	(0.001)	(0.001)
Blade Wear, mm:	0.0508	0	0	0
(in.)	(0.002)			

These rubs were not evaluated.

Rub No.:	344	343	340	339
Rate, μm/sec:	254	254	254	254
(in./sec)	(0.01)	(0.01)	(0.01)	(0.01)
Blade Wear, mm:	0	0	0	0

b. Enlargement of Rub 340 Showing Layering from Material Pullout 6X

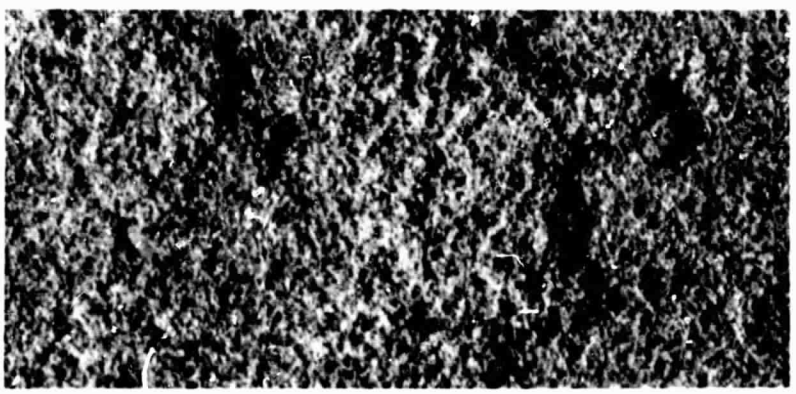

Figure 29. Room-Temperature Rub-Test Panels, AlBr + 20% Ekonol, from Ti-6Al-4V Blade Rubs With and Without Feltmetal 515B Underlayer.

The layering effect seen on the rub paths is related directly to the coating microstructure. The aluminum bronze and Ekonol were deposited in layers with the Ekonol showing up primarily as coarse particles or clumps of particles (note layered structure in Figure 30). Subsequent examination of the spray-process records showed that periodic pulsing occurred in the powder flow as a result of powder-clogging problems. The layering in the coating microstructure probably originated from the pulsing.

The Lynn (elevated temperature) rub-test results are summarized in Table XVII. No blade wear occurred for either Ti-6Al-4V or Inconel 718 blades under the test conditions investigated. These rub panels (Figure 31) also exhibited the layered material-pullout effect seen in the room-temperature rub tests. Rub-force measurements were included in the Lynn tests. Measurable shear forces of 1.8 to 3.1 N (0.4 to 0.7 lbf) were observed for all the 254 μm/sec (0.01 in./sec) incursions into rub panels, with and without Feltmetal 515B underlayer, but no measurable shear forces occurred during rubs at the 25.4 and 2.54 μm/sec (0.001 and 0.0001 in./sec) incursion rate. It must be assumed that the shear forces are related to the higher volume of material removed during a single blade encounter (i.e., greater bite per blade) since no evidence for differences in coating compaction or frictional heating was observed between the high incursion rate and the two lower incursion rates.

Particulate-erosion resistance was also considered since abradable coatings must have the ability to maintain an aerodynamically smooth finish over a long period of time under dust-ingestion conditions encountered in field service. The erosivity tests were conducted on 2.54 x 5.08 cm (1 x 2 in.) flat panels in the manner described earlier (Section 4.1). The results on as-sprayed and preexposed coatings are summarized in Table XVIII. The as-sprayed AlBr + 20% Ekonol showed an erosivity number of 12.9 [seconds to remove 25.4 μm (0.001 in.) of coating]; this is similar to that of Task I, Phase III material. However, the as-sprayed AlBr + 20% Ekonol/Feltmetal had a low erosivity number (≈7). The preexposed coatings with and without Feltmetal produced erosivity numbers ranging from 5.9 to 7.9 and were completely penetrated (see Figure 32).

Thermal-shock samples showed no evidence of cracking, spallation, or blistering on the AlBr + 20% Ekonol or AlBr + 20% Ekonol/Feltmetal coatings. Figure 30 shows macro- and microphotographs of thermal-shock samples. The layered coating structure discussed earlier was particularly evident in the macrophotograph; the microphotograph was typical of the bond-line integrity seen after 50 thermal cycles. Note in the microphotograph that there is little evidence of oxidation even though the Ekonol has burned out completely.

The ability to produce an aerodynamically smooth finish on fabricated material has been an important consideration in selecting seal materials at General Electric. Therefore, machinability was investigated by single-point turning and precision-grinding processes. Figure 33 shows the tooling set-up, and Table XIX gives the machinability test plan that was investigated. The best results obtained by each method are shown in Figue 34. Grinding produced the best finish on the as-sprayed coatings: 1.37 and 1.45 μm (54 and 57 microinch) AA. The best finish obtained by turning was 4.95 μm (195

a. Ti-6Al-4V Blades (48), 152 Surface m/sec (500 ft/sec) Tip Speed, 755 K (900° F); Preexposure was 50 Hours at 755 K (900° F)

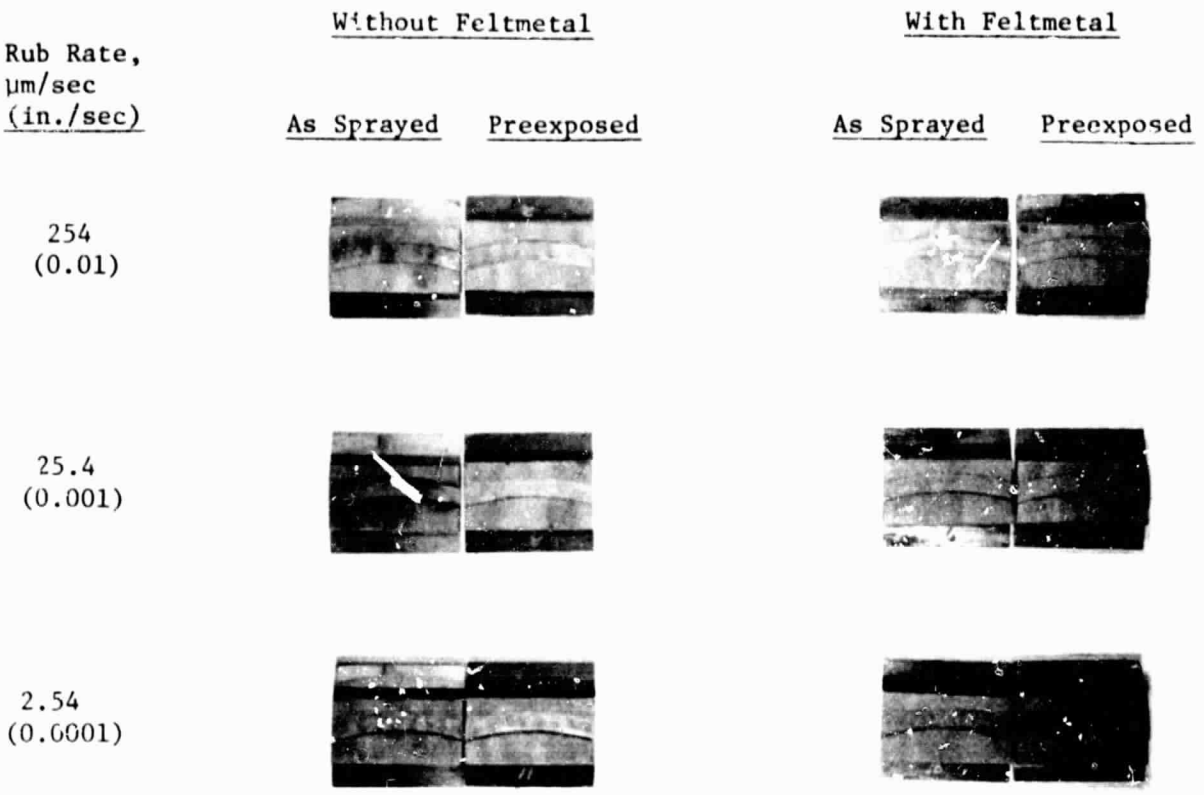

b. Inco 718 Blades (48), 152 Surface m/sec (500 ft/sec) Tip Speed, 867 K (1100° F); Preexposure was 50 Hours at 867 K (1100° F)

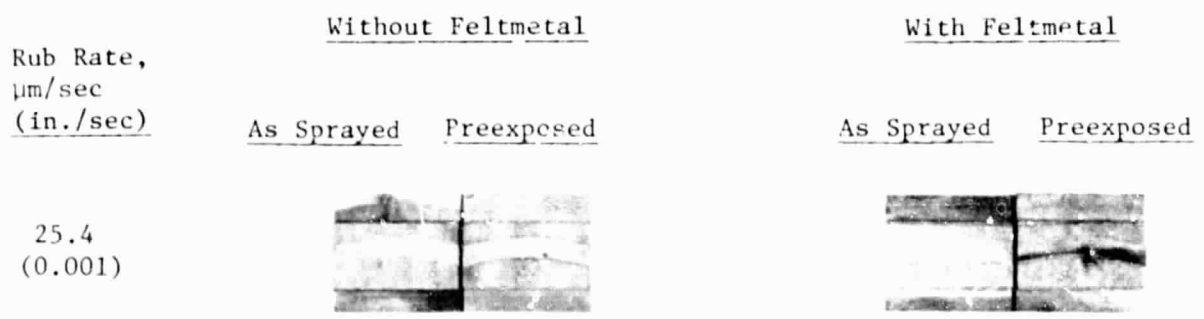

Figure 30. Elevated-Temperature Rub-Test Panels, AlBr + 20% Ekonol, With and Without Feltmetal Underliner.

Table XVII. AlBr + 20% Ekonol Elevated-Temperature Rub Test.

- All tests conducted with six blades at 228 m/sec (750 ft/sec) Tip Speed.

Coating	Blade Material	Temperature of 50-Hour Coating Preexposure, K (° F)	Incursion Rate, μm/sec (in./sec)	Coating Wear, mm (in.)	Blade Wear, mm (in.)
AlBr + 20% Ekonol	Ti-6Al-4V	---	2.54 (0.0001)	0.229 (0.009)	0.114 (0.0045)
AlBr + 20% Ekonol	Ti-6Al-4V	---	25.4 (0.001)	0.152 (0.006)	0.051 (0.002)
AlBr + 20% Ekonol	Ti-6Al-4V	---	254 (0.01)	0.813 (0.032)	0.000
AlBr + 20% Ekonol	Ti-6Al-4V	755 (900)	2.54 (0.0001)	0.889 (0.035)	0.000
AlBr + 20% Ekonol	Ti-6Al-4V	755 (900)	25.4 (0.001)	0.838 (0.033)	0.000
AlBr + 20% Ekonol	Ti-6Al-4V	755 (900)	254 (0.01)	0.889 (0.035)	0.000
AlBr + 20% Ekonol	Inco 718	---	2.54 (0.0001)	0.635 (0.025)	0.000
AlBr + 20% Ekonol	Inco 718	---	25.4 (0.001)	0.635 (0.025)	0.000
AlBr + 20% Ekonol	Inco 718	---	254 (0.01)	0.864 (0.034)	0.000
AlBr + 20% Ekonol	Inco 718	755 (900)	2.54 (0.0001)	0.914 (0.036)	0.000
AlBr + 20% Ekonol	Inco 718	755 (900)	25.4 (0.001)	1.016 (0.040)	0.000
AlBr + 20% Ekonol	Inco 718	867 (1100)	25.4 (0.001)	0.737 (0.029)	0.000
AlBr + 20% Ekonol/Feltmetal	Ti-6Al-4V	---	2.54 (0.0001)	1.016 (0.040)	0.000
AlBr + 20% Ekonol/Feltmetal	Ti-6Al-4V	---	25.4 (0.001)	0.813 (0.032)	0.000
AlBr + 20% Ekonol/Feltmetal	Ti-6Al-4V	---	254 (0.01)	0.787 (0.031)	0.000
AlBr + 20% Ekonol/Feltmetal	Ti-6Al-4V	755 (900)	2.54 (0.0001)	0.889 (0.035)	0.000
AlBr + 20% Ekonol/Feltmetal	Ti-6Al-4V	755 (900)	25.4 (0.001)	0.813 (0.032)	0.000
AlBr + 20% Ekonol/Feltmetal	Ti-6Al-4V	755 (900)	254 (0.01)	0.965 (0.038)	0.000
AlBr + 20% Ekonol/Feltmetal	Inco 718	---	2.54 (0.0001)	0.864 (0.034)	0.000
AlBr + 20% Ekonol/Feltmetal	Inco 718	---	25.4 (0.001)	0.737 (0.029)	0.000
AlBr + 20% Ekonol/Feltmetal	Inco 718	---	254 (0.01)	0.914 (0.036)	0.000
AlBr + 20% Ekonol/Feltmetal	Inco 718	755 (900)	2.54 (0.0001)	0.838 (0.033)	0.000
AlBr + 20% Ekonol/Feltmetal	Inco 718	755 (900)	25.4 (0.001)	0.864 (0.034)	0.000
AlBr + 20% Ekonol/Feltmetal	Inco 718	867 (1100)	25.4 (0.001)	0.737 (0.029)	0.000

No Feltmetal

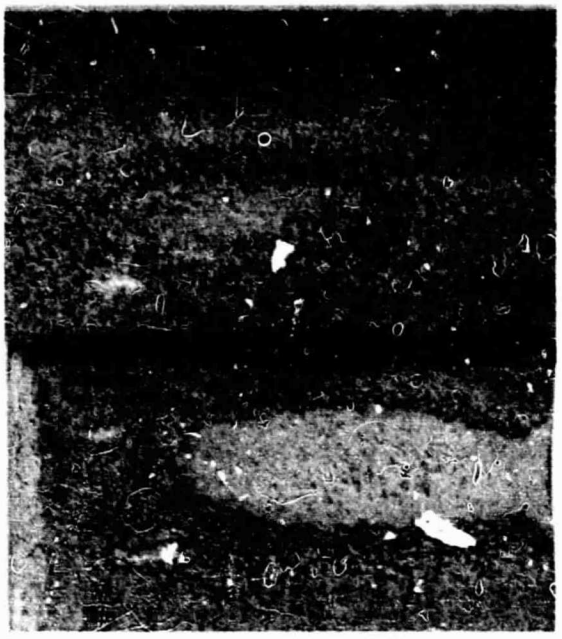

With Feltmetal Underliner

Figure 31. Erosion Samples of AlBr + 20% Ekonol.

Table XVIII. Erosion Test Results.

- All tests conducted at room temperature using 600 g of 50-μm Al_2O_3 powder with a 20° impingement angle.

Coating	Temperature of 50-Hour Coating Preexposure, K (° F)	Erosivity*
AlBr + 20% Ekonol	- -	12.9
AlBr + 20% Ekonol	- -	12.9
AlBr + 20% Ekonol	755 (900)	7.7
AlBr + 20% Ekonol	755 (900)	6.7
AlBr + 20% Ekonol	867 (1100)	7.2
AlBr + 20% Ekonol	867 (1100)	7.7
AlBr + 20% Ekonol/Feltmetal	- -	7.0
AlBr + 20% Ekonol/Feltmetal	- -	7.1
AlBr + 20% Ekonol/Feltmetal	755 (900)	5.9
AlBr + 20% Ekonol/Feltmetal	755 (900)	5.9
AlBr + 20% Ekonol/Feltmetal	867 (1100)	7.0
AlBr + 20% Ekonol/Feltmetal	867 (1100)	6.9

*Seconds to erode 25.4 μm (1 mil)

a. Macrophotographs: Note Layered Structures 2X

AlBr + 20% Ekonol,
M152 Substrate

AlBr + 20% Ekonol,
Feltmetal 515B,
M152 Substrate

b. Microphotograph: AlBr + 20% Ekonol Showing Bondline 50X

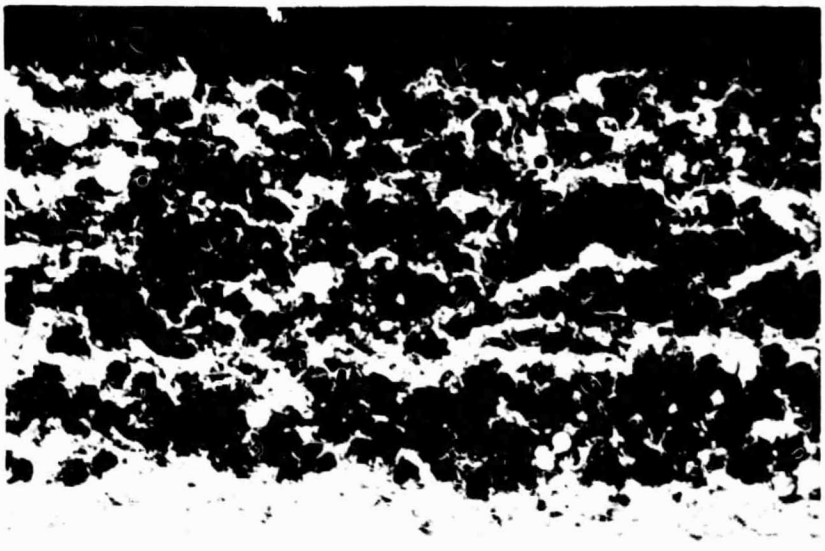

AlBr + 20% Ekonol

} M450 Bondcoat

M152 Substrate

Figure 32. Thermal-Shock Specimens.

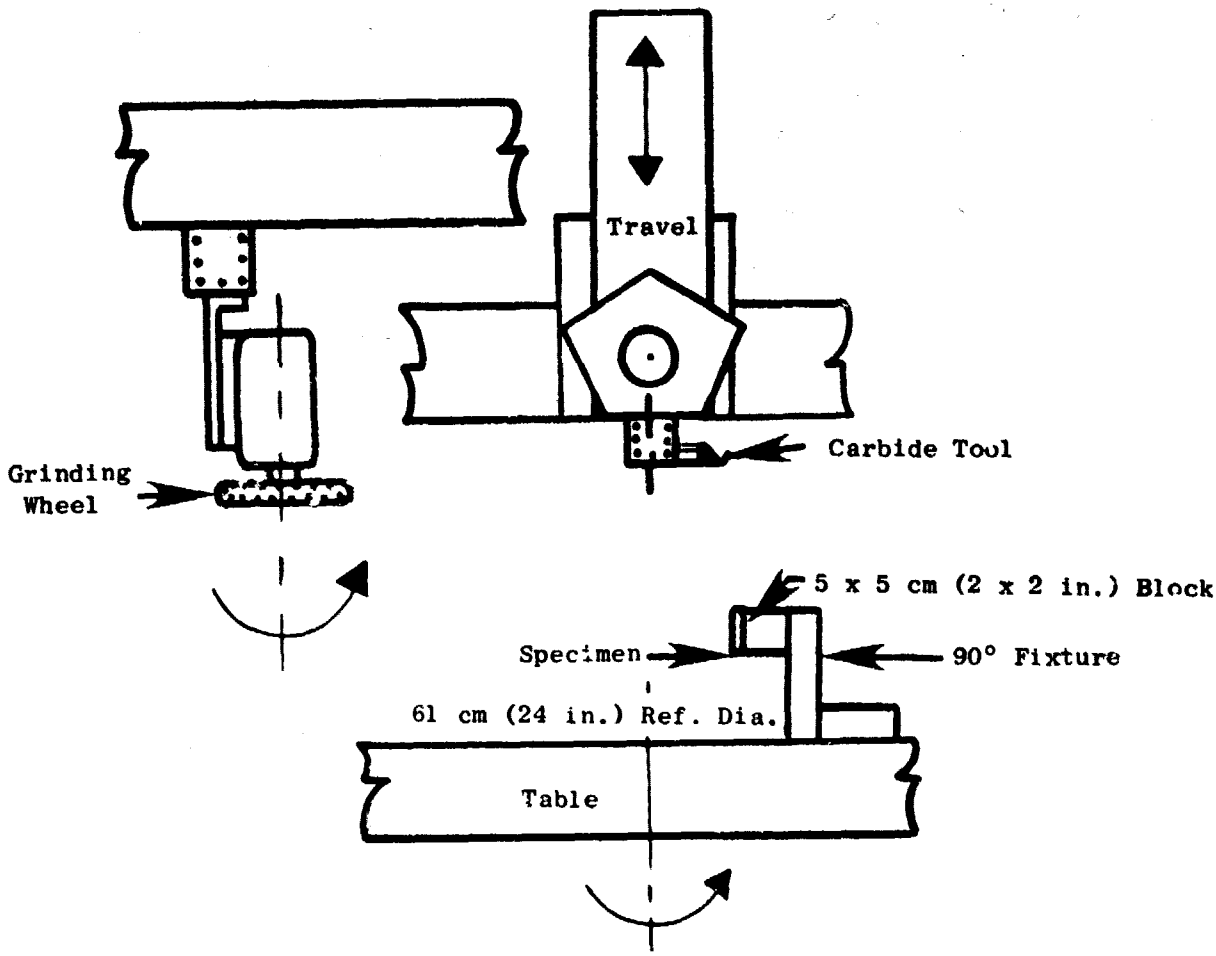

Figure 33. Single-Point Turn and Precision Grind.

a. AlBr + 20% Ekonol, Turned, 4.95 µm (195 µin) AA

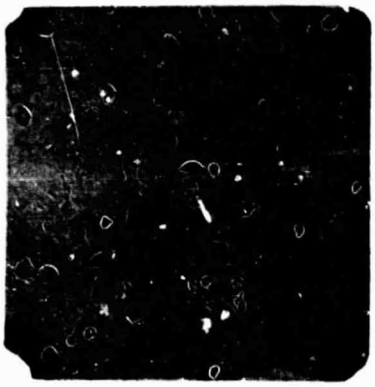

b. AlBr + 20% Ekonol/Feltmetal, Turned, 4.95 µm (195 µin) AA

c. AlBr + 20% Ekonol, Ground, 1.45 µm (57 µin) AA

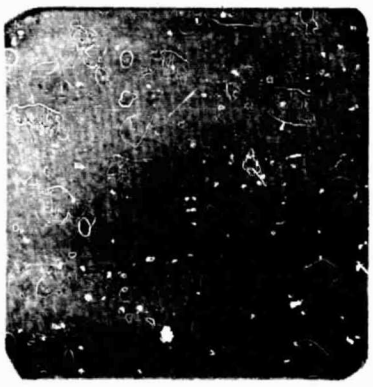

d. AlBr + 20% Ekonol/Feltmetal, Ground, 1.37 µm (57 µin) AA

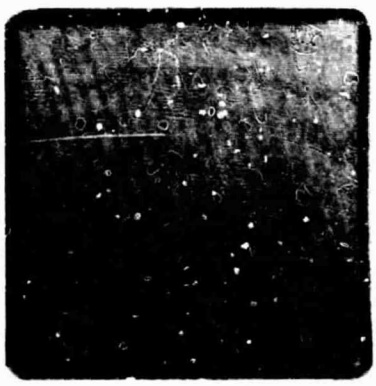

Figure 34. Best Finishes by Turning and Grinding. AlBr + 20% Ekonol.

Table XIX. Machinability-Test Plan.

Test No.	Material	Single-Point Turn[1]				Precision Grind[2]			
		Work Speed, Surface m/sec (ft/min)		Feed, mm/Rev (in./Rev)		Work Speed, Surface m/sec (ft/min)		Feed, mm/Rev (in./Rev)	
1.	AlBr Ekonol	1.02	(200)	0.127	(0.005)	0.25	(50)	0.762	(0.030)
2.	AlBr Ekonol	2.54	(500)	0.127	(0.005)	0.25	(50)	2.540	(0.100)
3.	AlBr Ekonol	1.02	(200)	0.254	(0.010)	0.51	(100)	0.762	(0.030)
4.	AlBr Ekonol	2.54	(500)	0.254	(0.010)	0.51	(100)	2.540	(0.100)
5.	AlBr Ekonol	Optional		---		Optional		---	
6.	AlBr Ekonol/ Feltmetal	1.02	(200)	0.127	(0.005)	0.25	(50)	0.762	(0.030)
7.	AlBr Ekonol/ Feltmetal	Optional		---		Optional		---	

1. Depth of cut: 0.127 mm (0.005 in.), coolant: dry, work diameter: 0.61 m (24 in.), toolholder: Style A; TPG433 Grade 883 carbide insert.

2. Wheel speed: 13.7 surface m/sec (2700 ft/min) with a 152 mm (6 in.) diameter, 25.4 mm (1 in.) wide, Grade A46K10V grinding wheel; 0.000 to 0.102 mm (0.004 in.) in-feed traverse, dry coolant; grinding wheel trued by diamond dressing and edges hand-radiused thereafter.

microinch) AA. The recommended machining conditions for consistently obtaining smooth surface finishes less than 1.60 μm (63 microinch) AA are as follows:

Equipment : Precision Grinder
Work Speed : 254 Surface mm/sec (50 tt/min)
Wheel Speed : 13.7 Surface m/sec (2700 ft/min)
Wheel Grade : A46 J8V (or equivalent)
In-feed : 0.000 to 0.102 mm (0.004 in.) Traverse
Traverse : 0.406 mm (0.016 in.) per Revolution
Coolant : Dry
Truing : Diamond-dress and hand-radius edges

The conclusions drawn from the first-iteration testing of AlBr + 20% Ekonol with and without the Feltmetal 515B underlayer were:

1. The sprayed-coating microstructure needs to be improved. The large Ekonol particles and layering of the aluminum bronze and Ekonol resulted in an unacceptably rough rub surface.

2. The aluminum bronze powder mesh analysis was still different from the targeted mesh analysis, but it resulted in coatings with good abradability at room temperature and 755 K (900° F) for Ti-6Al-4V blades and room temperature and 867 K (1100° F) for Inconel 718 blades.

3. The erosion resistance of the AlBr + 20% Ekonol coating was marginal at best, and after exposure it deteriorated to unacceptable levels due to the Ekonol burning out. The erosion resistance of the AlBr + 20% Ekonol/Feltmetal 515B was unacceptable in the as-sprayed and preexposed conditions. The low thermal conductivity of the Feltmetal underlayer apparently insulated the AlBr/Ekonol from the substrate enough to allow a temperature rise sufficient to soften the Ekonol. This eliminated the beneficial structural support the Ekonol provided to the otherwise porous aluminum bronze structure.

4. The coatings had good thermal-cycle capability and oxidation resistance.

5. Smooth-surface-finish capability was very good when the coating was ground in the as-sprayed condition.

4.4.4 Second-Iteration Coating

The second-iteration coating ended up as an AlBr + 15% Ekonol (by weight) composition as a result of an effort to improve the coating microstructure. It was recognized that careful control of coating microstructure would be essential for the success of a porous aluminum bronze abradable-seal material. In first-iteration testing, the layering of AlBr and Ekonol adversely affected rub-surface finishes and may have played a role in the marginal erosion resistance. The goal of obtaining a homogeneous microstructure in the aluminum bronze/Ekonol spray coating was approached by: (1) reducing the powder size for the Ekonol and (2) spraying the coatings in the new Material and Process Technology Laboratories (MPTL) thermal-spray facility at Evendale where closer process control was maintained.

Preliminary efforts defined handling problems with Ekonol powder and the blended aluminum bronze/Ekonol powders. These were caused by static-charge buildup and excessive moisture retention in the Ekonol. The corrective measures applied included:

1. The Ekonol (polyester plastic) was treated with a home-laundry antistatic solution such as those used on polyester clothing.

2. The treated Ekonol powder was thoroughly dried at temperatures in excess of 339 K (150° F) for a minimum of several hours.

3. The Ekonol was screened to obtain -200 mesh powder.

4. The blending time and subsequent handling of the blended, dry powders were minimized.

A quick hand-spray evaluation was made using the Task I; Phase III spray parameters (Section 4.2.3.1). The resulting AlBr + 20% Ekonol coating microstructure (Figure 35) exhibited good homogeneity of the Ekonol component. However, checks on the coating density (2.50 Mg/m^3), coating cohesive strength [3.1 MPa (462 psi)], and erosivity number (8.5) indicated that a reduced Ekonol content was necessary. On that basis, a second blend of AlBr + 15% Ekonol was prepared and sprayed following the newly developed procedures. Specimens prepared included Evendale and Lynn panels, density/erosion panels, tensile-bond buttons, and thermal-shock samples. Typical microstructures of the as-sprayed and preexposed [755 K (900° F)/50 hours] second-iteration coatings are shown in Figure 36. The density of the as-sprayed coating was 3.06 Mg/m^3, and the desired homogeneous Ekonol distribution was achieved. The microstructure of the 867 K (1100° F) preexposed coating was similar to that of the 755 K (900° F) preexposed coating; both showed complete burnout of the Ekonol. (The resultant porosity has been epoxy-filled during the mounting for metallographic preparation.)

The results of erosivity and coating-cohesive-strength tests, summarized in Table XX, indicated the as-sprayed coating had an erosivity of 10 to 11 seconds per 25.4 μm (0.001 in.) of material removed and a strength of 4.0 MPa (595 psi). The lower erosivity number for the 15% Ekonol coating relative to the first-iteration (20% Ekonol) coating can be attributed to not having to penetrate dense aluminum bronze layers periodically. The preexposed second-iteration coating erosion samples showed the same erosivity numbers as those from first-iteration tests (6.5 to 7.5), but the numbers by themselves were misleading. The AlBr + 15% Ekonol erosion samples (Figure 37) clearly had a much smaller volume of material removed than the AlBr + 10% Ekonol (Figure 32) even though the penetration rate was nearly the same. The AlBr coating strength decreased as a result of burning out the Ekonol during the preexposures. More will be said about the effects of preexposure on erosion resistance and coating strength in Section 4.5.

Thermal-shock samples were run as described previously. No evidence of cracking, spallation, or blistering were seen after 50 thermal-exposure cycles. Metallography confirmed the excellent bond-line integrity at the AlBr/M450 bond coat and the M450/M152 substrate interfaces (Figure 38).

A set of as-sprayed and preexposed AlBr + 15% Ekonol samples were machined by the grinding parameters established for the first-iteration coating. The as-sprayed coating consistently gave excellent surface finishes of 0.635 to 1.270 μm (25 to 50 microinch) AA. The preexposed [755 K (900° F)/50 hours] samples exhibited rough areas [9.78 μm (385 μin.) AA] covering up to 50% of the ground surface on some samples. The remainder of the surface was a smeared aluminum bronze layer with a [0.885 to 1.016 μm (35 to 40 μin.) AA] finish. Figure 39 shows typical machined surfaces on as-sprayed and preexposed coatings.

Figure 35. Preliminary, Hand-Sprayed, Second-Iteration AlBr + 20% Ekonol Showing a More Homogeneous Microstructure. 50X

Table XX. Erosion and Coating-Cohesive-Strength Test Results for AlBr + 15% Ekonol Coating.

- All erosion tests were conducted at room temperature using 600 g of 50-μm Al_2O_3 powder with a 20° impingement angle.
- Cohesive-strength data are average of three samples from one spraying.

Temperature of 50-Hour Coating Preexposure, K (° F)	Erosivity*	Cohesive Strength, MPa (psi)
---	10.20	4.10 (595)
---	10.93	
755 (900)	7.30	3.45 (500)
755 (900)	7.40	
755 (900)	6.60	
867 (1100)	6.65	3.16 (458)
867 (1100)	7.05	
867 (1100)	6.93	

*Seconds to erode 25.4 μm (1 mil).

a. As-Sprayed; Well-Distributed Ekonol Phase

b. Preexposed at 755 K (900° F)/50 Hours;
Complete Ekonol Burnout

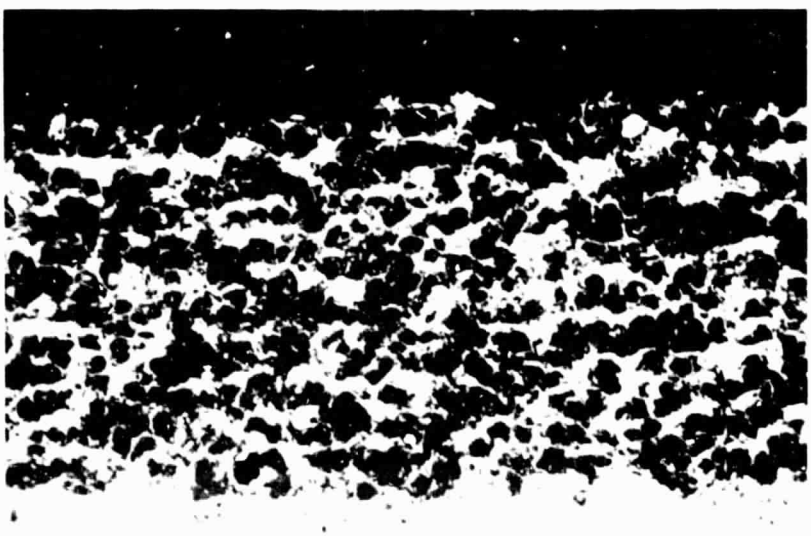

Figure 36. AlBr + 15% Ekonol Coatings. 50X

a. As Sprayed

b. Preexposed at 755 K (900° F)/50 Hours

c. Preexposed at 867 K (1100° F)/50 Hours

Figure 37. AlBr + 15% Ekonol Erosion Samples.

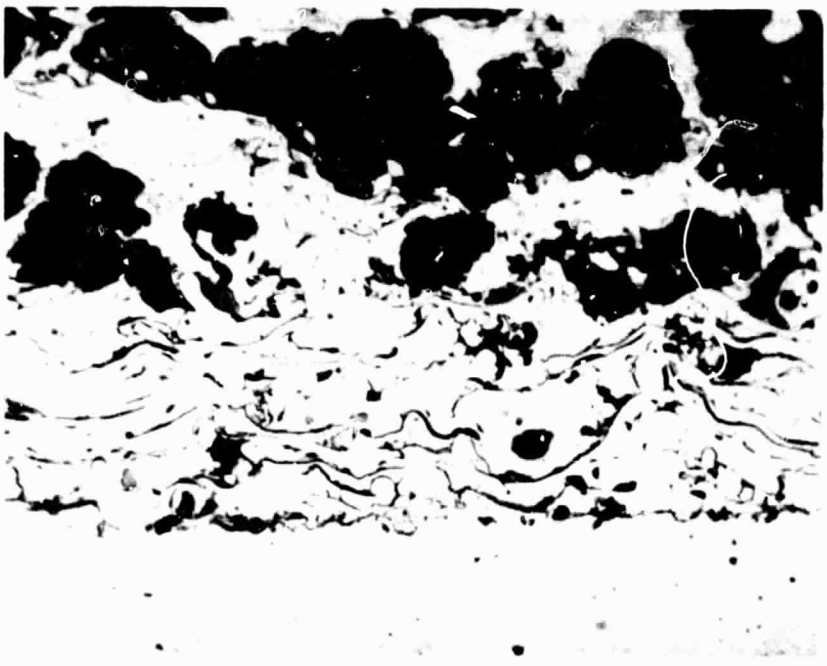

Figure 38. AlBr Thermal-Cycle-Panel Bond Lines. 250X

a. As Sprayed, 0.635 to 1.27 μm (25 to 50 μin) AA

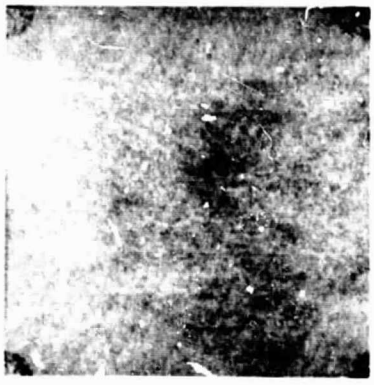

b. Preexposed at 755 K (900° F)/50 Hours, 0.89 to 0.92 μm (35 to 40 μin) AA in Smeared Areas and Typically 9.78 μm (385 μin) AA in Rough Areas

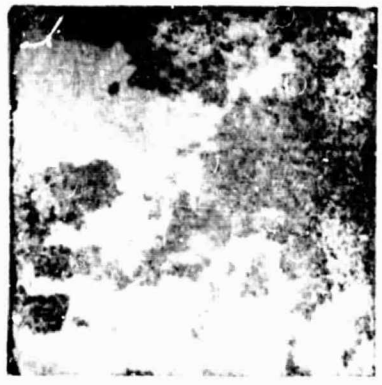

Figure 39. AlBr + 15% Ekonol Machinability Samples.

The Evendale room-temperature and Lynn elevated-temperature rub results are given in Tables XXI and XXII. Titanium blade wear against the as-sprayed AlBr + 15% Ekonol was higher than for the AlBr + 20% Ekonol in room-temperature rubs. This titanium blade wear decreased as the incursion rate increased and was eliminated for all except the 2.54 μm (0.0001 in./sec) incursion rate in the preexposed coatings where the Ekonol was burned out. No blade wear occurred for any of the Inconel 718 blade room-temperature rubs.

In the Lynn elevated-temperature tests, some difficulties in temperature control resulted in two of the 755 K (900° F) Ti-6Al-4V blade tests being conducted at 810 K (1000° F). The as-sprayed AlBr 15% Ekonol coating showed zero blade wear at the 2.54 μm/sec (0.0001 in./sec) incursion rate and 50.8 μm (0.002 in.) of blade wear at the 25.4 μm/sec (0.001 in./sec) incursion rate; prior to the latter test, a 15-minute exposure to a large overtemperature was experienced and may account for this unexpected result.

The preexposed sample tested at the 2.54 μm/sec (0.0001 in./sec) incursion rate showed 127 μm (0.005 in.) of blade wear. Inspection of the rub sample indicated the incursion depth was sufficient to penetrate the AlBr/Ekonol, rub the M450 bond coat, and wear the blades.

The as-sprayed coating was also tested at 867 K (1100° F) with Inconel 718 blades. The incursion rate was 25.4 μm/sec (0.001 in./sec), and it gave 50.8 μm (0.002 in.) of blade wear. Metallographic studies were conducted on the AlBr + 15% Ekonol rub paths. The appearance of the second-iteration, room-temperature rub surfaces (Figure 40) was improved over the AlBr + 20% Ekonol; material pullout due to the layered microstructure was eliminated. Areas under the rub paths show compaction of the coating in room-temperature rub tests. Coating microstructures from rub areas of the 254 μm/sec (0.01 in./sec) incursion-rate tests at room temperature are shown for Ti-6Al-4V blades in Figure 41 and Inconel 718 blades in Figure 42. Little or no coating densification and scabbing were seen at the rub surface even when significant blade wear occurred. This was apparent from the sections through the rub path for the 2.54 μm/sec (0.0001 in./sec) incursion-rate, as-sprayed-coating, room-temperature, rub test with Ti-6Al-4V blades (Figure 43).

This was not always the case with the elevated-temperature rubs (Lynn rub tests). For the 2.54 μm/sec (0.0001 in./sec) incursion rate with Ti-6Al-4V blades on the as-sprayed coating, little or no compaction was observed at the rub surface (Figure 44). The titanium blades showed a very thin AlBr transfer layer across most of the blade tip and an extremely small plastic-deformation zone on the leading edge only (Figure 45). In contrast, Figure 46 shows the longitudinal and transverse sections taken through the rub path of the 25.4 μm/sec (0.001 in./sec) incursion-rate, elevated-temperature rub test on the as-sprayed coating with Ti-6Al-4V blades. Scabbed areas over compacted coating regions are evident in these microphotographs. The titanium blades from this test showed buildup on the leading edges and a small amount of martensite formation on the trailing edges (Figure 47).

Table XXI. AlBr + 15% Ekonol Room-Temperature Rub Test.

- Antistatic-Treated, -200 Mesh Ekonol Powder
- Six Blades at 228 Surface m/sec (750 ft/sec) Tip Speed

Blade	Temperature of 50-Hour Coating Preexposure, K (° F)	Incursion Rate, μm/sec (in./sec)	Coating Wear, μm (in.)	Blade Wear, μm (in.)
Ti-6Al-4V	---	2.54 (0.0001)	0.229 (0.009)	0.216 (0.0085)
Ti-6Al-4V	---	25.4 (0.001)	0.406 (0.016)	0.089 (0.0035)
Ti-6Al-4V	---	254 (0.01)	0.533 (0.021)	0.013 (0.0005)
Ti-6Al-4V	755 (900)	2.54 (0.0001)	0.533 (0.021)	0.013 (0.0005)
Ti-6Al-4V	755 (900)	25.4 (0.001)	0.533 (0.021)	0.000
Ti-6Al-4V	755 (900)	25.4 (0.001)	0.762 (0.030)*	0.000
Inco 718	---	2.54 (0.0001)	0.533 (0.021)	0.000
Inco 718	---	25.4 (0.001)	0.533 (0.021)	0.000
Inco 718	---	254 (0.01)	0.686 (0.027)	0.000
Inco 718	755 (900)	2.54 (0.0001)	0.559 (0.022)	0.000
Inco 718	755 (900)	25.4 (0.001)	0.553 (0.021)	0.000
Inco 718	867 (1100)	2.54 (0.0001)	0.584 (0.023)	0.000

*AlBr pickup on blade tips; 0.711 mm (0.028 in.) incursion.

Table XXII. AlBr + 15% Ekonol Elevated-Temperature Rub Test.

- Antistatic-Treated, -200 Mesh, Ekonol Powder
- Forty-Eight Blades at 152 Surface m/sec(500 ft/sec) Tip Speed

Blade Material	Temperature of 50-Hour Coating Preexposure K (° F)	Incursion Rate, μm/sec (in./sec)	Test[1] Temperature K (° F)	Coating Wear, μm (in.)	Blade Wear, μm (in.)
Ti-6Al-4V	---	2.54 (0.0001)	755 (900)	1.067 (0.042)	0.000
Ti-6Al-4V	---	25.4 (0.001)	811 (1000)[2]	1.016 (0.040)	0.051 (0.002)
Ti-6Al-4V	755 (900)	2.54 (0.0001)	811 (1000)	0.813 (0.032)	0.127 (0.005)[3]
Inco 718	---	25.4 (0.001)	867 (1100)	0.584 (0.023)	0.051 (0.002)

1. Temperature-control problems encountered.
2. Sample underwent a 15-minute, high-overtemperature exposure.
3. Blades were through the coating, into the bond coat; t[illegible] caused blade wear.

a. Uniform Rub Paths; Six Blades, 229 Surface m/sec (750 ft/sec)

	Ti-6Al-4V Blades		Inco 718 Blades		
50-Hour Preexposure:	As Sprayed	755 K (900° F)	As Sprayed	755 K (900° F)	867 K (1100° F)
Rub No.:	491	493	514	515	520
Rate, µm/sec:	2.54	2.54	2.54	2.54	2.54
(in./sec)	(0.0001)	(0.0001)	(0.0001)	(0.0001)	(0.0001)
Blade Wear, mm:	0.2159	0.0127	0	0	0
(in.)	(0.0085)	(0.0005)			
Rub No.:	492	494	Test	516	
Rate, µm/sec:	25.4	254	Not	25.4	
(in./sec)	(0.001)	(0.01)	Valid	(0.001)	
Blade Wear, mm:	0.0889	0.00		0	
(in.)	(0.0035)				
Rub No.:	496	495	517	518	
Rate, µm/sec:	254	2.54	2.54	254	
(in./sec)	(0.01)	(0.001)	(0.001)	(0.01)	
Blade Wear, mm:	0.0127	0.00	0	0	
(in.)	(0.0005)				
Rub No.:			519		
Rate, µm/sec:			254		
(in./sec)			(0.01)		
Blade Wear, mm			0		

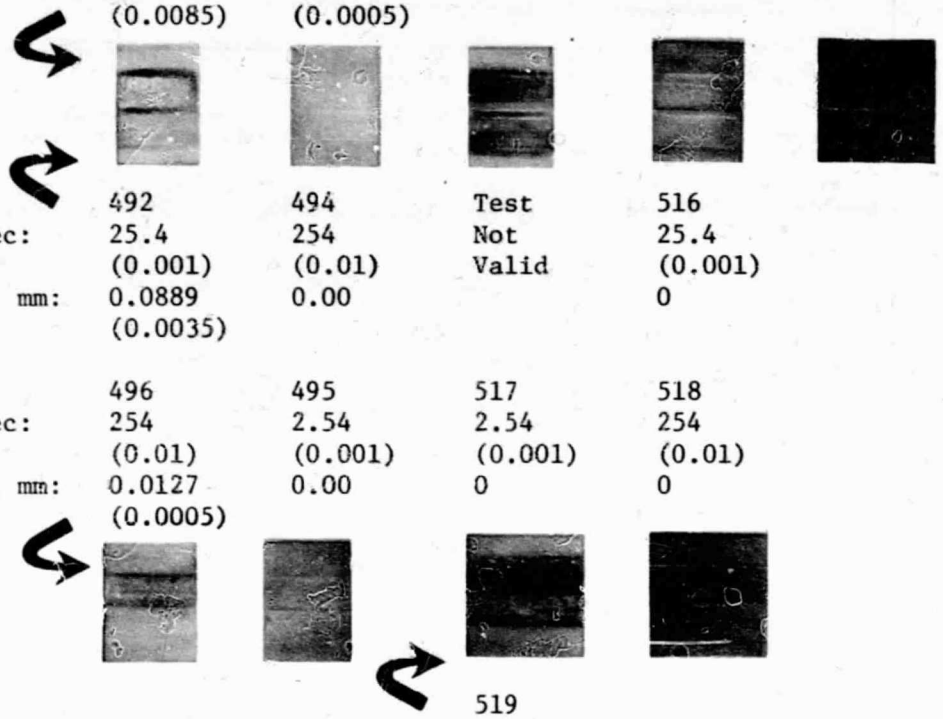

b. Enlargement of Typical Rub Shows Absence of Layered Surface (See Figure 29) 6X

Figure 40. AlBr + 15% Ekonol Room-Temperature-Rub Panels.

C-2

a. As Sprayed

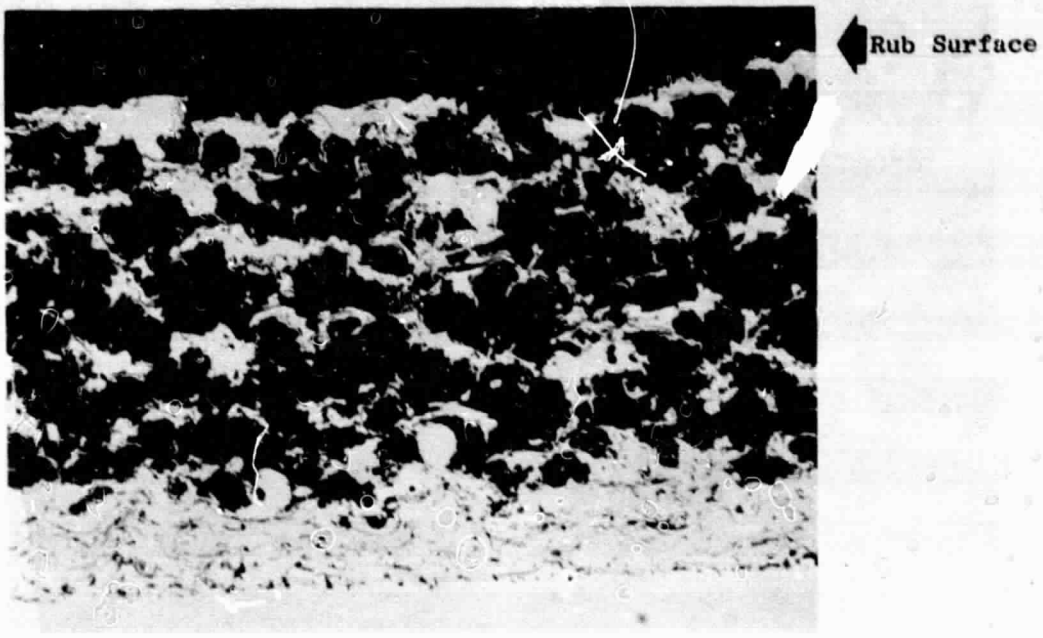

b. Preexposed at 755 K (900° F)/50 Hours

Figure 41. Rub Paths for AlBr + 15% Ekonol with Ti-6Al-4V Blades at Room Temperature, 254 μm/sec (0.01 in./sec) Incursion Rate. 100X

a. As Sprayed

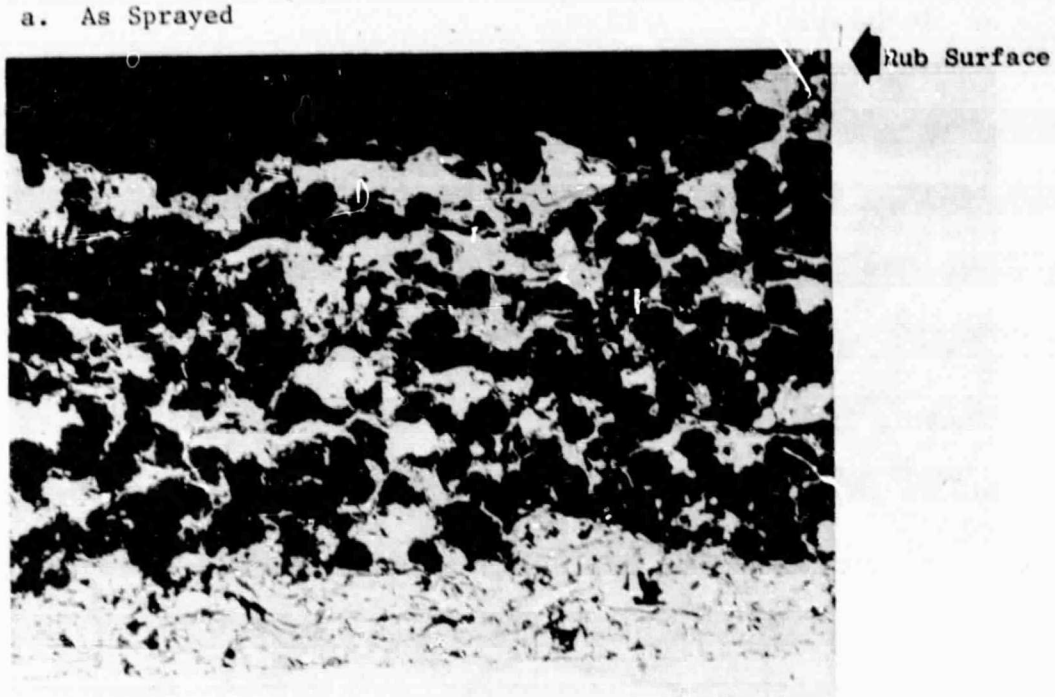

b. Preexposed at 755 K (900° F)/50 Hours

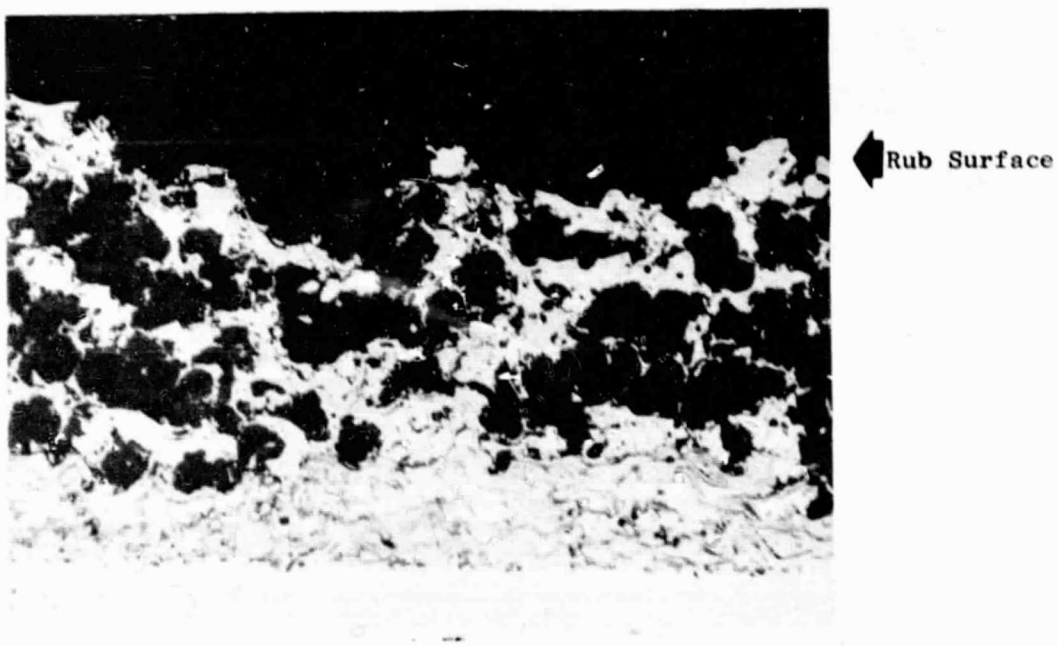

Figure 42. Rub Paths for AlBr + 15% Ekonol with Inco 718 Blades at Room Temperature, 254 μm/sec (0.01 in./sec) Incursion Rate. 100X

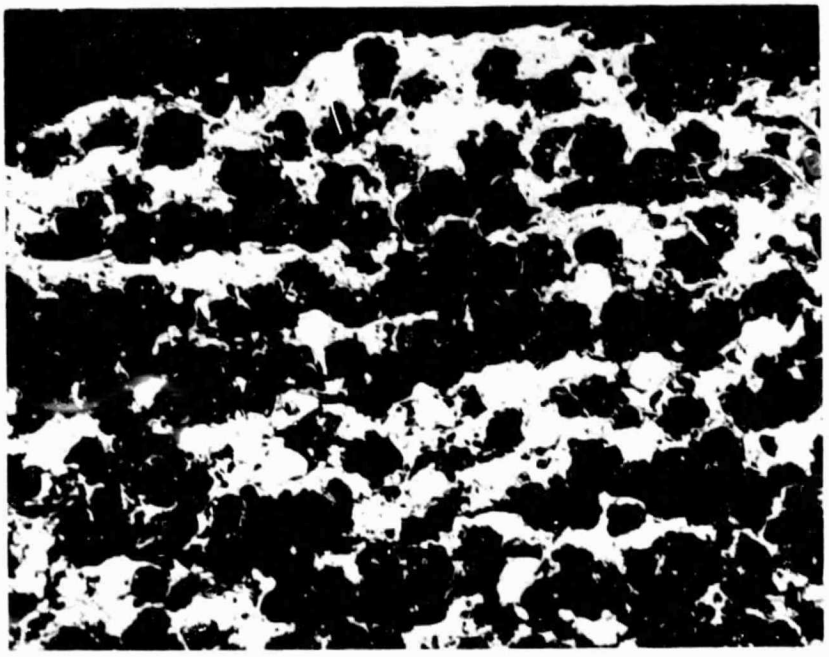

Figure 43. Ti-6Al-4V Blades, Area Under Rub Path for Room-Temperature Rub on As-Sprayed AlBr + 15% Ekonol at the 2.54 µm/sec (0.0001 in./sec) Incursion Rate. 100X

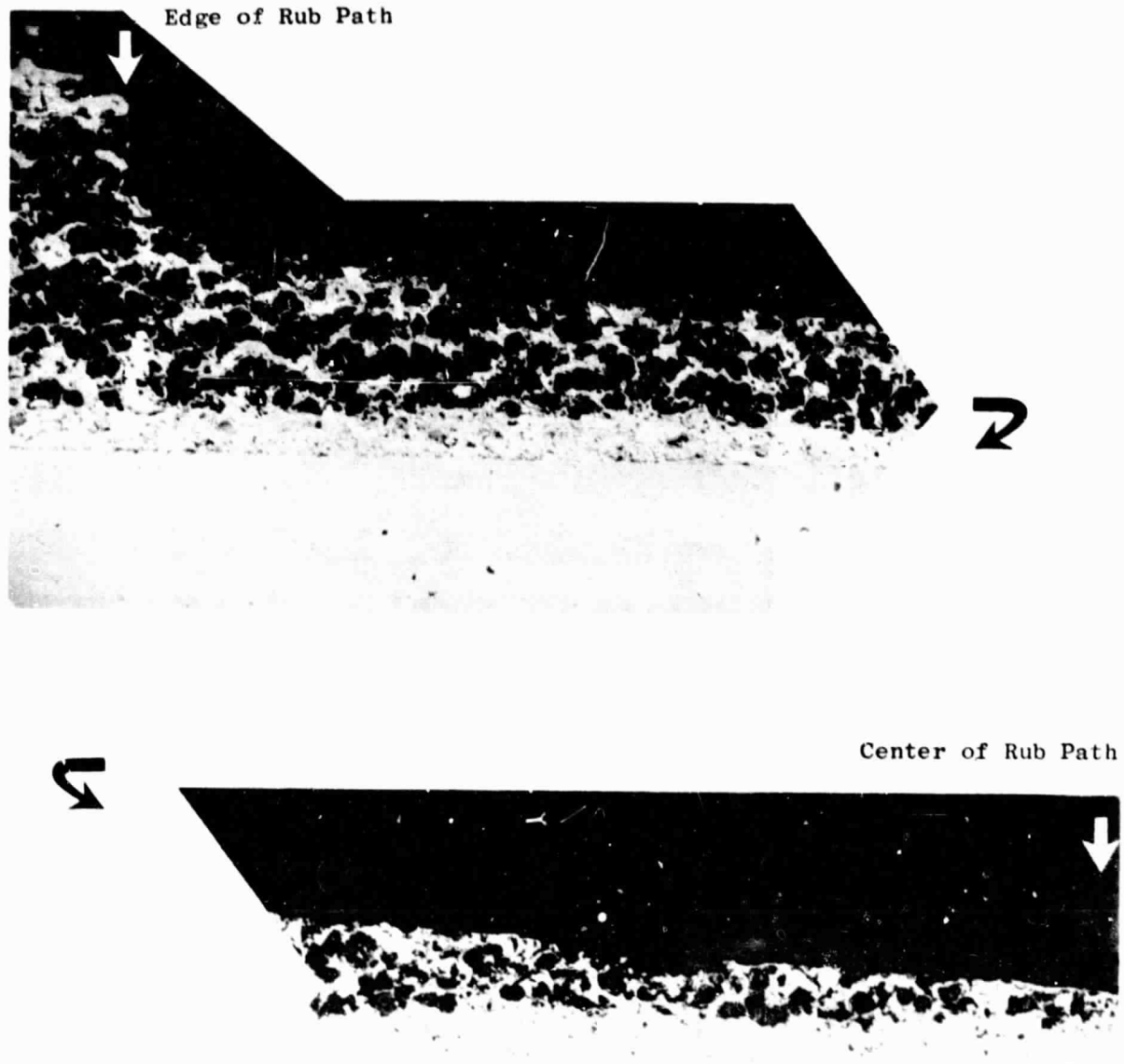

Figure 44. Elevated-Temperature Rub with Ti-6Al-4V Blades at the 2.54 μm/sec (0.0001 in./sec) Incursion Rate. 50X

a. Thin AlBr Layer at Tip 250X

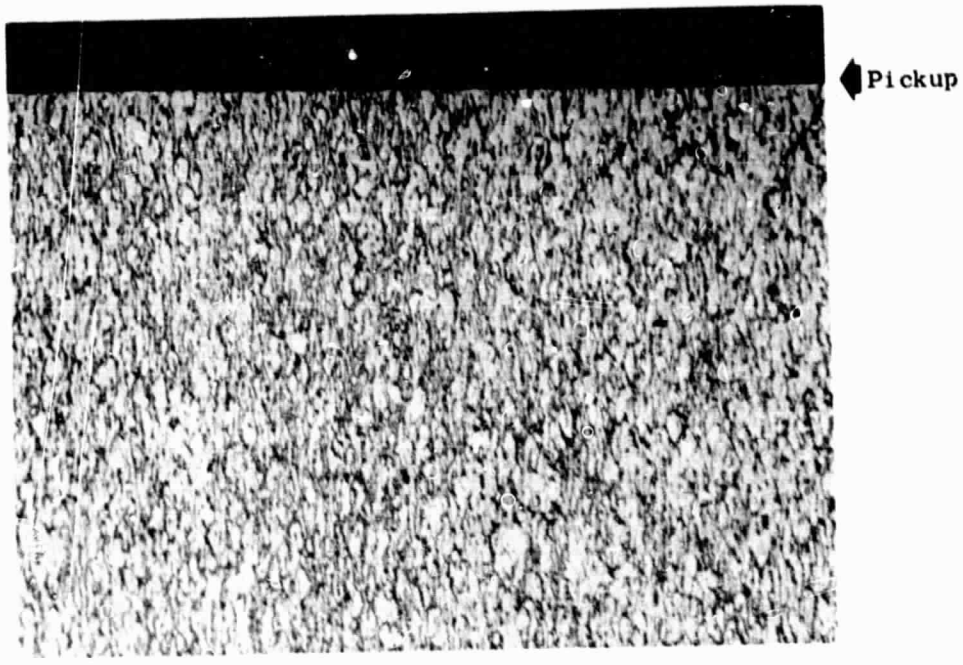

b. Plastic Deformation on Leading Edge 750X

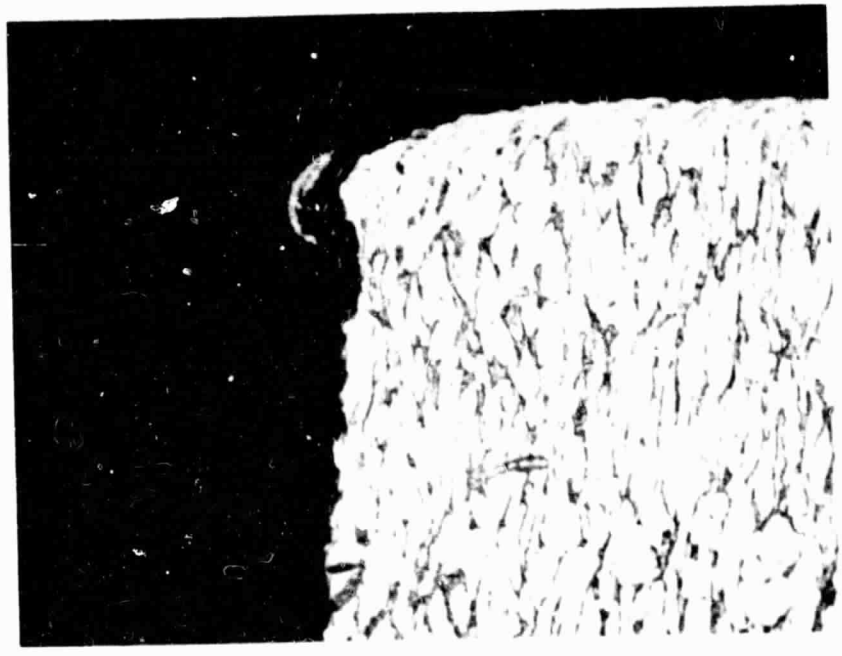

Figure 45. Ti-6Al-4V Blade from 2.54 μm/sec (0.0001 in./sec)/ 755 K (900° F) Rub on AlBr + 15% Ekonol.

a. Transverse Section Under Rub

b. Longitudinal Section Under Rub

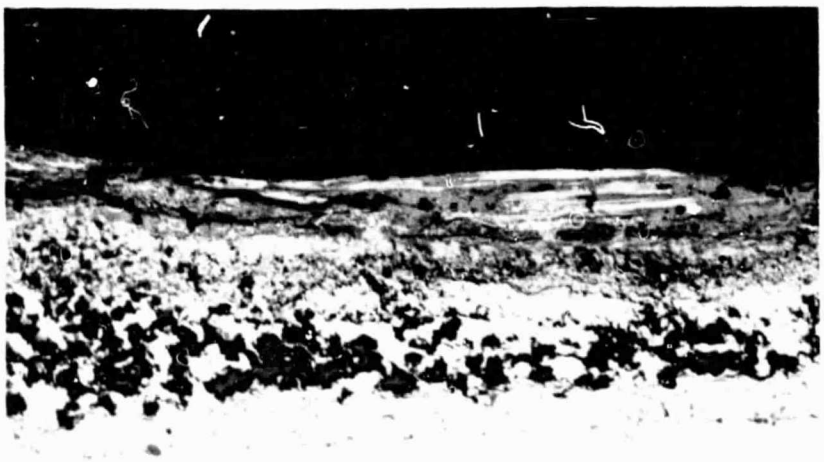

Figure 46. Elevated-Temperature Rubs on AlBr + 15% Ekonol with Ti-6Al-4V Blades at 25.4 μm/sec (0.001 in./sec) Incursion Rate. 50X

a. Blade Tip with Leading-Edge Buildup 100x

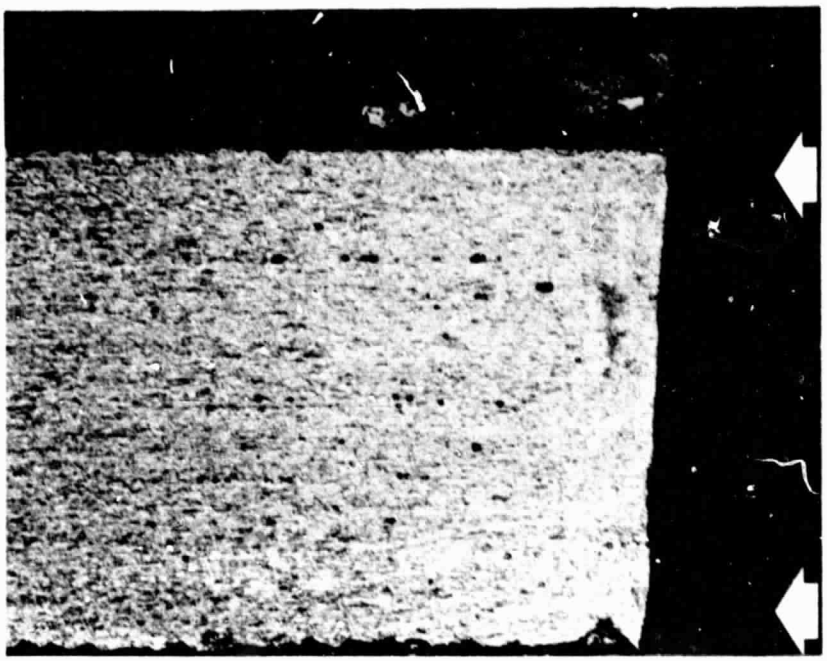

b. Martensitic Formation at Trailing Edge 500X

Figure 47. Ti-6Al-4V Blade from 25.4 μm/sec (0.001 in./sec) Rub on AlBr + 15% Ekonol at 755 K (900° F).

The conclusions drawn from second-iteration testing of the AlBr + 15% Ekonol were:

1. The sprayed-coating microstructure was improved by the Ekonol antistatic treatment and reducing the Ekonol mesh size.

2. The coating showed good abradability with Inconel 718 blades at room temperature and 867 K (1100° F) but required burnout of the Ekonol to achieve acceptable abradability at room temperature with Ti-6Al-4V blades. The abradability was good at 755 K (900° F) with Ti-6Al-4V blades. All rub surfaces were improved over the first-iteration coating.

3. The erosion resistance of the as-sprayed coating was still marginal and deteriorated to unacceptable levels after Ekonol burnout by preexposure.

4. The coatings had good thermal-cycle capability and oxidation resistance.

5. The as-sprayed coating gave excellent surface finishes by the grinding methods established in first-iteration testing. The preexposed coating did not grind smoothly over the whole surface. This might be improved with different grinding practices or by increasing the metal content in the coatings.

4.4.5 Third-Iteration Coating

An AlBr + 10% Ekonol coating composition was selected for full-scale, third-iteration testing after a preliminary evaluation of 5% and 10% Ekonol compositions. The thrust of third-iteration testing was to determine the Ekonol content required in an AlBr + Ekonol coating to achieve a desirable balance of properties between abradability and erosivity. The erosivity at the abradability limits for Ti-6Al-4V blades had been established as unacceptable with as-sprayed coatings. It remained to be seen if this were true for Ti-6Al-4V blades rubbing preexposed, lower Ekonel-containing, aluminum bronze coatings and for Inconel 718 blades rubbing both as-sprayed and preexposed coatings since these blade/coating pairs remained abradable at the 15% Ekonol spray-blend composition.

The preliminary evaluation consisted of room-temperature rubs selected on the basis of trends established in the first- and second-iteration coatings, determination of erosion resistance and coating cohesive strength, and microstructural examinations of the sprayed AlBr + 5% Ekonol and AlBr + 10% Ekonol. The coating densities obtained for these preliminary spray runs were 5.09 and 4.48 Mg/m^3, respectively, for the 5% and 10% Ekonol coatings. The as-sprayed microstructures (Figure 48) were homogeneous. Metallography on preexposed samples showed complete Ekonol burnout and interconnected porosity. Results on the selected room-temperature rub tests showed excessive blade wear in all AlBr + 5% Ekonol rubs. The 755 K (900° F) preexposed AlBr + 10%

a. AlBr + 10% Ekonol

b. AlBr + 5% Ekonol

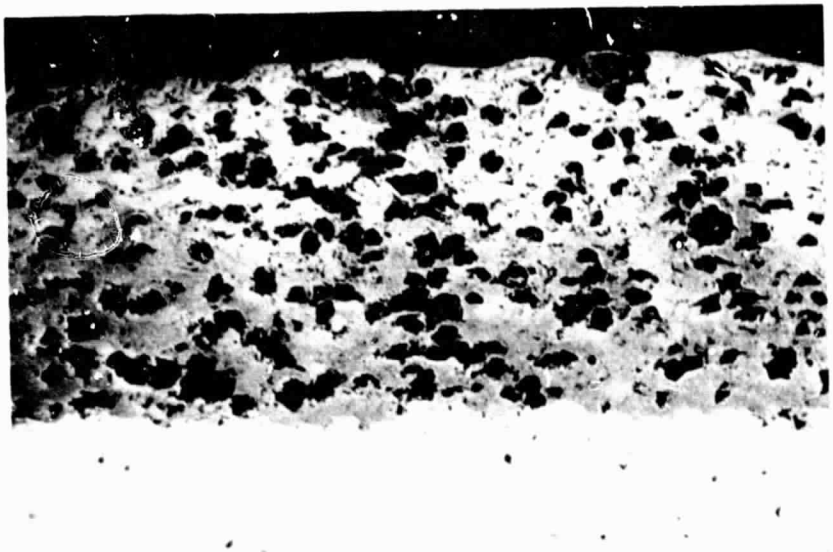

Figure 48. Preliminary, Third-Iteration, Spray-Coating Microstructures.

Ekonol showed zero blade wear for the 2.54 μm/sec (0.0001 in./sec) incursion rate with Inconel 718 blades. Significant blade wear occurred at the other conditions tested.

The erosion resistance was excellent; Lynn erosivity numbers were greater than 20 in all tests. The 755 K (900° F) preexposed AlBr + 10% Ekonol coating gave the lowest result (20.8 average), and the 755 K (900° F) preexposed AlBr + 5% Ekonol gave the highest result (≈30.5 average). The coating cohesive strengths were 7.58 MPa (1100 psi) for the as-sprayed and preexposed AlBr + 10% Ekonol. The AlBr + 5% Ekonol had significantly higher cohesive strengths that were judged to be excessive even for use with Inconel 718 blades based on past experience at General Electric. The erosivity and cohesive-strength data for these preliminary spray runs are summarized in Table XXIII.

The AlBr + 10% Ekonol coating was selected for full evaluation for the following reasons:

1. It exhibited some abradability in room-temperature rubs and was expected to be better in elevated-temperature rubs on the basis of first- and second-iteration tests which wore blades.

2. The erosion resistance was good.

3. The cohesive strength did not change drastically as a result of the Ekonol burnout.

The AlBr + 10% Ekonol samples were sprayed using the standard spray parameters and procedures established earlier. Samples sprayed included Evendale room-temperature rub panels, Lynn elevated-temperature rub panels, M152 thermal-shock panels, tensile-bond buttons, and machinability samples. The as-sprayed AlBr + 10% Ekonol coating exhibited a homogeneous microstructure (Figure 49).

Results of the Evendale room-temperature rub tests are summarized in Table XXIV, and Figure 50 shows the rubbed panels. Significant blade wear occurred in all tests. The as-sprayed coating rubbed by Ti-6Al-4V blades showed the most wear at the 254 μm/sec (0.01 in./sec) incursion rate and the smallest amount of wear at the 25.4 μm/sec (0.001 in./sec) incursion rate.

The titanium blade wear with the preexposed, 755 K (900° F)/50 hours, AlBr + 10% Ekonol also showed the least wear at the 25.4 μm/sec (0.001 in./sec) incursion rate. The preexposed coating gave nearly equal blade wear for the 25.4 and 254 μm/sec (0.001 and 0.01 in./sec) incursion rates. Transverse sections taken from the rub paths of these preexposed coatings are shown in Figures 51 through 53. Figure 51 shows the 25.4 μm/sec (0.001 in./ sec) rub gave little or no coating densification at the rub surface. Figures 52 and 53 clearly show evidence of nearly equal amounts of coating densification at the rub surfaces of the 2.54 and 254 μm/sec (0.0001 and 0.01 in./sec) rubs.

The interpretation of the results for the 2.54 μm/sec (0.0001 in./sec) incursion rate is that frictional heating over the longer test time (200 seconds) is able to significantly lower the flow stress of the AlBr so that

Table XXIII. Erosion and Coating-Cohesive-Strength Test Results.

- All erosion tests were conducted at room temperature using 600 g of 50-μm Al_2O_3 powder with a 20° impingement angle.
- Cohesive-strength data are average of three tests from one spray run.

Coating	Temperature of 50-Hour Coating Preexposure K (° F)	Erosivity*	Cohesive Strength, MPa (psi)
AlBr + 5% Ekonol	---	29.35	10.84 (1573)
AlBr + 5% Ekonol	---	29.35	
AlBr + 5% Ekonol	755 (900)	29.35	12.38 (1795)
AlBr + 5% Ekonol	755 (900)	31.70	
AlBr + 10% Ekonol	---	22.53	7.67 (1112)
AlBr + 10% Ekonol	---	23.15	
AlBr + 10% Ekonol	755 (900)	20.53	7.69 (1115)
AlBr + 10% Ekonol	755 (900)	21.05	

*Seconds to erode 25.4 μm (1 mil)

Table XXIV. AlBr + 10% Ekonel Room-Temperature Rub Test.

- Antistatic-Treated, -200 Mesh Ekonol Powder
- Six Blades at 228 Surface m/sec (759 ft/sec) Tip Speed

Blade Material	Temperature of 50-Hour Coating Preexposure, K (° F)	Incursion Rate, μm/sec (in./sec)	Coating Wear, mm (in.)	Blade Wear, mm (in.)
Ti-6Al-4V	--	2.54 (0.0001)	0.127 (0.005)	0.279 (0.011)
Ti-6Al-4V	---	25.4 (0.001)	0.076 (0.003)	0.216 (0.0085)
Ti-6Al-4V	---	254 (0.01)	0.229 (0.009)	0.4[illegible] .016)
Ti-6Al-4V	755 (900)	2.54 (0.0001)	0.203 (0.008)	0.254 (0.010)
Ti-6Al-4V	755 (900)	25.4 (0.001)	0.178 (0.007)	0.165 (0.0065)
Ti-6Al-4V	755 (900)	254 (0.01)	0.152 (0.006)	0.229 (0.009)
Inco 718	---	2.54 (0.0001)	0.203 (0.008)	0.165 (0.0065)
Inco 718	---	25.4 (0.001)	0.356 (0.014)	0.127 (0.005)
Inco 718	---	254 (0.01)	0.279 (0.011)	0.127 (0.005)
Inco 718	755 (900)	2.54 (0.0001)	0.254 (0.010)	0.064 (0.0025)
Inco 718	755 (900)	25.4 (0.001)	0.178 (0.007)	0.203 (0.008)
Inco 718	867 (1100)	2.54 (0.0001)	0.127 (0.005)	0.178 (0.007)

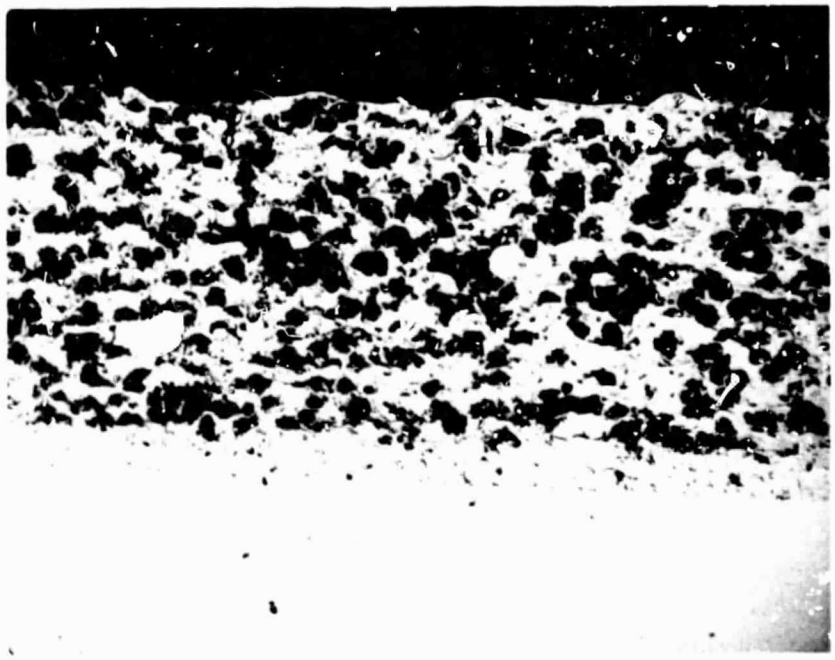

Figure 49. As-Sprayed AlBr + 10% Ekonol Microstructure from Third-Iteration Coating Spray Run. 50X

a. Room-Temperature Rubs, 229 Surface m/sec (750 ft/sec)

	Ti-6Al-4V Blades		Inco 718 Blades		
50-Hour Preexposure:	As Sprayed	755K (900° F)	As Sprayed	755K (900° F)	867 K (1100° F)
Rub No.:	80-6	80-1	80-11		80-12
Rate, μm/sec:	2.54	254	254		2.54
(in./sec)	(0.0001)	(0.01)	(0.01)		(0.0001)
Blade Wear, mm:	0.2794	0.2286	0.1270		0.1778
(in.)	(0.011)	(0.009)	(0.005)		(0.007)
				Invalid Test	
Rub No.:	80-2	80-4	80-8	80-9	
Rate, μm/sec:	254	25.4	25.4	25.4	
(in./sec)	(0.01)	(0.001)	(0.001)	(0.001)	
Blade Wear, mm:	0.4064	0.1651	0.1270	0.2032	
(in.)	(0.016)	(0.0065)	(0.005)	(0.008)	
					
Rub No.:	80-3	80-5	80-7	80-10	
Rate, μm/sec:	25.4	2.54	2.54	2.54	
(in./sec)	(0.001)	(0.0001)	(0.0001)	(0.0001)	
Blade Wear, mm:	0.2159	0.2540	0.1651	0.0635	
(in.)	(0.0085)	(0.010)	(0.0065)	(0.0025)	

b. Elevated-Temperature Rubs, 152 Surface m/sec (500 ft/sec)

Blade Material:	Ti-6Al-4V	Ti-6Al-4V	Ti-6Al-4V	Inco 718	Inco 718
Test Temperature:	755 K	755 K	755 K	867 K	867 K
50-Hour	(900° F)	(900° F)	(900° F)	(1100° F)	(1100° F)
Preexposure:	As Sprayed	As Sprayed	755 K	As Sprayed	867 K
Rate, μm/sec:	2.54	25.4	2.54	25.4	25.4
(in./sec)	(0.0001)	(0.001)	(0.0001)	(0.001)	(0.001)
Coating Wear, mm:	0.6096	0.6096	0.0508	0.6858	0.6858
(in.)	(0.024)	(0.024)	(0.002)	(0.027)	(0.027)
Blade Wear, mm:	0.2794	0.3048*	0.6350*	0.0508*	0.0508*
(in.)	(0.011)	(0.012)*	(0.025)*	(0.002)*	(0.002)*
*Indicates Pickup					

Figure 50. AlBr + 10% Ekonol Rub Panels.

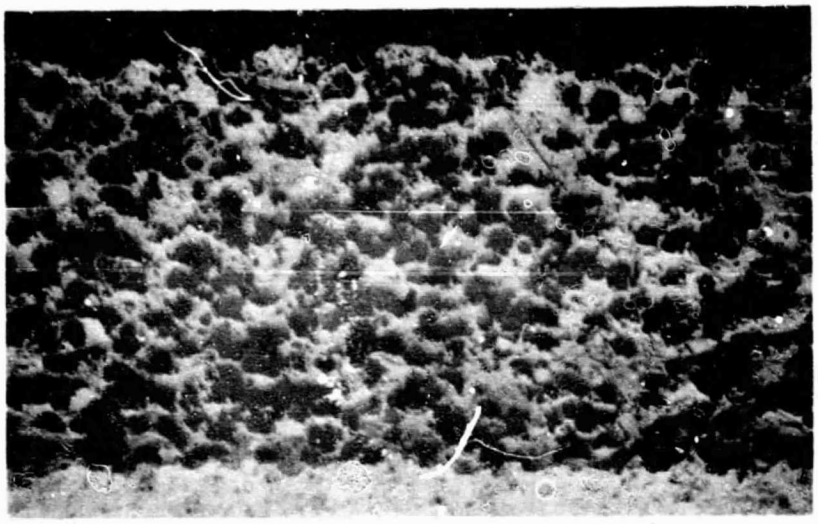

Figure 51. Transverse Section Through Preexposed, 755 K (900° F)/50 Hours, AlBr + 10% Ekonol Rub Path Tested with Ti-6Al-4V Blades, 25.4 μm/sec (0.001 in./sec) Incursion Rate, Room Temperature. 50X

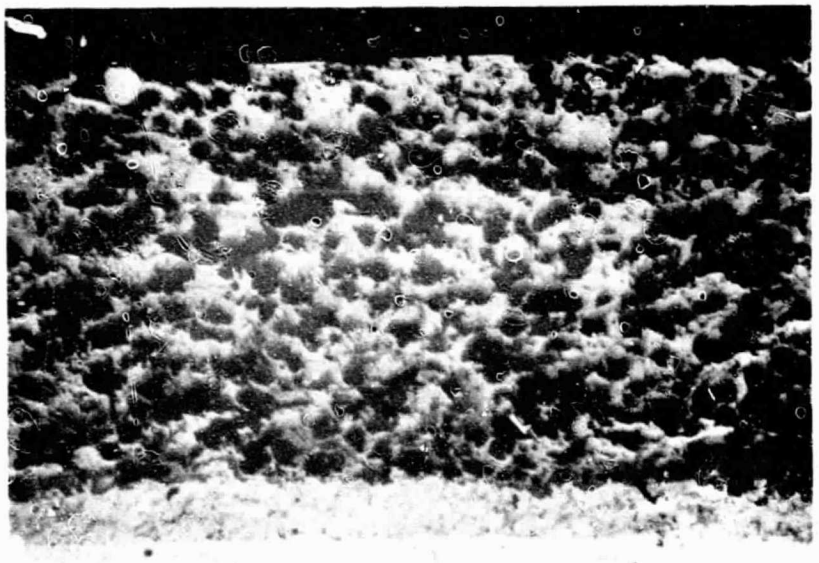

Figure 52. Transverse Section Through Preexposed, 755 K (900° F)/50 Hours, AlBr + 10% Ekonol Rub Path Tested with Ti-6Al-4V Blades, 2.54 μm/sec (0.0001 in./sec) Incursion Rate, Room Temperature. 50X

Figure 53. Transverse Section Through Preexposed, 755 K (900° F)/50 Hours, AlBr + 10% Ekonol Rub Path Tested with Ti-6Al-4V Blades, 254 μm/sec (0.01 in./sec) Incursion Rate, Room Temperature. 50X

densification occurs. Visual support for this interpretation is seen in the as-sprayed rub panels (Figure 50) where charring of the Ekonol occurs over a more extensive region for the lowest incursion rate. In the case of the 254 μm/sec (0.010 in./sec) incursion rate, the depth of bite for each blade encounter is an order of magnitude larger than for the 25.4 μm/sec (0.001 in./sec) rate: 1.5 versus 0.15 nm (5.9 versus 0.59 microinches). Thus the rub-surface densification in this case may be directly related to crushing of the coating by impacting blades.

The Inconel 718 blades showed less wear in general than the Ti-6Al-4V blades. The 25.4 μm/sec (0.001 in./sec) incursion rate showed the most blade wear for the as-sprayed coating, but the lowest blade wear for the preexposed 755 K (900° F)/50 hours coatings. Figures 54 and 55 are transverse sections of the 2.54 and 25.4 μm/sec (0.0001 and 0.001 in./sec) incursion-rate rub panels of the preexposed 755 K (900° F)/50 hr coatings. These coatings are highly densified at the rub surfaces and appear to have more overall, uniform compaction than the titanium blade rubs. Once again the extent of densification at the rub surface correlates to the amount of blade wear. The greater rub panel coating densification and lower blade wear with Inconel 718 probably result from higher flow stress for Inconel 618 blades than for the Ti-6Al-4V blades.

The Lynn elevated-temperature rub-test data are summarized in Table XXV, and the rub panels have been included in Figure 50. The Inconel 718 blade rubs at 867 K (1100° F) (Figure 56) were unworn over most of the blade tips except for some localized notching in rubs against the preexposed [867 K (1100° F)/50 hr] rub panels. Typical features of the Inconel 718 blades from these rubs are shown in Figure 57. An aluminum bronze pickup layer on one of the unworn blades was evident for the unetched blade (top photo). The same area did not show a heat-affected zone (middle photo) after etching. Most of the transferred aluminum bronze was removed by the acid etch (100 cm^3 methanol, 80 cm^3 HCl, 40 cm^3 acetic acid, 10 cm^3 HF, and 10 cm^3 $CuCl_2$). A transverse section (i.e., perpendicular to the rub direction) through one of the Inconel 718 blade tips rubbed against the preexposed aluminum bronze rub liner showed localized notching up to 0.2 mm (0.008 in.) deep (bottom photo) and located near the blade corner. The preexposed rub panel exhibited complementary deep-groove formation at the rub-path edge. No groove formation like this was seen on the earlier AlBr/15% Ekonol preexposed coating.

The Ti-6Al-4V blade rubs at 755 K (900° F) (Figure 58) showed varied results. Both as-sprayed coatings wore 0.635 mm (0.025 in.) but gave 0.279 mm (0.011 in.) blade wear for the 2.54 μm/sec incurion rate and showed 0.305 mm (0.012 in.) of localized AlBr pickup for the 25.4 μm/sec (0.001 in./sec) incursion rate. In contrast to this the 755 K (900° F)/50 hours preexposed coating tested at 2.54 μm/sec (0.0001 in./sec) incursion rate showed 0.635 (0.002 in.,) of scab buildup on the rub panels. Figure 59 shows one of the Ti-6Al-4V blades with the AlBr pickup that caused grooves. One of the Inconel 718 blades is also shown for comparison purposes. Figure 60 shows features seen on the Ti-6Al-4V blades. The top microphotograph showed the extensive martensitic formation that accompanied the high blade wear seen for the 2.54 μm/sec (0.0001 in./sec) incursions into as-sprayed and preexposed coatings.

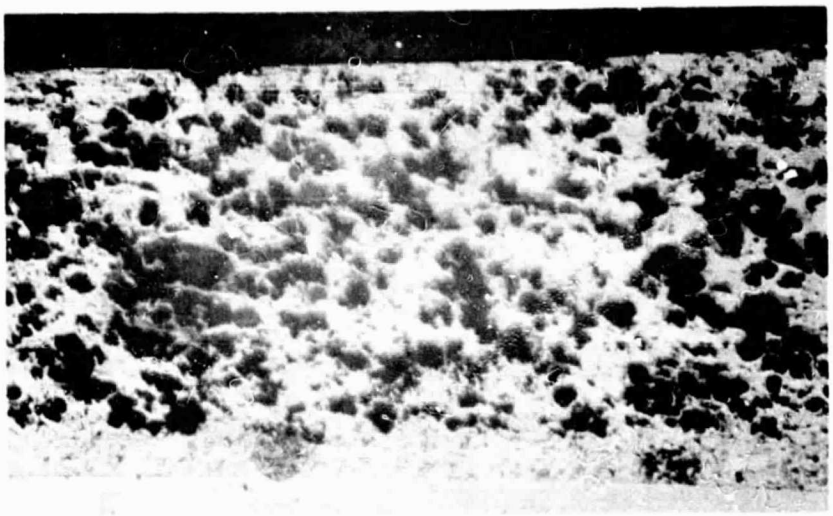

Figure 54. Transverse Section Through Preexposed, 755 K (900° F)/50 Hours, AlBr + 10% Ekonol Rub Path Tested with Inco 718 Blades, 2.54 μm/sec (0.0001 in./sec) Incursion Rate, Room Temperature. 50X

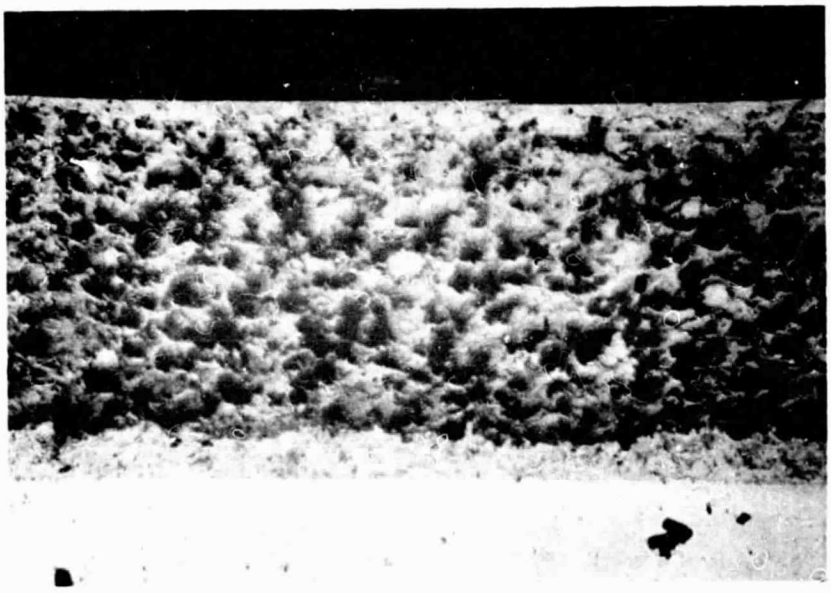

Figure 55. Transverse Section Through Preexposed, 755 K (900° F)/50 Hours, AlBr + 10% Ekonol Rub Path Tested with Inco 718 Blades, 25.4 μm/sec (0.001 in./sec) Incursion Rate, Room Temperature. 50X

a. As Sprayed

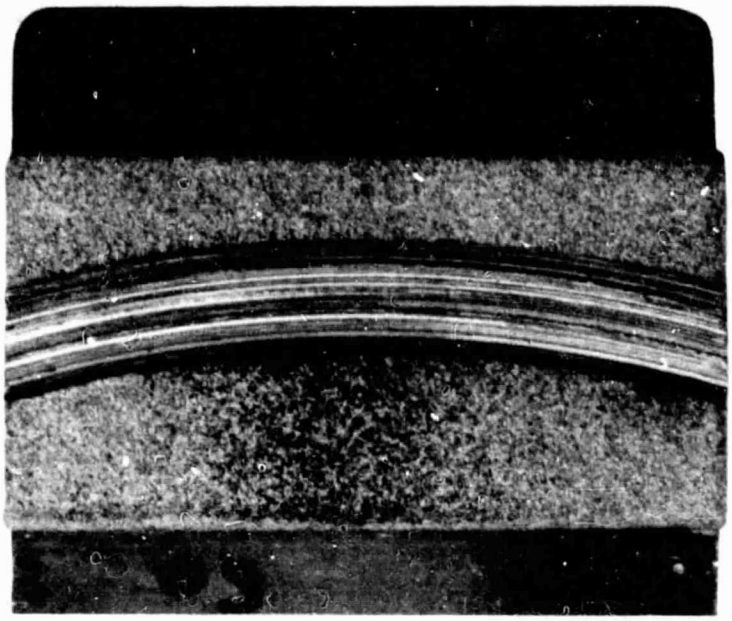

b. Preexposed 867 K (1100° F)/50 Hours

Figure 56. AlBr + 10% Ekonol Rub Panels from 867 K (1100° F) Test with Inco 718 Blades, 25.4 μm/sec (0.001 in./sec) Incursion Rate. 2X

a. Thin, Transfered AlBr Layer on Unetched Blade
400X

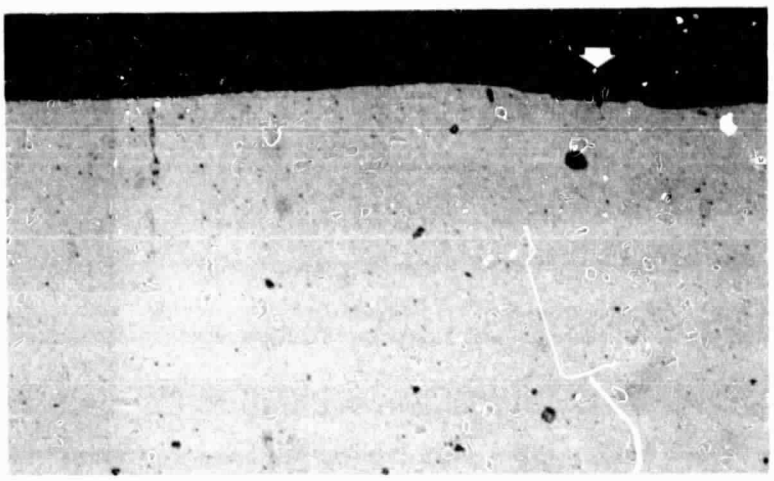

b. No Noticable Heat-Affected Zone Was Seen After Etching
400X

c. Transverse Section Showing Localized Grooves up to 0.203 mm (0.008 in.) Usually Occuring Near the Blade Corner Where Heat-Transfer Conditions Were Different
50X

Figure 57. Inco 718 Blades from 867 K (1100° F) Rub Tests.

a. As-Sprayed, 2.54 µm/sec (0.0001 in./sec) Incursion Rate

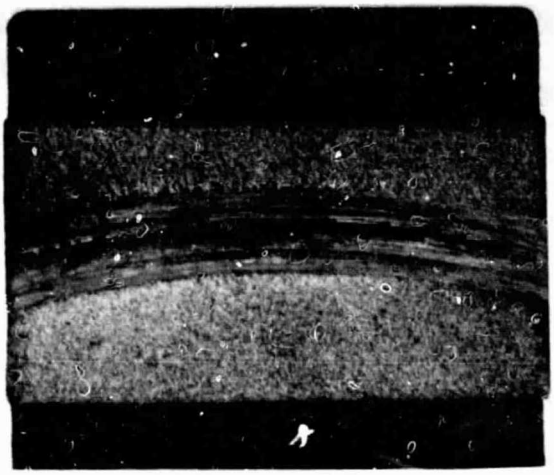

b. As-Sprayed, 25.4 µm/sec (0.001 in./sec) Incursion Rate

The 25.4 µm/sec (0.001 in./sec) rub was fairly smooth with some grooving, but the 2.54 µm/sec (0.0001 in./sec) rub was rougher due to more scabbing.

c. Preexposed at 755 K (900° F)/ 50 Hours, 2.54 µm/sec (0.001 in./sec) Incursion Rate

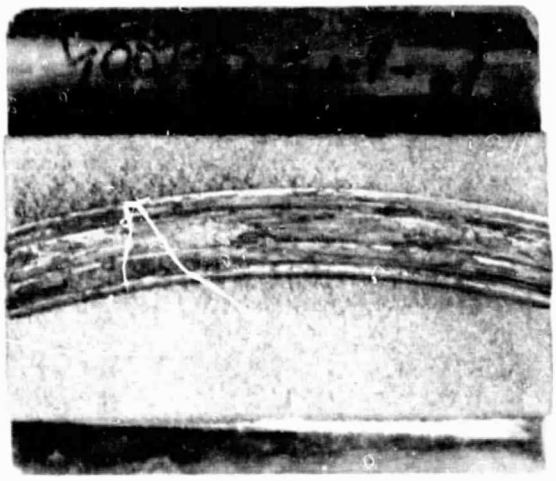

Figure 58. AlBr + 10% Ekonol Rub Panels from 755 K (900° F) Test with Ti-6Al-4V Blades. 1.5X

Inco 718 blade, 867 K (1100° F) test; note slight grooving and edge buildup. 7X

Ti-6Al-4V blade, 755 K (900°F) test; note large local buildups that caused deep notching on the rub panels. 7X

Blade Tip

Side Profile

Figure 59. Elevated-Temperature Rub-Test Blades from As-Sprayed AlBr + 10% Ekonol Rubs, 25.4 μm/sec (0.001 in./sec) Incursion Rate.

a. Extensive Martensite Formed at the Blade Tip When Blades Wore

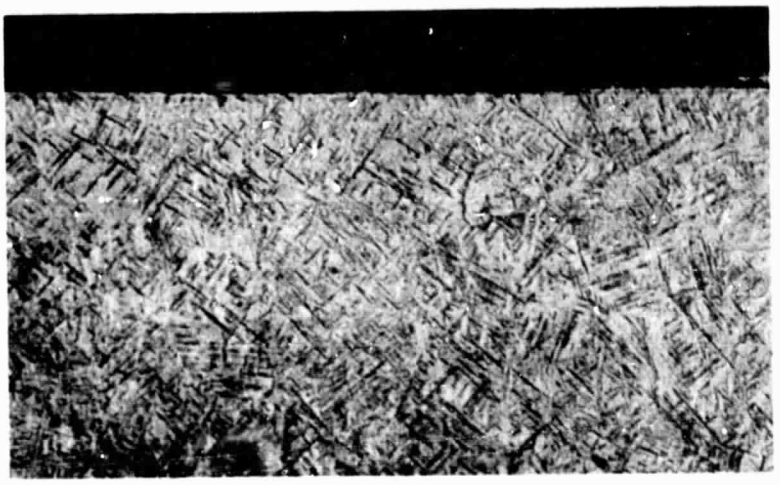

b. Transverse Section from Blades Where Excessive Localized Pick-Up Ocurred

The arrow indicates shrink pores formed by the cooling of molten material.

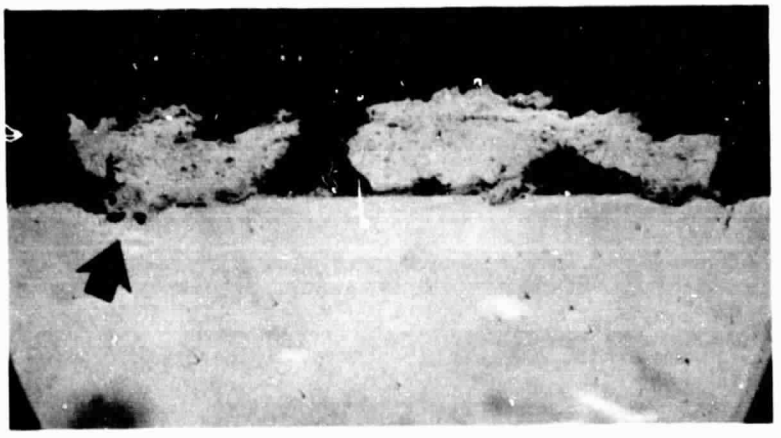

c. Longitudinal Section from the Same Blade Shows No Martensite in Other Areas

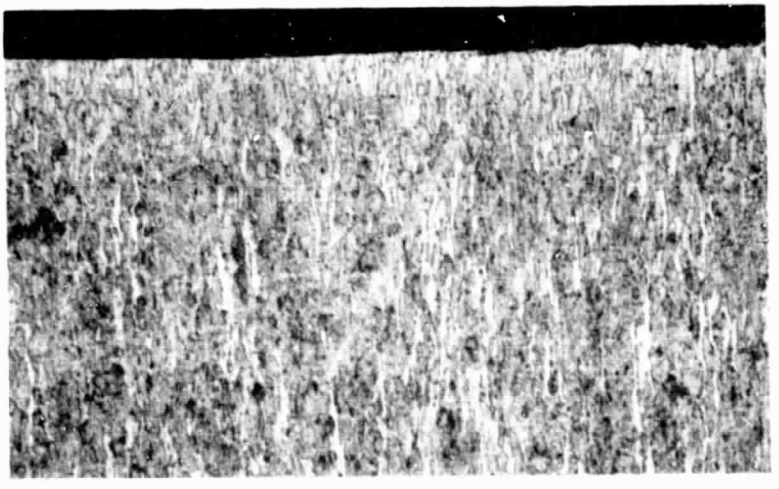

Figure 60. Ti-6Al-4V Blades from 755 K (900° F) Rub Tests. 400X

Table XXV. AlBr + 10% Ekonol Elevated-Temperature Test.

- Antistatic-Treated, -200 Mesh Ekonol Powder
- Forty-Eight Blades at 152 Surface m/sec (500 ft/sec) Tip Speed

Blade Material	Temperature of 50-Hour Coating Preexposure, K (° F)	Incursion Rate, μm/sec (in./sec)	Ambient Test Temperature, K (° F)	Coating Wear, mm (in.)	Blade Wear, mm (in.)
Ti-6Al-4V	---	2.54 (0.0001)	755 (900)	0.610 (0.024)	0.279 (0.011)
Ti-6Al-4V	---	25.4 (0.001)	755 (900)	0.610 (0.024)	0.305 (0.012)*
Ti-6Al-4V	755 (900)	2.54 (0.0001)	755 (900)	0.051 (0.002)*	0.635 (0.025)
Inco 718	---	25.4 (0.001)	867 (1100)	0.686 (0.027)	0.051 (0.002)*
Inco 718	867 (1100)	25.4 (0.001)	867 (1100)	0.686 (0.027)	0.051 (0.002)*

*Pickup

The middle microphotograph shows a transverse section through the localized aluminum bronze blade pickup shown in Figure 59. The small, shrinkage pores at the blade tip were dramatic confirmation that molten metal was present when the pickup was initiated. This further confirms the importance of eutectics or other metallurgical interactions during rubs. The bottom microphotograph was taken from a longitudinal section through the same blade at an area away from the localized pickup. The martensite was formed in these areas when blade wear did not occur.

The erosion and tensile-bond test results for the AlBr + 10% Ekonol coating are shown in Table XXVI. The Lynn erosivity numbers [seconds to erode 25.4 μm (0.001 in.) of material] were 19.50 to 23.00 depending on coating condition. These values are as expected based on prior experience with the preliminary AlBr + 10% Ekonol spray run. Figure 61 shows the erosion-test panels. The cohesive strength of the coatings was also as expected for the as-sprayed condition, 8.225 MPa (1192 psi), but was higher than expected for the 755 K (900° F)/50 hours preexposed coatings, 11.902 MPa (1725 psi). This indicated that long-term exposure effects of abradability must be looked at more closely before the AlBr + Ekonol system can be used in hotter compressor stages.

Table XXVI. Erosion and Coating-Cohesive-Strength Test Results for AlBr + 10% Ekonol Coating.

- All erosion tests conducted at room temperature using 600 g of 50-μm Al_2O_3 powder with a 20° impingement angle.
- Cohesive-strength data are average of three tests from one spray run.

Temperature of 50-Hour Coating Preexposure, K (° F)	Erosivity*	Cohesive Strength MPa (psi)
---	22.33	8.22 (1192)
---	21.83	
755 (900)	20.05	10.35 (1501)
755 (900)	19.50	
867 (1100)	22.63	11.89 (1725)
867 (1100)	23.00	

*Seconds to erode 25.4 μm (1 mil).

a. As-Sprayed

b. Preexposed at 755 K (900° F)/50 Hours

c. Preexposed at 867 K (1100° F)/50 Hours

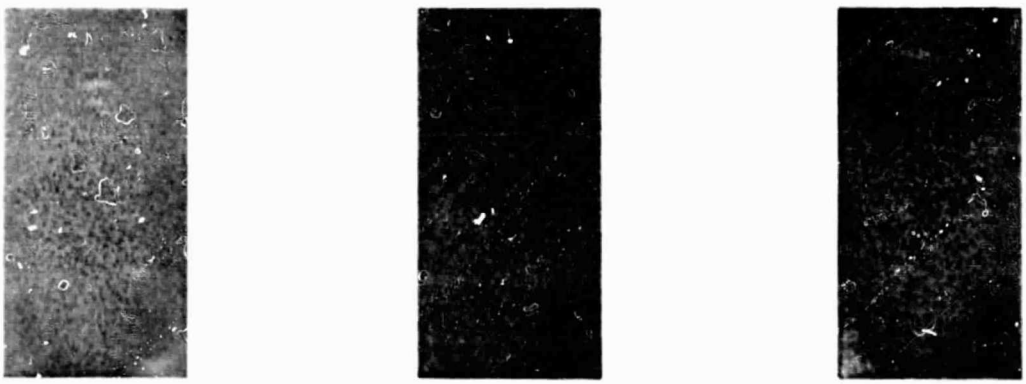

Figure 61. Erosion-Test Panels for AlBr + 10% Ekonol, Third-Iteration Coating. 50X

Machinability tests were also conducted on AlBr + 10% Ekonol coating. The machining consisted of precision-grinding as-sprayed and preexposed [755 K (900° F)/50 hr] samples using the grinding parameters estblished in earlier work. A slight modification in fixturing was incorporated for easier positioning of the curved panels. The as-sprayed panels gave surface-finish values of 0.533 to 1.524 μm (21 to 60 μin.) AA; the preexposed samples gave values of 0.965 to 1.600 μin. (38 to 63 μin.) AA. The preexposed 10% Ekonol coating gave a uniform, smear-ground surface finish with a fine crazing pattern. No rough areas remained after grinding; this represents an improvement over the preexposed 15% Ekonol coating. Figure 62 shows typical as-sprayed and preexposed panel surfaces after grinding.

Thermal-cycle tests consisted of placing samples in a hot furnace at 755 K (900° F) for one hour and then force-cooling, with a large fan, to room temperature. After 50 cycles no cracking, spalling, or edge uplifting were seen. Figure 63 is a typical metallographic section showing the bond-line integrity.

The conclusions drawn from third-iteration testing were:

1. Excessive blade wear occurred in room-temperature rub tests for Ti-6Al-4V and Inconel 718 blades due to coating densification and scabbing.

2. Ti-6Al-4V blades gave unpredictable behavior in 755 K (900° F) rub tests. They either wore excessively and formed thin scabs on the seal, or they showed localized aluminum bronze pickup that scoured deep grooves in the seal. Both behavior patterns were unacceptable for engine use.

3. Inconel 718 blades showed some aluminum bronze transfer in 867 K (1100° F) rubs but gave fairly smooth rub paths with some grooving, particularly near corners.

4. The erosion resistance was excellent and exceeded engine needs based on General Electric's background experience in this area.

5. The thermal-shock and oxidation resistance were acceptable.

6. Machinability was exellent for as-sprayed and preexposed coatings using the precision-grinding methods established in the first iteration of Task III.

7. The coating microstructure and density indicated good process control over a substantial range of AlBr/Ekonol blend rates.

a. As-Sprayed, 0.53-1.52 µm (21-60 µin) AA

b. Preexposed at 755 K (900° F)/ 50 Hours, 0.96-1.60 µm (38-63 µin) AA

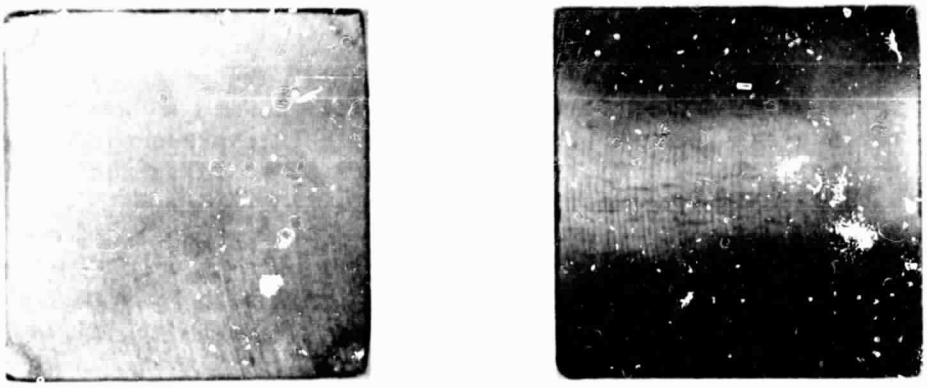

Figure 62. AlBr + 10% Ekonol Machinability Samples. 50X

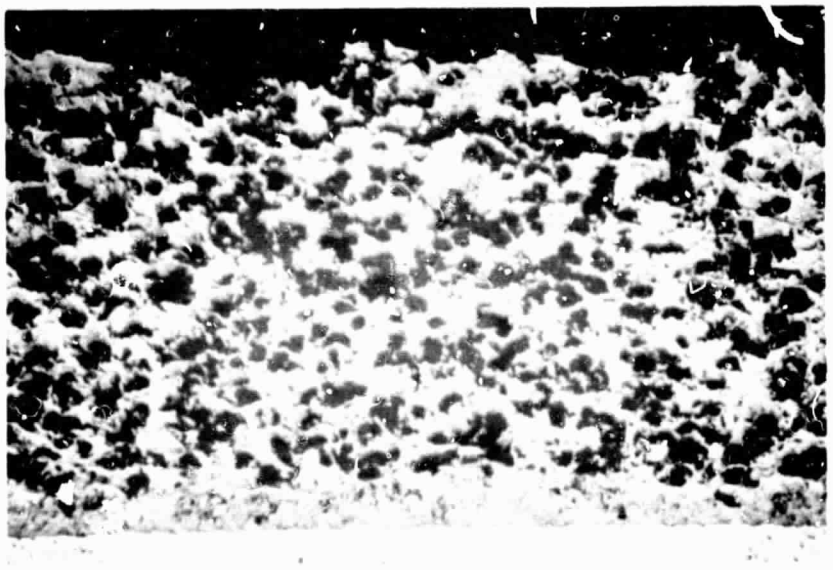

Figure 63. AlBr + 10% Ekonol Thermal-Cycle Panels Showed No Cracking or Spalling. 50X

4.4.6 Final Coating Recommendation and Testing

4.4.6.1 Material Selection and Preparation

Abradability and coating properties were reviewed after the completion of third-iteration testing. The room-temperature Ti-6Al-4V blade wear increases steadily with decreasing amounts of Ekonol for the as-sprayed coatings. For preexposed coatings, titanium blade wear was acceptable at all but the lowest Ekonol content (10%) where it wore blades almost as severly as the as-sprayed coating. The room-temperature Inconel 718 blade wear was zero for the as-sprayed and preexposed 20% and 15% Ekonol compositions, but it was unacceptably high for the as-sprayed and preexposed 10% Ekonol compositions. This data has been summarized in Figure 64. The limited elevated-temperature rub data did not lend itself to clear graphical presentation. In general, however, the Inconel 718 blades performed well in 867 K (1100° F) rubs with all coating compositions in the as-sprayed and preexposed conditions. The Ti-6Al-4V blade rubs at 755 K (900° F) showed zero wear with as-sprayed and preexposed AlBr + 20% Ekonol coatings and little or no wear for the as-sprayed AlBr + 15% Ekonol coatings. There was inconsistent behavior for the as-sprayed and preexposed AlBr + 10% Ekonol coatings; they varied from excessive Ti-6Al-4V blade wear to extreme scouring of the seal coatings (caused by localized blade pickup).

The coating properties considered in making a final power-blend composition recommendation were erosivity, cohesive strength, and deposited density. Only those coatings which were sprayed with standard parameters and -200 mesh treated Ekonol were considered. These properties are summarized in Figure 65. The as-sprayed coating showed a linear relationship between powder-blend composition and all three of these benchmark properties over the 5% to 15% Ekonol range. Quantitative microscopy on these coatings indicated a range of about 65% to 30% metal (by volume) in the deposited coatings. However, the as-sprayed AlBr + 20% Ekonol coating deviated from the linear relationship. This could have been caused by the fact that this coating was hand-sprayed; however, a more likely explanation is the powder-blend composition exceeded the point where that portion of the heat partitioned to the Ekonol during dwell time in the plasma flame was sufficient to cause softening of the Ekonol particles. As a result, the deposition characteristics of the blend were changed.

Erosivity and cohesive strength both showed significant variations with preexposure. The 15% Ekonol coating exhibited property losses, and the 5% and 10% Ekonol showed property increases. In general, the changes in cohesive strength were quite dramatic and were probably a major factor in the increased Inconel 718 blade wear seen with the AlBr + 10% Ekonol coating.

Based on the above review of Task III efforts, a final coating composition of AlBr + 12.5% Ekonol was recommended for the planned Evendale Compressor Rub Simulator tests at 755 K (900° F) and 366 m/sec (1200 ft/sec). The reasons for this recommendation were:

1. It appeared that a composition between 15% and 10% would give stabilized coating properties at temperatures encountered in the compressor section of gas-turbine engines.

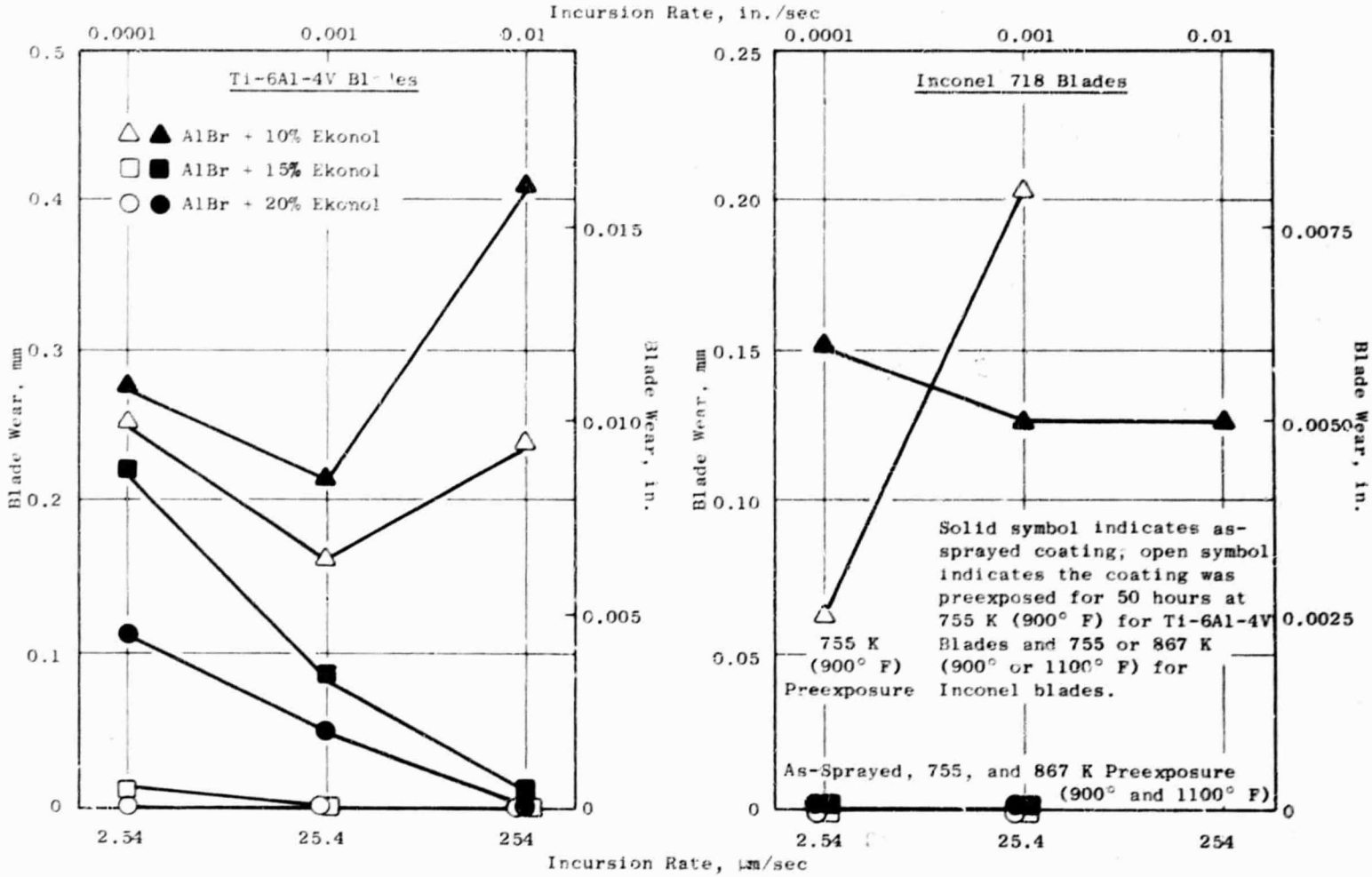

Figure 64. Room-Temperature Blade Wear Versus Incursion Rate Summarized for the First Three Coating Iterations of Task III.

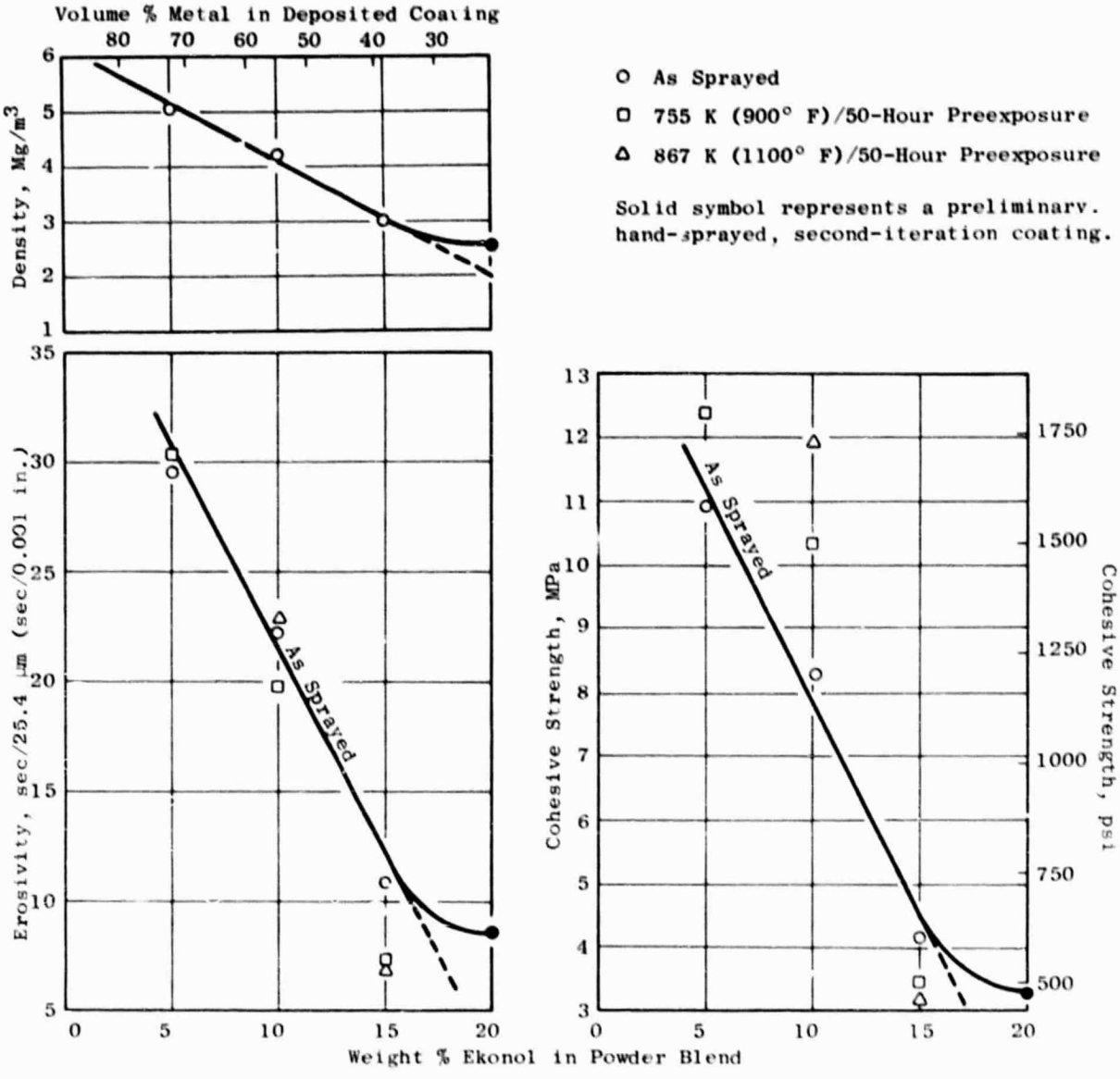

Figure 65. Coating Properties of AlBr/Ekonol Compositions Examined Under Task III.

2. A comparison of abradability trends for room-temperature and elevated-temperature tests indicated Inconel 718 blade wear should be acceptable at this composition, and Ti-6Al-4V blade wear might be acceptable for preexposed coatings.

3. The erosivity data indicated this composition represented the maximum Ekonol content consistent with the desired erosion resistance for an abradable seal material.

Test hardware was sprayed with the AlBr + 12.5% Ekonol powder blend using the standard spray parameters and powder-handling procedures developed earlier. The hardware included Evendale Compressor Rub Simulator case liners, sufficient curved panels for selected room-temperature rub tests, tensile-bond test buttons, and erosion/density panels for coating-property characterization.

4.4.6.2 Property Evaluation and Selected Room Temperature Abradability Testing

Characterization of the AlBr + 12.5% Ekonol coating selected for final testing included metallography on the as-sprayed coating (Figure 66), tensile-bond strength, erosivity, and selected room-temperature rubs. The standard 229 m/sec (750 ft/sec) and 0.5 mm (0.020 in.) incursion tests included 2.54 and 25.4 μm/sec (0.0001 and 0.001 in./sec) incursion rates on preexposed coating [50 hours at 755 K (900° F) for Ti-6Al-4V blade rubs and 867 K (1100° F) for Inconel 718 blade rubs]. The 2.48 μm/sec (0.0001 in./sec) rate gave more severe blade wear than the 25.4 μm/sec (0.001 in./sec) rate with titanium blades. For both incursion rates, the Inconel 718 blades showed about half the blade wear of the lowest wear for the titanium blades. These data are summarized in Table XXVII.

Table XXVII. AlBr + 12.5% Ekonel Room-Temperature Test.

- Six Blades at 228 Surface m/sec (750 ft/sec) Tip Speed

Blade Material	Temperature of 50-Hour Coating Preexposure, K (° F)	Incursion Rate, μm/sec (in./sec)	Coating Wear, mm (in.)	Blade Wear, mm (in.)
Ti-6Al-4V	755 (900°)	2.54 (0.0001)	0.102 (0.004)	0.330 (0.013)
Ti-6Al-4V	755 (900)	25.4 (0.001)	0.279 (0.011)	0.203 (0.008)
Inco 718	867 (1100)	2.54 (0.0001)	0.051 (0.002)	0.305 (0.012)
Inco 718	867 (1100)	25.4 (0.001)	0.051 (0.002)	0.356 (0.014)

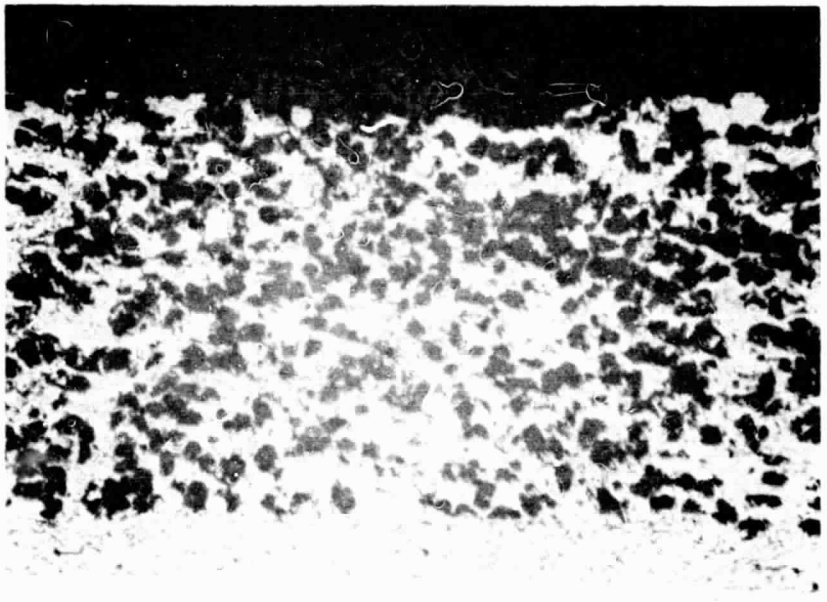

Figure 66. As-Sprayed AlBr + 12.5% Ekonol Microstructure. 50X

The coating density (3.58 Mg/m^3) was on target, and the erosivity was about as expected. The as-sprayed coating erosivity number was 17.4, and cohesive strength was 7.93 MPa (1150 psi). The 755 K (900° F)/50 hour preexposed-coating erosivity was 15.5, and the cohesive strength was 8.96 MPa (1299 psi). The 867 K (1100° F)/50 hour preexposed coating had an erosivity of 19.5 and a cohesive strength of 9.24 MPa (1340 psi). These data, summarized in Table XXVIII, show the erosivity numbers were about as expected, but the cohesive strengths were unusually high and were reflected in the higher than expected blade wear. These data also indicated an instability in the structure of the metal matrix - possibly due to some of the initial stages of sintering.

Table XXVIII. Erosion and Coating-Cohesive-Strength Test Results for AlBr + 12.5% Ekonol Coating.

- Erosion tests at room temperature using 600 g of 50-μm Al_2O_3 powder with a 20° impingement angle
- Cohesive-strength data are average of three tests from one spray run.

Temperature of 50-Hour Coating Preexposure, K (° F)	Erosivity*	Cohesive Strength, MPa (psi)
---	16.83	7.93 (1192)
---	18.05	
755 (900)	17.90	8.88 (1288)
755 (900)	15.10	
867 (1100)	19.83	9.24 (1340)
867 (1100)	19.18	

*Seconds to erode 25.4 μm (1 mil).

4.4.6.3 Compressor Simulative Rub Testing

Compressor simulative rub tests were conducted in the single-point rub mode. The ambient test temperature was 755 K (900° F), and a blade tip speed of 298 m/sec (1200 ft/sec) was employed. Forty-four blades were used, and the target incursion was 0.5 mm (0.020 in.) for all tests.

Four tests were conducted under the above conditions. Figures 67 and 68 show the tested rub liners and detailed features of the rub paths; Figures 69 through 72 show typical blades from each test. In the first test, the as-sprayed coating was rubbed by Inconel 718 blades at the 24.8 μm/sec (0.001 in./sec) incursion rate. Blade wear was high, 0.41 to 0.58 mm (0.016 to 0.023 in.), and most severe on the forward blade corner. (The blade tips are inclined relative to the axis of rotation and so that one corner of the blade passes a reference point on the rub liner before the other passes the same reference point.) There was a large amount of transferred aluminum bronze on the leading edge, and Tempil Laq on the back side of the case liners indicated temperatures during the rub were 867 and 922 K (1100° and 1200° F).

The second rub test was on a preexposed [755 K (900° F)/50 hr] rub liner segment by Inconel 718 blades at the same 25.4 μm/sec (0.001 in./sec) incursion rate. The blade wear and aluminum bronze pickup were not as severe in this test as in the first test, but the blade wear was still high, 0.013 to 0.048 mm (0.005 to 0.019 in.). Due to a miscalculated rotor growth, two attempts were needed to obtain the 0.5-mm (0.020-in.) incursion. Tempil Laq indicators showed the rear of the rub-liner segment exceeded 867 K (1100° F) on the first incursion and fell between 978 and 1033 K (1300 and 1400° F) on the second incursion. This observation was consistent with limited laboratory experience which suggests that multiple incursions to obtain a given total incursion depth are more severe than single incursions to obtain the same total incursion depth.

The third rub test was on a preexposed [755 K (900° F)/50 hr] rub liner segment with Inconel 718 blades at an incursion rate of 2.54 μm/sec (0.0001 in./sec). Blade wear was about the same as in the first test; however, these blades did not show as much aluminum bronze buildup on the leading edge as did those of the first test. Tempil Laq once again indicated a temperature in excess of 867 K (1100° F) on the rear face of the rub-liner segment.

The fourth rub test was on a preexposed [755 K (900° F)/50 hr] rub-liner segment with Ti-6Al-4V blades at the 25.4 μm/sec (0.001 in./sec) incursion rate. Blade wear was more severe than for Inconel 718 blades under the same test conditions. Leading-edge buildup of the aluminum bronze was comparable to that seen for the first test. The blade trailing edges were also burred, and this was not seen with Inconel 718 blades. Tempil Laq indicated a rear rub-liner temperature in excess of 1078 K (1500° F). This was significantly hotter than was seen with Inconel 718 blades but was not unexpected. The thermal conductivity of Ti-6Al-4V is much lower than that of Inconel 718 and should force a larger fraction of the frictional heat to partition to the rub liner.

The above results, summarized in Table XXIX, clearly indicate unacceptable rub behavior in a compressor environment. All tests gave at least some areas of blade material scabbing onto the rub coatings, areas of coating pull-out, and leading-edge aluminum bronze buildup. Metallography typical of these features is illustrated in Figures 73 through 77. Figure 73 shows a transverse section of a titanium blade with aluminum bronze rub debris buildup on the leading edge. Figure 74 is a higher magnification of the same blade tip after

a. As-Sprayed,
Versus Inco 718 Blades,
25.4 µm/sec (0.001 in./sec) Incursion Rate

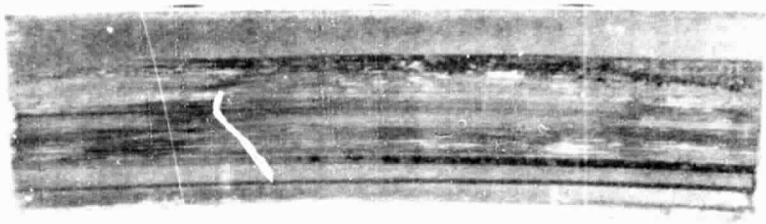

b. Preexposed at 755 K (900° F)/50 Hours,
Versus Inco 718 Blades,
2.54 µm/sec (0.0001 in./sec) Incursion Rate

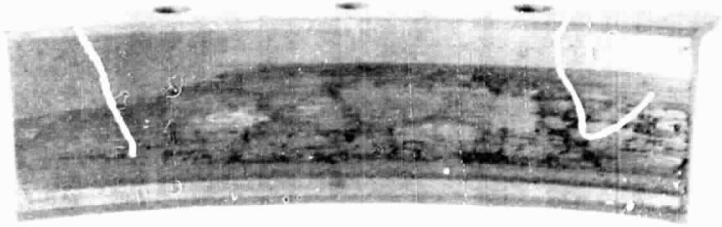

c. Preexposed at 755 K (900° F)/50 Hours,
Versus Inco 718 Blades,
25.4 µm/sec (0.001 in./sec) Incursion Rate

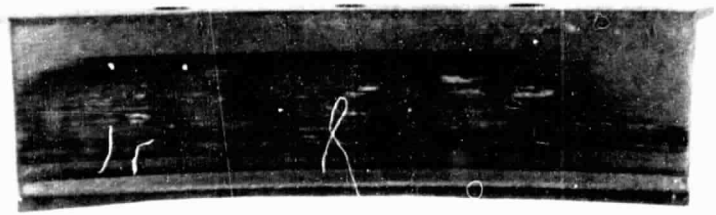

d. Preexposed at 755 K (900° F)/50 Hours,
Versus Ti-6Al-4V Blades,
25.4 µm/sec (0.001 in./sec) Incursion Rate

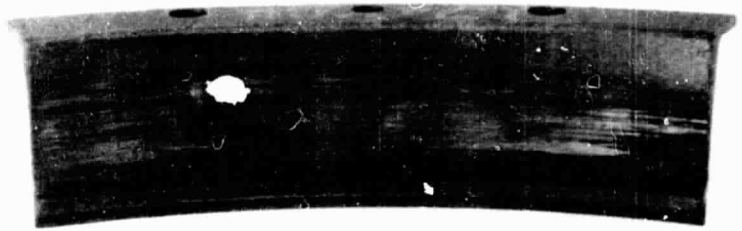

Figure 67. AlBr + 12.5% Ekonol 755 K (900° F) Rubs. ≈0.8X

Figure 68. Closeups of A through D of Figure 67. ≈4X

a. Looking Down on Tip

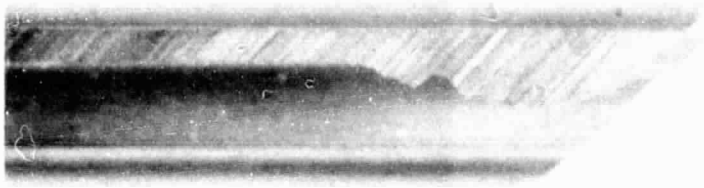

b. Looking in at Front Edge

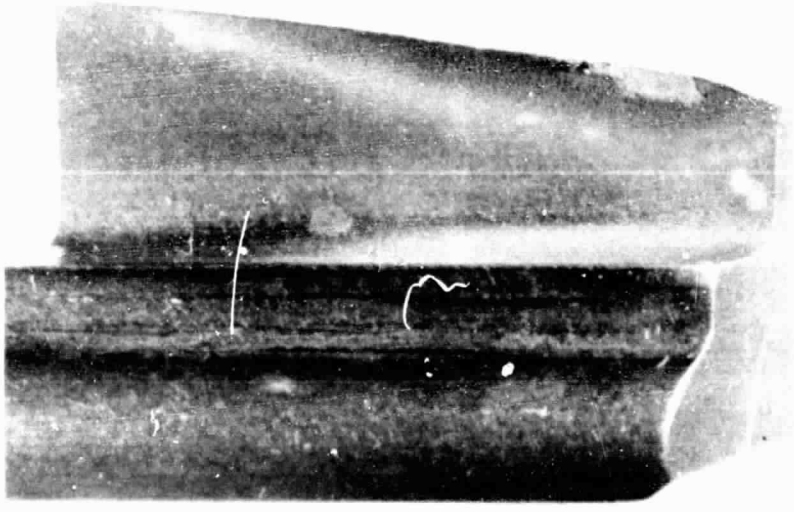

Figure 69. Blades from AlBr + 12.5% Ekonol As-Sprayed Vs. Inco 718 Blades, 25.4 µm/sec (0.001 in./sec) Incursion Rate. 4X

a. Looking Down on Tip

b. Looking in at Front Edge

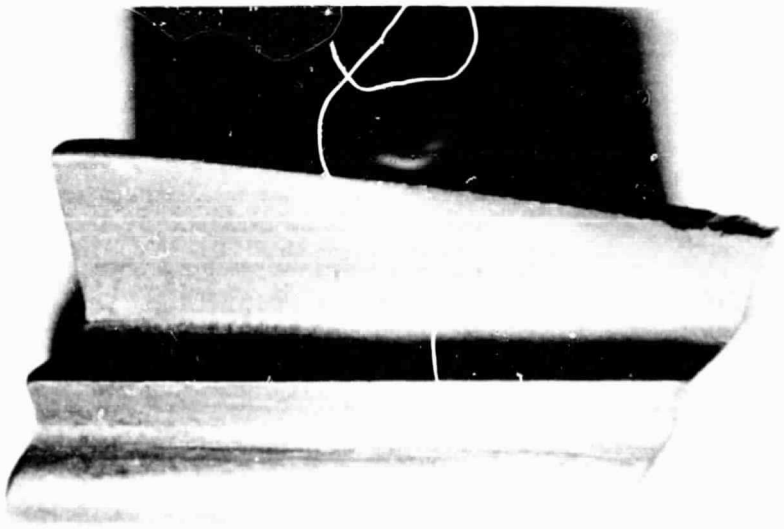

Figure 70. Blades from AlBr + 12.5% Ekonol Preexposed at 755 K (900° F)/50 Hours Vs. Inco 718 Blades, 2.54 μm/sec (0.0001 in./sec) Incursion Rate. 4X

a. Looking Down on Tip

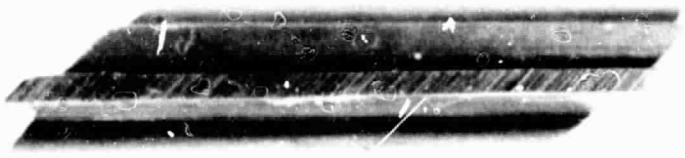

b. Looking in at Front Edge

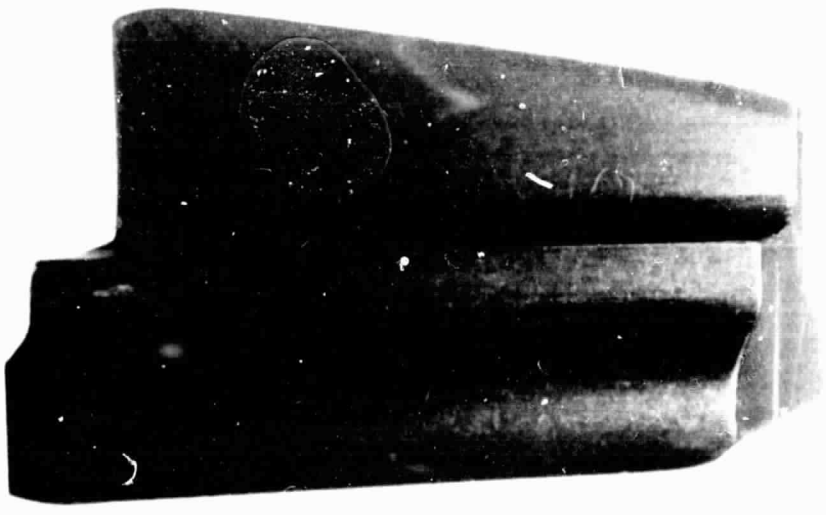

Figure 71. Blades from AlBr + 12.5% Ekonol Preexposed at 755 K (900° F)/50 Hours Vs. Inco 718 Blades, 25.4 μm/sec (0.001 in./sec) Incursion Rate. 4X

a. Looking Down on Tip

b. Looking in at Front Edge

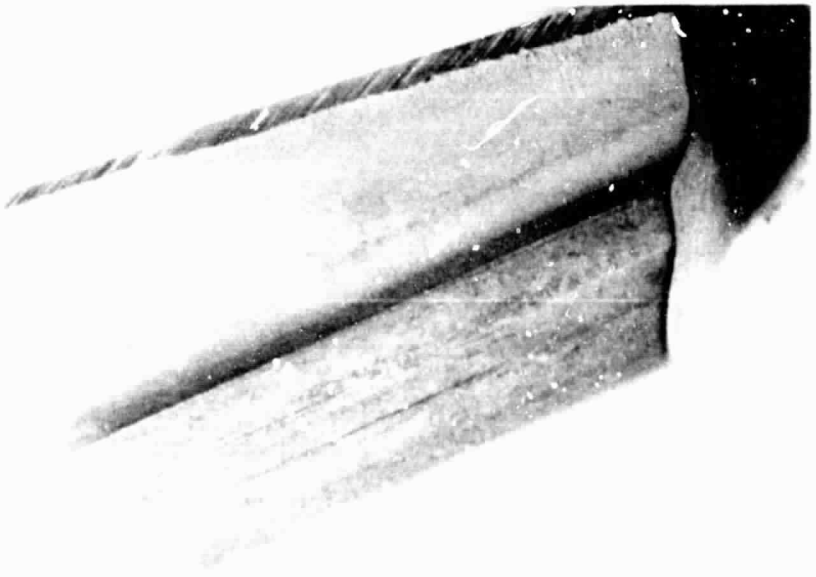

Figure 72. Blades from AlBr + 12.5% Ekonol Preexposed at 755 K (900° F)/50Hours Vs. Ti-6Al-4V Blades, 25.4 μm/sec (0.001 in./sec) Incursion Rate. 4X

Table XXIX. AlBr + 12.5% Ekonol 755 K (900° F), 298 m/sec (1200 ft/sec) Tip Speed Rub Test.

• Six Blades at 228 Surface m/sec (750 ft/sec) Tip Speed

Blade Material	Temperature of 50-Hour Coating Preexposure, K (° F)	Incursion Rate, μm/sec (in./sec)	Coating Wear, mm (in.)	Blade Wear, mm (in.)	Coating Wear / Blade Wear
Inco 718	---	25.4 (0.001)	0.356 (0.014)	0.508 (0.020)	0.7
Inco 718	755 (900)	2.54 (0.0001)	0.254 (0.010)	0.508 (0.020)	0.5
Inco 718	755 (900)	25.4 (0.001)	0.305 (0.012)	0.178 (0.007)	1.7
Ti-6Al-4V	755 (900)	25.4 (0.001)	0.330 (0.013)	0.254 (0.010)	1.3

Coating was preexposed for 50 hours at 755 K (900° F). Note extreme build-up of AlBr rub debris on the leading edge.

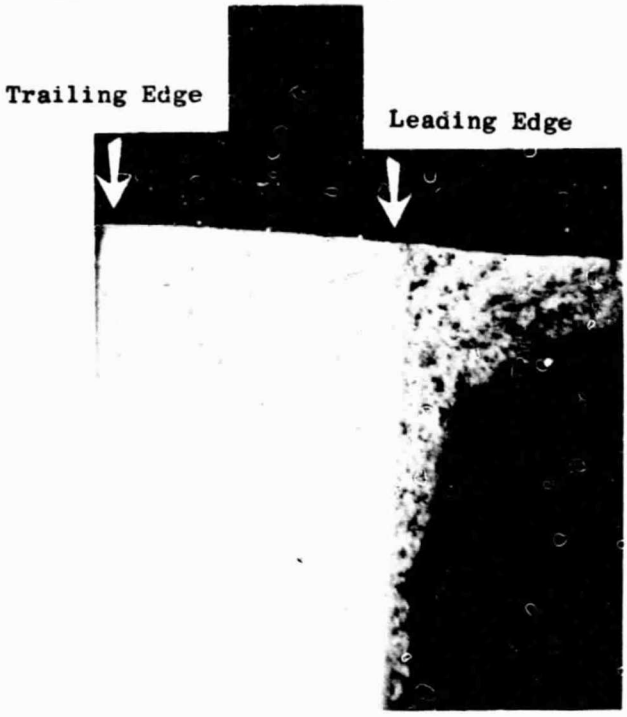

Figure 73. Ti-6Al-4V Blade Tip from 755 K, 298 m/sec (900° F, 1200 ft/sec) Rub Against AlBr + 12.5% Ekonol at 25.4 μm (0.001 in.) Incursion Rate. 50X

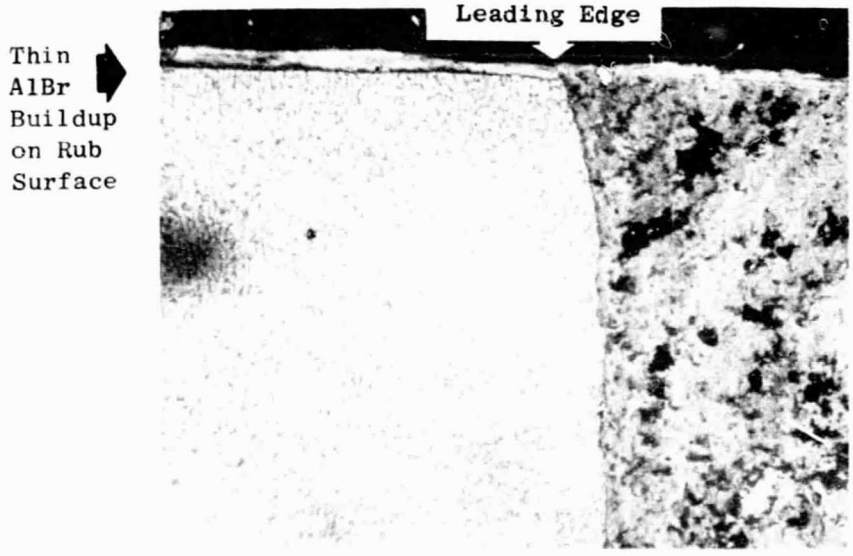

Figure 74. Same Blade After Etching. 200X

a. Transverse Section of Inconel 718 Blade Rubbed Into AlBr + 12.5% Ekonol Preexposed 50 Hours at 755 K (900° F); Rub Conditions Included 755 (900° F) Ambient Temperature, 298 m/sec (1200 ft/sec) Blade Tip Speed, and a 0.508 mm (0.02 in.) Incursion at 2.54 µm/sec (0.0001 in./sec) 50X

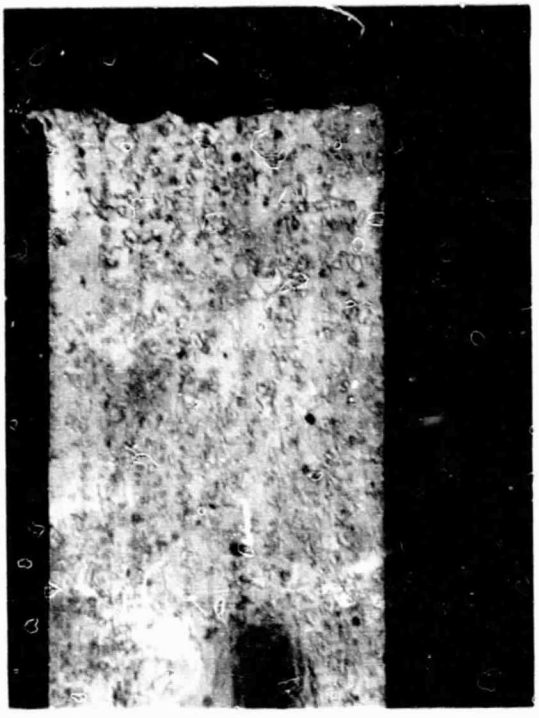

b. Longitudinal Section 50X

Figure 75. Heat-Affected Zone.

a. Compacted Surface Layer with Pullout Area

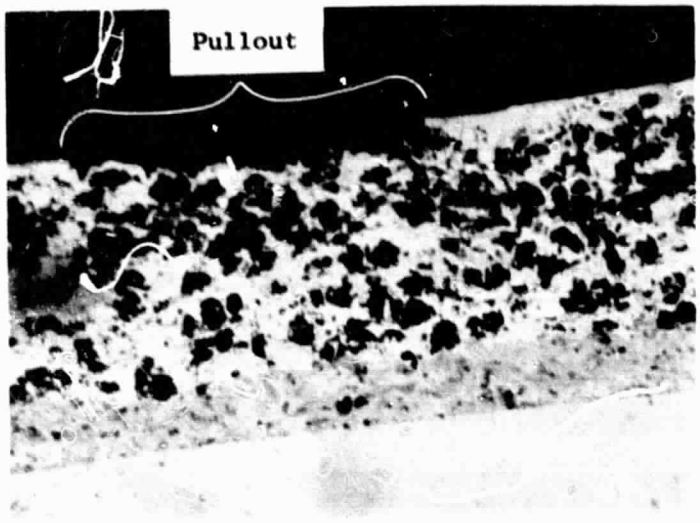

b. Scab Formation Has Apparently Been Pushed Into Porous Coating and Caused Additional Compacting

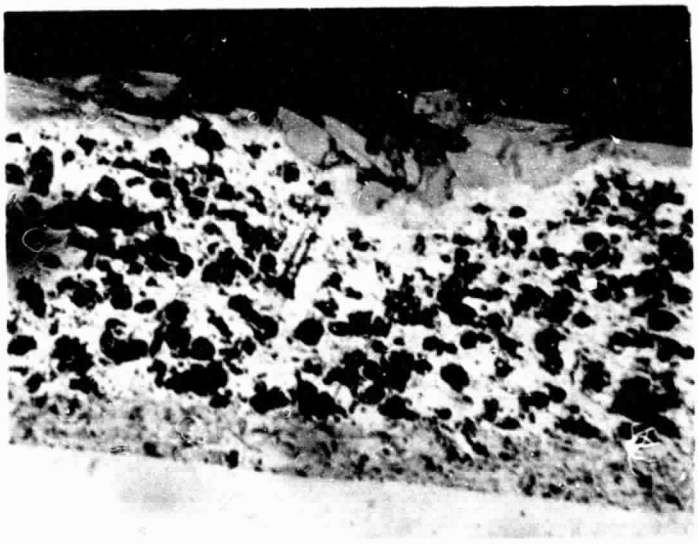

Figure 76. AlBr + 12.5% Ekonol Rub Liner from the 755 K (900° F), 298 m/sec (1200 ft/sec) Tip Speed Test with Titanium Blades at the 2.54 μm/sec (0.001 in./sec) Incursion Rate. 50X

a. Scabbing on a Compacted Surface Layer in a Region of Shallow Rub Depth (High Blade Wear)

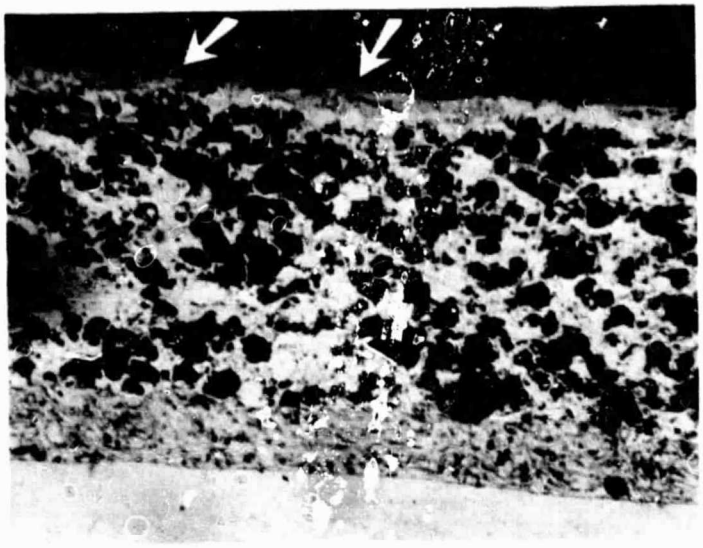

b. Generalized Coating Compaction in a Region of High Rub Depth (Low Blade Wear)

Figure 77. AlBr + 12.5% Ekonol Rub Liner from the 755 K (900° F), 298 m/sec (1200 ft/sec) Tip Speed Test with Inco 718 Blades at the 25.4 µm/sec (0.001 in./sec) Incursion Rate. 50X

etching. The most noticeable features are the lack of martensite at the tip and the different appearance of the thin layer of transfer material across the tip when compared to the leading-edge buildup of aluminum bronze.

Figure 75 shows one of the Inconel 718 blades from the 2.54 μm/sec (0.0001 in./sec) incursion into preexposed AlBr + 12.5% Ekonol. The most noticeable features here are the lack of the transferred layer of aluminum bronze, the burr formation on the trailing edge of the blade tip, the uneven wear in the transverse section (not seen on the titanium blades), and a 2.54 to 5.08 mm (0.01 to 0.02 in.) deep heat-affected zone.

Figure 76 shows typical rub-liner features seen on the titanium blade rub at 755 K (900° F), 298 m/sec (1200 ft/sec) and 25.4 μm/sec (0.001 in./sec) incursion rate. The top photograph shows the formation of a compacted surface layer of the right and left sides. In the center region, the compacted layer appears to have been pulled off. This suggests the tip buildup layer seen in Figure 73 may be formed initially by adhesive transfer. The bottom photograph shows a scabbed area. It appears that scab formation has been initiated on a continuous, compacted, aluminum bronze layer. Once initiated, the scab has continued to grow and was pushed down into the porous structure beneath it. This caused more extensive densification of the aluminum bronze immediately beneath that portion of the scab pushed down into the coating.

Figure 77 shows typical rub-liner features from the Inconel 718 blade rub at 755 K (900° F), 298 m/sec (1200 ft/sec) and 25.4 μm/sec (0.001 in./sec) incursion rate. The top photograph shows a typical scabbed area where little densification of the underlying coating has occurred beneath the initially compacted surface layer. The bottom photograph shows a region where considerable rub depth was achieved. Apparently, much of this was compaction of the porous structure rather than wear.

4.5 DISCUSSION

The disappointing results of the Task III effort to develop a porous, aluminum bronze, abradable seal pointed out several basic problems. The first of these was the conflict between the material properties required for good abradability and the desirable features of a coating that is stable in the compressor environment. Good erosion resistance, low oxidation and corrosion rates, and nonsticky debris are material-property requirements that are often divergent from those required by abradability considerations. The most obvious example in the current work was the conflict between abradability and erosion resistance.

This comes as no surprise since treatments for wear and erosion both indicate an inverse dependence on flow stress for ductile materials. Archard's Law of Wear (Reference 22) is:

$$W_v = \frac{KLD}{P}$$

where

W_v = Wear Volume

K = Wear Coefficient

L = Normal Load

D = Sliding Distance

P = Material Flow Stress

For erosion of ductile material, Finny (ibid) has found the following expression to be useful:

$$Q = \frac{MV^2}{2} \frac{1}{P} f(a)$$

where

Q = Volume removed by erosion

M = Total mass of the eroding particles

V = Particle velocity

P = Material Flow Stress

f(a) = A geometric factor dependent on the attack angle of the particles

According to these equations, improving the abradability (increasing W_v) by varying the coating strength will also result in a decreased erosion resistance (increased Q) because both Q and W_v are inversely proportional to P.

The conflicts between abradability and oxidation resistance of nonsticky debris are perhaps less obvious. The oxidation resistance of metals is improved by alloying; however, this also increases the strength of the metal and is thus deterimental to abradability according to Task I results.

The nonsticky-debris requirement is imposed by compressor design. The compressor stall margin is drastically reduced by the adherence of sticky debris to airfoil leading edges. However, nonsticky debris requires a high-melting-point coating. This, once again, decreases abradability since metal flow strengths are roughly proportional to melting temperature.

The second area highlighted by Task II results was the metallurgical and microstructural stability requirements for the abradable seal. This was most effectively pointed out by the correlation between blade wear and coating strength. The 5, 10, and 12.5% Ekonol coatings all had relatively high tensile strength (compared to the 15% Ekonol coating), and all produced wear on

blades. The tendency for the tensile strength of the 5, 10, and 12.5% Ekonol compositions to increase with increasing exposure temperatures caused concern that some of the early stages of sintering may be occurring in these coatings.

The initial metal-particle bonding in these plasma-sprayed coatings results in flattened individual particles with microvoids at the junctions. The radius of curvature at these junctions would be quite small. Thus, one of the early stages of sintering, neck-rounding, could occur even at fairly low temperatures since the driving force for neck-rounding is proportional to the neck radius. The neck radius should increase with increasing temperature or time. This could increase the coating strength, from a fracture mechanics point of view, without appreciably affecting the coating density. A cursory examination of as-sprayed and preexposed coatings at high magnifications indicated there could be some validity to the above ideas, but they were not pursued further under the scope of this work.

If such a mechanism were verified, it could reflect on the third area of concern seen in Task III. Metallographic examinations of longitudinal and transverse sections through the rub path indicated all of the following may occur in a given rub test:

1. Uniform coating densification and/or even wear.

2. Localized surface densification only.

3. Scabbing at surface densification.

4. Material pullout at surface densification.

This amounts to unpredicatable coating response to a rub, depending on which of the above events is initiated first. The explanation lies in local coating microstructural details too fine to control through thermal-spray processes at these porosity levels. Based on the above discussion of sintering, one could easily envision local plastic instabilities in the deformation process at the coating surface causing random responses of the types listed above. The changes in porous properties and unpredictable rub behavior suggest the porous microstructure needs to be further stabilized. This might best be accomplished by a coating with a lower volume fraction of metal content where coating strength is too low to show effects like the proposed strengthening by the early stage of sintering. Included in this open structure would be an inert, friable, filler material that retains its basic characteristics in the compressor environment. This would provide structural stability in the coating. The controlled process parameters would then provide the required property and microstructural control.

The final area highlighted by Task III was the difference in the abradable-seal material performance with different blade materials. The titanium alloy blades always experienced more wear than the Inconel 718 blades. Two factors influence this:

1. Heat-partitioning effects and the resulting thermal gradients in the blade and seal materials.

2. The relative flow strengths of the two alloys as a function of temperature.

The partitioning of the available frictional heat under a given rub situation is determined by the relative thermal conductivities of the blade and seal materials. The thermal conductivity of Ti-6Al-4V is about 60% that of Inconel 718. This causes the frictional heat generated by the rub to be more localized at the surface for titanium blades than for Inconel blades. Thus, the resultant surface temperatures should be higher for titanium blades. On this basis alone, one would expect Inconel blades to rub better than titanium blades since the flow strength decreases with temperature. However, more detailed examination of the flow strengths shows the situation to be even worse. The flow strengths of Inconel 718 and Ti-6Al-4V are similar at room temperature, 1.128 and 0.896 GPa (165 and 130 ksi) respectively, but at 811 K (1000° F) (a temperature easily attained during rub interaction) Inconel 718 has lost only 15% of its strength while Ti-6Al-4V has suffered a 65% strength loss that further enhances the tendency to wear.

This suggests that a change of blade material is necessary for further improvements in compressor blade-tip-to-casing gas seals. Specifically, blade tips that retain high flow strengths at temperature and result in lower heat generation or less severe thermal gradients may have a better chance of success. This would have to be accomplished by a tip treatment since it is not immediately feasible to change the blade material without redesigning the entire compressor. This could be accomplished by either a case-hardening treatment or a coating. The following three approaches could be taken:

1. A high-flow-strength, low-friction tip that would be wear resistant.

2. An abrasive tip that would efficiently cut the seal material and alter heat partitioning such that a significant portion of it goes to the seal material and rub debris.

3. A combination of the above.

5.0 CONCLUSIONS

1. Physical and mechanical properties of bulk materials help explain some of the features of the rub behavior of dense coatings but do not completely account for the differences observed in the various alloys studied.

2. Rub energy does not correlate with blade wear and cannot be used as a screening test for coating materials.

3. All additions to Cu reduced both blade wear and scabbing.

4. An interlayer of Feltmetal between the substrate and coating was found to reduce the severity of rubs (in terms of blade wear) but did not significantly affect the rub force or energy. However, it also reduced erosion resistance.

5. The addition of porosity to the coating produced smooth rubs but also reduced the erosion resistance of the coating.

6. Significant substrate temperature rises occur only when measurable blade wear or pick-up occurred. The higher rub forces were also associated with blade wear or pick-up.

7. Subtle changes in spray parameters, powder size distributions, and rub conditions were found to affect the performance and acceptability of the coatings.

8. Best spray parameters and use of treated -200 mesh Ekonol gave a controlled microstructure over a large range of coating composition.

9. If the Ekonol is not burned out of the coating it wears titanium blades at all compositions investigated.

10. Titanium alloy blades always wore more than Inconel 718 blades due to the combined effects of heat partitioning and temperature dependence of flow strengths.

11. At compositions where the erosion resistance and surface-finish capability of the coating were considered adequate after Ekonol burnout, blade wear was high.

12. Initiation of scabbing and blade wear on porous coatings were associated with formation of a dense, plastically flowed layer of aluminum bronze at the coating surface.

13. Coating cohesive strength provided the best indicator of when blade wear would occur.

14. Even short-time exposures at temperatures encountered in the latter compressor stage causes significant coating cohesive-strength increases.

15. Final compressor simulative rub testing indicated excessive aluminum bronze debris buildup on the leading edges of blades. This may indicate a sticky-debris problem.

REFERENCES

1. Rhines, F.N., Phase Diagrams in Metallurgy, McGraw-Hill, New York-London-Toronto, 1965, p. 3.

2. Pearson, W.B., A Handbook of Lattice Spacings and Structures of Metals and Alloys, Pergamon Press, New York-London-Paris-Los Angles, 1958.

3. Hansen, M., Constitution of Binary Alloys, McGraw-Hill, New York-London-Toronto, 1958.

4. Metals Handbook, 8th Edition, American Society for Metals, Metals Park, Ohio, 1965.

5. Rosenburg, S.J., NBS Monograph 106, U.S. Government Printing Office, Washington DC, 1978.

6. Toulonkian, Y.S., Powell, R.W., Ho, C.Y., and Klemens, P.G. (Editors), Thermophysical Properties of Matter, Volume I, IFI/Plenum Press, New York-Washington DC, 1970, p. 1142.

7. Sykes, C. and Evans, H., "Some Peculiarities in the Physical Properties of Iron-Aluminum Alloys," Proc. Roy. Soc. London, Series A, Vol. 145, 1934, pp. 529-539.

8. Kaster, W. and Franz, H., "Poisson's Ratio for Metals and Alloys," Met. Rev., Vol. 6, No. 21, 1961, pp. 1-55.

9. Leamy, H.J., Gibson, E.D., and Kayser, F.A., "The Elastic Stiffness Coefficients of Iron-Aluminum Alloys - I. Experimental Results and Thermodynamic Analysis," Acta Met., Vol. 5, December 1967, pp. 1827-1838.

10. Dieter, G.E., Mechanical Metallurgy, McGraw-Hill, New York-London-Toronto, 1961, p. 38.

11. Honeycombe, R.W.K., The Plastic Deformation of Metals, Edward Arnold Ltd., Great Britan, 1978, pp. 6-19.

12. Case, S.L. and VanHorn, K.R., Aluminum in Iron and Steel, John Wiley and Sons, New York and Chapman and Hall, London, 1953, pp. 300-303.

13. Alloy Digest, Engineering Alloy Digest Inc., Upper Mondain, New Jersy, 1961, Filming Code Ni-69.

14. Williams, J.A. and Bane, N., "Some Observations on the Flow Stress of Metals During Metal Cutting," Wear, Vol. 42, April 1977, pp. 341-353.

15. Materials Selector 77, Reinhold Publishing Co., Stamford, Connecticut, 1976.

16. Sykes, C and Bampfylde, J.W., J. Iron and Steel Inst., Vol. 130, 1934, pp. 389-ff.

17. Guy, A.G., Elements of Physical Metallurgy, Addison-Wesley Publishing Co., Reading, Massachusetts - London, 1960, p. 428.

18. Weertman, J. and Weertman, J.R., Elementary Dislocation Theory, MacMillan Co., New York, 1969, p. 98.

REFERENCES (Concluded)

19. Thornton, P.R., Mitchell, T.E., and Hirsch, P.B., "The Dependence of Cross-Slip on Stacking-Fault Energy in Force-Centered Cubic Metals and Alloys," Phil. Mag., Vol. 7, No. 80, August 1962, pp. 1349-1369.

20. Bowden, F.P. and Frietag, E.H., "The Friction of Solids at Very High Speeds - I. Metal on Metal; II. Metal on Diamond," Proc. Roy. Soc. London, Series A, Vol. 248, 1958, pp. 350-367.

21. Bill, R.C. and Ludwig, L.P., Wear of Seal Materials Used in Aircraft Propulsion Systems, NASA TM-79003 and AVRADCOM TR-78-47.

22. Engel, P.A., Impact Wear of Materials, Elsevier Scientific Publishing Inc., Amsterdan-London-New York, 1967.

23. Rabinowiccz, E., Friction and Wear of Materials, John Wiley and Sons, New York, 1965.

24. Hirschhorn, J.S., Introduction to Powder Metallurgy, American Powder Metallurgy Institute by Colonial Press Inc., Princeton, New Jersy, 1979.